Title
Cytotrophoblast extracellular vesicles promote maternal adaptation to pregnancy

Author
Taylor, Sara Kristine

Publication Date
2019

Peer reviewed|Thesis/dissertation

Cytotrophoblast extracellular vesicles promote maternal adaptation to pregnancy

by
Sara Kristine Taylor

DISSERTATION
Submitted in partial satisfaction of the requirements for degree of
DOCTOR OF PHILOSOPHY

in

Developmental and Stem Cell Biology

in the

GRADUATE DIVISION
of the
UNIVERSITY OF CALIFORNIA, SAN FRANCISCO

Approved:

DocuSigned by:
Robert Blelloch
91DFF4C4A2FF4FC...
Robert Blelloch
Chair

DocuSigned by:
Lewis Lanier
Lewis Lanier

DocuSigned by:
Adrian Erlebacher
Adrian Erlebacher

DocuSigned by:
Susan Fisher
3D7FD5EAA89E411...
Susan Fisher

Committee Members

Acknowledgements

I would like to thank my thesis advisor Susan Fisher for always pushing this project forward. It would not have been possible without her guidance, dedication, and big picture ideas. She taught me how to think like a scientist and approach problems critically. Her extensive depth of knowledge across biology provided perspective and insight with every new piece of data. Susan assembled a phenomenal group of scientists and I am grateful for their expertise.

A few lab members were critical for the success of my thesis work. My project would not have been possible without the skills and magic of Miko Kapidzic and Elaine Kwan, who isolated the massive numbers of primary cells required for extracellular vesicle generation. Matthew Gormley kickstarted this project and always made time to help. I am also thankful for Josh Robinson, who never hesitated to assist with data analysis and provide other scientific advice, and Yan Zhou, who I could always turn to for troubleshooting tips and tricks. I would also like to thank Hao Chen. Last, but absolutely not least, I would like to thank Harry Slomovits for his practical advice and refreshing sense of humor.

I would also like to express my gratitude to each member of my thesis committee: my chair Robert Blelloch, Lewis Lanier, and Adrian Erlebacher. I am thankful for their scientific expertise, insight, and support. I would also like to thank the DSCB program, especially Demian Sainz, for his advice and support throughout graduate school.

This project, spanning multiple tissue types, required the expertise of multiple collaborators. I would like to thank Linda Giudice and her lab for working with me on the endometrial functional experiments. Sahar Houshdaran was wonderful to work with and her expertise was instrumental. I would also like to thank Mike German and Luc Baeyens, who I collaborated with for the pancreas project and Birgit Schilling, who performed proteomic analyses.

I am so thankful for the many wonderful friends I made in graduate school. Thank you so much for all the memorable times. I would like to especially thank Liz Wheatley, Andrew Mancini, Buddy White, Bonnie Cole, Elijah Martin, and Ashley Libby, who were always ready for assorted (mis)adventures, and Bernadette Hsu and Elaine Kwan, who were always happy to get comfort food with me. I would also like to thank my friends from outside of UCSF for helping me keep things in perspective and patiently waiting for me to finish my thesis work.

My boyfriend, Jared Rudolph, has been an endless source of love and support. Thank you for always believing in me, even when I didn't. Your encouragement means the world to me and I'm excited to see what adventures our futures have in store.

I am grateful for my wonderful family. I would like to thank my mom, sister, and grandparents for their endless love and support. To my cousin Lauren, I had a blast living in the same city. I would also like to thank Jared's family, Harriet, Colin, and Abe for their love and support and welcoming me into the family. Last, I would like to thank Poe for always greeting me at the door no matter how late I came home after a time course experiment.

I thank everyone again who has supported my PhD journey. I look forward to sharing my own future directions with you.

Contributions

Chapters 1-3 of this work have been adapted largely as they will appear in a manuscript in preparation.

Chapter 4 of this work was performed in collaboration with Luc Baeyens and Michael S. German. Figures have been adapted from a manuscript in preparation. This chapter also reprints figures from the following publications:

OHARA-IMAIZUMI, M., KIM, H., YOSHIDA, M., FUJIWARA, T., AOYAGI, K., TOYOFUKU, Y., NAKAMICHI, Y., NISHIWAKI, C., OKAMURA, T., UCHIDA, T., FUJITANI, Y., AKAGAWA, K., KAKEI, M., WATADA, H., GERMAN, M. S. & NAGAMATSU, S. 2013. Serotonin regulates glucose-stimulated insulin secretion from pancreatic beta cells during pregnancy. *Proc Natl Acad Sci U S A,* 110**,** 19420-5.

PARSONS, J. A., BRELJE, T. C. & SORENSON, R. L. 1992. Adaptation of islets of Langerhans to pregnancy: increased islet cell proliferation and insulin secretion correlates with the onset of placental lactogen secretion. *Endocrinology,* 130**,** 1459-66.

Cytotrophoblast extracellular vesicles promote maternal adaptation to pregnancy

Sara Kristine Taylor

Abstract

Pregnancy requires integration between the embryo/fetus and the mother. The placenta promotes maternal adaptations to meet the physiologic, immunologic, and metabolic demands of the developing offspring. To mediate these changes, this temporary organ releases large quantities of extracellular vesicles (EVs) that facilitate communication between the embryo/fetus and the mother. Few studies have investigated the contents and functions of EVs from primary cytotrophoblasts (CTBs) at midgestation. In this study, I isolated EVs from second trimester CTBs by differential ultracentrifugation and characterized them by transmission electron microscopy, immunoblotting, and mass spectrometry. The 100,000 x g pellet was enriched for vesicles with a cup-like morphology typical of exosomes. They expressed the exosomal markers CD9 and hepatocyte growth factor-regulated tyrosine kinase substrate (HRS) and the trophoblast proteins placental alkaline phosphatase (PLAP) and HLA-G. Global proteomic profiling by mass spectrometry showed that the placental EVs contained proteins with roles in localization, transport, and immune functions. A cytokine array revealed that the CTB 100,000 x g pellet contained a significant amount of TNF-α. In terms of uterine functions, CTB EVs increased decidual stromal cell (dESF) transcription and secretion of NF-κB targets, including IL-8, as measured by qRT-PCR and cytokine array. A soluble form of the TNF-α receptor inhibited the ability of CTB 100,000 x g EVs to increase dESF secretion of IL-8. Together, the data suggest that CTB EVs enhance decidual cell release of inflammatory cytokines, which may be an important component of successful pregnancy. In terms of extra-uterine sites, CTB

100,000 x g EVs promoted pancreatic β-cell proliferation and insulin production both *in vivo* and *in vitro*. Ultimately, this work identified CTB EVs as drivers of maternal adaptation to pregnancy at local and distant sites and creates a foundation to investigate functions of these vesicles in other tissues and in the context of pregnancy complications.

Table of Contents

List of Figures

List of Tables

Chapter 1: Introduction

Sara K. Taylor[1,2,3], Susan J. Fisher[1,2,3,4,5,6]

1. Center for Reproductive Sciences, University of California, San Francisco, California 94143
2. Department of Obstetrics, Gynecology, and Reproductive Sciences, University of California, San Francisco, California 94143
3. Eli and Edythe Broad Center for Regeneration Medicine and Stem Cell Research, University of California, San Francisco, California 94143
4. Division of Maternal Fetal Medicine, University of California, San Francisco, California 94143
5. Department of Anatomy, University of California, San Francisco, California 94143
6. Human Embryonic Stem Cell Program, University of California, San Francisco, California 94143

Overview

In the following chapters, I give the background for my thesis research in terms of placental biology and the relevant literature regarding extracellular vesicles (Chapter 1). Next, I describe the major findings of my research, which focused on placental extracellular vesicles (EVs). I characterized the size, morphology, and protein contents of two types of second trimester cytotrophoblast (CTB) EVs. I profiled their proteomes using mass-spectrometry (Chapter 2). By using a cytokine array, I identified TNF-α in the 100,000 x g EVs. Because CTB-conditioned medium amplifies expression and secretion of NF-κB target, pro-angiogenic cytokines (Hess *et al.*, 2007), I investigated the role of CTB 100,000 x g EVs and TNF-α in this process (Chapter 3). Also, we explored whether these vesicles play a role at a systemic level, specifically, in pancreatic adaptation to pregnancy (Chapter 4). Finally, I summarize the many future directions in which the findings presented here may advance the field (Chapter 5).

The placenta orchestrates physiologic, immunologic, and structural integration of the maternal-fetal interface

Pregnancy presents unique physiologic and immunologic challenges to the mother and the embryo/fetus. The placenta mediates their physiologic integration. At a molecular level, this is accomplished by diverse molecules, including hormones and specialized placental proteins. At an immunologic level, the molecules and mechanisms are less clear, but likely include the numerous chemokines and cytokines produced at the maternal-fetal interface and the cytotrophoblast MHC class I molecule HLA-G (Ellis *et al.*, 1986; Hemberger, 2013; Kovats *et al.*, 1990).

The placenta also mediates the physical integration of the embryo/fetus with the uterus and the maternal circulatory system. Its structure is diagramed in Figure 1.1. The component functional units are termed chorionic villi, which are classified as either floating or anchoring

(Robinson *et al.*, 2017). Most of the placental surface is composed of floating villi, which are suspended in maternal blood (Maltepe and Fisher, 2015). Their surface is formed by syncytiotrophoblasts (STBs), multi-nucleated cells covered in microvilli, which increase the surface area and consequently diffusion, promoting nutrient and waste exchange (Smith *et al.*, 1977). Beneath the STB layer lie progenitor mononuclear cytotrophoblasts (CTBs), which fuse to form the syncytium (Robinson *et al.*, 2017). The stromal core lies deep to the CTB layer and contains the villous vascular tree and connective tissue elements, including a specialized population of macrophages (Hofbauer cells)(Gaw *et al.*, 2019; Red-Horse *et al.*, 2005; Reyes *et al.*, 2017). In anchoring villi, the CTB progenitors aggregate into columns, which leave the placenta and invade the decidua where they remodel spiral arteries redirecting blood flow to the floating villi (Red-Horse *et al.*, 2005). The cohabitation of placental cells from the embryo/fetus and maternal immune, decidual, and muscle cells within the uterus requires fine tuning of tolerizing and inflammatory mechanisms (Hemberger, 2013).

We know that this process is critical to determining pregnancy outcomes. For example, shallow CTB invasion and reduced maternal spiral artery remodeling are associated with preeclampsia (Ball *et al.*, 2006; Fisher, 2015).

Extracellular vesicles

Extracellular vesicles (EVs) have emerged as a form of cell-cell communication. There are multiple types of EVs, including exosomes and microvesicles, which vary in size, cellular compartment of origin, contents, and function.

Exosomes range from 30-150 nm in size and originate in the endosomal compartment (Patel *et al.*, 2019). They are formed by inward budding of endosomes into multivesicular bodies, which are transported to the cell surface where they fuse with the cell membrane and release exosomes into the extracellular space (Figure 1.2) (Harding *et al.*, 1984; Pan *et al.*, 1985). When visualized by transmission electron microscopy (TEM), they typically exhibit a cup-

like morphology, likely an artifact of dehydration in the TEM sample preparation process (Conde-Vancells *et al.*, 2008; Raposo *et al.*, 1996). Microvesicles are 100-1000 nm and are shed from the plasma membrane (Figure 1.2)(Raposo and Stoorvogel, 2013). The overlapping size of these two EV populations complicates the study of specific vesicle types. Thus, unless there are multiple purification steps, which may include immuno-affinity methods, samples will contain both exosomes and microvesicles.

EV cargo varies depending on what cells the vesicles are derived from and from where in the cell they originate. Overall, exosome contents reflect their origin in the endosomal compartment. They are enriched for tetraspanins, such as CD9, CD63, and CD81, and endosomal sorting components required for transport (ESCRT) pathway machinery, including tumor susceptibility gene 101 (Tsg101), Alix, and hepatocyte growth factor-regulated tyrosine kinase substrate (HRS)(Raposo and Stoorvogel, 2013). These molecules regulate the loading of other cargo into this subpopulation of EVs. For example, Tsg101 binds to the tetrapeptide motif P(S/T)AP to recruit other proteins, such as galectin-3 (Banfer *et al.*, 2018). Additionally, the WW domain present in the Nedd4 family of ubiquitin ligases is sufficient for protein packaging into exosomes via binding to Ndfip1 and ubiquitination (Sterzenbach *et al.*, 2017). There are likely other amino acid motifs that localize proteins to exosomes. These vesicles also contain a variety of RNA species. For example, exosomes are enriched with mRNAs that contain a 5' terminal oligopyrimidine motif (Shurtleff *et al.*, 2016). Contents also include small non-coding RNAs, including microRNAs (miRs) and transfer RNAs (tRNAs)(Shurtleff *et al.*, 2017). Packaging mechanisms may vary by cell type depending on which RNA-binding proteins and RNAs are among the contents (Shurtleff *et al.*, 2016). In terms of small RNAs, heterogeneous nuclear ribonucleoprotein A2B1 binds to the GGAG motif of miRs, which enables exosome loading (Villarroya-Beltri *et al.*, 2013). Additionally, the Y-box binding protein I (YBX1) selectively sorts small noncoding RNAs, including miRs and tRNAs, into exosomes (Shurtleff *et al.*, 2016; Shurtleff *et al.*, 2017). In terms of other nucleic acids, exosomes contain double-stranded DNA

(Thakur *et al.*, 2014) and mitochondrial DNA (Guescini *et al.*, 2010; Sansone *et al.*, 2017), but the mechanisms of packaging are unknown.

Fewer studies have investigated the cargo of microvesicles, but the contents of these EVs appear to overlap that of exosomes (van Niel *et al.*, 2018). They both contain proteins and nucleic acids. Microvesicles are enriched for protein contents that reflect their origin, such as plasma membrane structures, cargo that associates with lipid rafts, and cytoskeletal components (van Niel *et al.*, 2018). In terms of nucleic acids, they carry mRNA, small non-coding RNAs (including miRs), and DNA (Wei *et al.*, 2017). Additional studies are needed to understand mechanisms of cargo loading into microvesicles.

Exosome isolation methods

Multiple methods have been used to isolate exosomes from *in vitro*-cultured conditioned medium and bodily fluids. Each has its advantages and disadvantages. Stepwise ultracentrifugation culminating at high speeds (between 100,000 and 110,000 x g) is the most commonly used method due to the low cost and relatively moderate amount of time required (Thery *et al.*, 2006). However, the isolated pellet is not a pure population because the sizes of exosomes and microvesicles overlap. This exosome-enriched pellet also contains other contaminants, such as protein aggregates, lipoparticles, and apoptotic products (Hessvik and Llorente, 2018).

Due to the limitations of ultracentrifugation, other techniques to isolate exosomes have been developed. Size exclusion chromatography is a rapid method that does not perturb the morphology of the resulting EVs, but the vesicles outside the chosen cutoff ranges will be lost and some level of cross-contamination due to size overlap is inevitable (Coumans *et al.*, 2017; Gamez-Valero *et al.*, 2016). Ultrafiltration uses a filter with either pressure or ultracentrifugation to separate EVs from soluble proteins. This rapid method produces higher yields than ultracentrifugation, but the preparation is contaminated by larger EVs and the applied force can

cause aggregation (Coumans *et al.*, 2017). Polymer precipitation kits are a quick isolation technique with high recovery, but result in contamination by microvesicles, lipoparticles, and protein aggregates unless followed by additional purification steps (Duong *et al.*, 2019; Hessvik and Llorente, 2018). Additionally, EVs generated by this method reduce viability of target cells *in vitro,* possible evidence of reagent spillover (Gamez-Valero *et al.*, 2016). Therefore, downstream analyses should be considered when choosing an isolation method.

Exosome preparations can be further purified after the initial isolation step by density-gradient centrifugation and/or immunological isolation. For the former, the concentrated EVs are layered above or below a density gradient and ultracentrifuged, allowing for collection of exosomes at a density of 1.15 to 1.19 g/ml; however, this method is takes time and reduces yield (Hessvik and Llorente, 2018; Thery *et al.*, 2006). Additionally, if the sample is concentrated by ultracentrifugation before this step, aggregation and physical disruption of vesicles may result in lower recovery (Duong *et al.*, 2019). One study comparing exosome isolation methods followed by a density gradient step found that: (1) ultracentrifugation results in the lowest yields but highest purity; (2) polymer precipitation with a cushioned density gradient perform similarly; and (3) ultrafiltration produces the lowest purity preparations (Duong *et al.*, 2019). Immunological isolation with an exosomal marker is another frequently used purification method, but it is time consuming and heterogenous expression of target antigens among exosome subpopulations may result in a significant loss of EVs (Ji *et al.*, 2019; Shah *et al.*, 2018). Overall, the tradeoff between yield and purity poses a barrier to studying exosomes if the starting material is limiting.

Extracellular vesicles as a method of cell-cell communication

EVs are an emerging form of intercellular transport and communication. Signals to the recipient cell can take many forms. Multiple groups have used the Cre-loxP system to demonstrate exosomal cargo transfer to recipient cells in mouse model systems. EVs carrying

plasmid DNA, mRNA, and tagged protein for Cre-recombinase are taken up by their target cells, resulting in recombination (Kanada *et al.*, 2015; Sterzenbach *et al.*, 2017; Zomer *et al.*, 2015). Another study took advantage of species-specific differences and found that exosomal miRNAs and mRNAs can be delivered to recipients, with subsequent translation of the latter (Valadi *et al.*, 2007).

Proteins on the surface of EVs are critical for uptake by recipient cells. The EV protein repertoire includes integrins and extracellular matrix proteins, which are required for homing to and uptake by target cells (Costa-Silva *et al.*, 2015; Hoshino *et al.*, 2015). Vesicular integrin expression does not always mirror that of parent cells (Hoshino *et al.*, 2015). Small EVs isolated by ultracentrifugation at 100,000 x g have a variety of glycan modifications, including N-acetylglucosamine and sialic acid residues (Williams *et al.*, 2019). Perturbation of glycosylation changes uptake by recipient cells (Williams *et al.*, 2019). More studies are needed to understand mechanisms by which EVs home to their targets.

EV functions have been described for many diseases and contexts, including cancer, immunity, and reproduction, specifically placentation. In the following sections, vesicles isolated by ultracentrifugation and an additional purification method, such as density gradient centrifugation or immuno-isolation, will be referred to as exosomes. EVs isolated by ultracentrifugation alone will be identified by the speed used to pellet them.

Extracellular vesicle functions in cancer

EV function has been extensively studied in the context of cancer. They are present at higher concentrations in the blood of patients as compared to that of healthy control individuals (Capello *et al.*, 2019). On a practical level, immortalized cancer cell lines facilitate production of the large quantities of conditioned medium required to isolate and purify exosomes from other EVs and contaminating material. Vesicles can function locally or at distant sites, facilitating

interactions of cancer cells with a variety of other cell types, including in the niche and at metastatic sites.

EVs as a signaling mechanism between cancer cells

Multiple groups have reported that tumors use EVs to promote more aggressive behavior of subsets of their component cells. For example, malignant cells release EVs that carry mRNAs associated with migration and metastasis; these vesicles enhance these aggressive behaviors in less malignant recipient tumor cells (Zomer *et al.*, 2015). Additionally, apoptotic glioblastoma cells promote proliferation and therapy resistance in the surviving cancer cells by transferring EVs containing oncogenic splicing factors (Pavlyukov *et al.*, 2018). Furthermore, migrating HT1080 fibrosarcoma cells leave behind an exosome trail that promotes paracrine motility (Sung *et al.*, 2015). Fibronectin on the surface of these vesicles enhances speed but not direction of movement (Sung *et al.*, 2015; Sung and Weaver, 2017). Together, these studies demonstrate that EVs promote different aspects of tumor progression within cancer cell populations.

EVs from the stroma as mediators of cancer progression

The stroma also releases vesicles that modulate cancer cell metabolism, therapy resistance, and disease progression. For example, bone marrow mesenchymal stem cells release 100,000 x g EVs that induce a dormant phenotype in metastatic breast cancer cells, reducing their proliferation and ultimately rendering them resistant to chemotherapy (Ono *et al.*, 2014). This is likely due to miR-23b present in the vesicles, as overexpression of this miRNA similarly decreases proliferation (Ono *et al.*, 2014). Conversely, horizontal transfer of mitochondrial DNA in cancer-associated fibroblast EVs to dormant human breast cancer stem-like cells restores metabolic activity and hormone therapy resistance (Sansone *et al.*, 2017). Stromal cells also release EVs in response to tumor cell signals. When breast cancer cells

trigger NOTCH-MYC in fibroblasts, the stromal cells release unshielded RNA via exosomes (Nabet *et al.*, 2017). Breast cancer cells take up these vesicles, which activate the pattern recognition receptor RIG-I, resulting in STAT1 antiviral and NOTCH3 signaling that drives the growth of therapy resistant cells and metastasis (Boelens *et al.*, 2014; Nabet *et al.*, 2017). Thus, EVs act as a form of intercellular communication between the stroma and cancer cells.

EVs as a mechanism to modulate the primary and metastatic tumor microenvironments

Cancer EVs promote a favorable microenvironment at primary and pre-metastatic sites. These vesicles act in a paracrine manner at the primary tumor niche. For example, mouse GL261 glioma cells transfer miR-21 to microglia via 100,000 x g EVs in vivo, which down-regulates miR-21 targets, including *Btg2*; downregulation of this gene increases microglia proliferation and supports tumor progression (Abels *et al.*, 2019). Cancer EVs can also promote angiogenesis directly or through stromal cells. Hypoxic colorectal cancer cells release exosomes to promote the proliferation and migration of endothelial cells via Wnt/β-catenin signaling (Huang and Feng, 2017). Cancer cell exosomes trigger differentiation of fibroblasts to myofibroblasts via TGF-β1 (Webber *et al.*, 2010). These exosome-induced myofibroblasts promote angiogenesis of human umbilical vein endothelial cells (HUVECs) *in vitro* and enhance tumor growth *in vivo*; TGF-β1 inhibition or blocking exosome production via Rab27a knockdown abolishes these effects (Webber *et al.*, 2015). Soluble TGF-β1 does not recapitulate these pro-angiogenic or tumor-promoting features, suggesting that the exosomal form of this growth factor has distinct functions and/or that these EVs contain other molecules that modulate the effects of TGF-β1 (Webber *et al.*, 2010; Webber *et al.*, 2015). Overall, these studies demonstrate multiple functions of tumor EVs in modulating nearby cells to promote tumor progression.

Cancer cells also release EVs into the circulation, where they establish the pre-metastatic niche at distant sites in multiple cancer types. Metastatic melanoma exosomes

educate bone marrow-derived cells (BMDCs) through MET signaling and induce vascular leakiness and BMDC recruitment at the pre-metastatic niche, thus promoting metastasis (Peinado *et al.*, 2012). Pancreatic ductal adenocarcinoma (PDAC) 100,000 x g EVs induce formation of a pre-metastatic niche and increase liver metastatic burden in mice (Costa-Silva *et al.*, 2015). These EVs are taken up by Kupffer cells, increasing their secretion of TGF-β and upregulating hepatic stellate cell production of fibronectin, a pro-adhesion factor (Costa-Silva *et al.*, 2015). This fibrotic environment increases recruitment of bone marrow-derived macrophages to the liver, which promotes metastasis (Costa-Silva *et al.*, 2015). The adhesion and extracellular matrix (ECM) molecules on EVs determine exosome homing sites and where the pre-metastatic niche will form (Hoshino *et al.*, 2015). Specifically, EV integrins $\alpha_6\beta_4$ and $\alpha_6\beta_1$ promote lung metastasis, while integrin $\alpha_V\beta_5$ promotes liver metastasis. Inhibition of integrins decreases EV organotropism, but overexpression increases EV uptake. Additionally, pretreatment with lung-tropic tumor EVs redirects metastasis of bone-tropic tumor cells to the lung (Hoshino *et al.*, 2015). Thus, cancer EVs can function at distant sites to promote the formation of the pre-metastatic niche and disease progression.

EVs as a mechanism of immune escape

Cancer cells release EVs to modulate the immune system and evade destruction. Tumor vesicles suppress differentiation, interfere with receptor binding, and contain immunosuppressive cargo. Uptake of cancer cell EVs interferes with normal differentiation of immune cells. For example, breast cancer exosomes suppress monocyte differentiation into antigen-presenting cells (Yu *et al.*, 2007). Similarly, tumor cell 110,000 x g EVs prevent monocyte differentiation into dendritic cells, instead promoting the development of myeloid cells that suppress T cell function (Valenti *et al.*, 2006).

Tumor cell EVs also exhibit decoy functions and interfere with the binding of immune molecules to targets. For example, prostate cancer cells generate exosomes containing membrane-bound ICAM-1, which binds to LFA-1 on leukocytes to block their adhesion to activated endothelial cells (Lee *et al.*, 2010). This prevents immune cell migration into the tissue, protecting the tumor. Additionally, the surface of pancreatic cancer cell exosomes is enriched for tumor-associated antigens that induce an antibody response as compared to whole cell lysates (Capello *et al.*, 2019). These vesicles act as a decoy for antibodies and inhibit complement-dependent cytotoxicity of pancreatic cancer cells in a dose dependent manner (Capello *et al.*, 2019). Overall, tumor EVs can bind to immune cell receptors and antibodies, preventing them from reaching their intended ligands or targets.

Cancer cell EVs also promote apoptosis or inhibit activation of immune cells via immunomodulatory molecules, including TGF-β1, Fas ligand (FasL), HLA-G, and PD-L1. For example, melanoma cells release EVs containing functional FasL that mediates apoptosis of Jurkat T cells (Andreola *et al.*, 2002). Additionally, human cancer cell exosomes inhibit IL-2-mediated proliferation of peripheral lymphocytes, induce regulatory T cells, and suppress natural killer (NK) cell-mediated cytotoxicity (Clayton *et al.*, 2007). These EVs contain TGF-β1, and antibody neutralization of this growth factor partially restores lymphocyte proliferation. Renal carcinoma cancer stem cells secrete EVs containing HLA-G that inhibit peripheral monocyte differentiation into dendritic cells; anti-HLA-G antibody partially blocks this effect (Grange *et al.*, 2015). Together, the inability to completely block the inhibitory effects of these EVs suggests that they contain other immunomodulatory cargo. Multiple groups have found that vesicles modulate immune cells via PD-L1, an immunosuppressive molecule (Chen *et al.*, 2018; Dong *et al.*, 2002; Haderk *et al.*, 2017; Poggio *et al.*, 2019). For example, chronic lymphocytic leukemia exosomes induce PD-L1 expression in monocytes that can be recapitulated by transfer of noncoding Y RNA hY4 and blocked by TLR7 deficiency or TLR signaling inhibition

(Haderk *et al.*, 2017). In addition, multiple cancer types release EVs that directly inhibit T cell activation and proliferation via PD-L1 (Chen *et al.*, 2018; Poggio *et al.*, 2019; Ricklefs *et al.*, 2018). The inability to release exosomal PD-L1 inhibits tumor growth *in vivo*, which can be rescued by systemic exosomal PD-L1 (Poggio *et al.*, 2019). Thus, cancer cells use EVs to exploit multiple mechanisms for immune suppression and evasion.

Extracellular vesicle functions in immune cells

EVs have many other immunomodulatory functions beyond cancer context. Multiple groups have studied their role in antigen presentation. Antigen presenting cells (APCs), which include dendritic cells and B cells, release 100,000 x g EVs and/or exosomes that contain major histocompatibility complex (MHC) class II molecules loaded with peptides and induce antigen-specific T cell activation *in vitro* and *in vivo* (Raposo *et al.*, 1996; Zitvogel *et al.*, 1998). Vesicles can present antigens by multiple mechanisms: direct stimulation of T cells; internalization by dendritic cells that reload the peptides onto their own MHC class II; or presentation on the dendritic cell surface without phagocytosing and processing (Segura *et al.*, 2007; Wakim and Bevan, 2011). The latter two mechanisms enhance T cell activation, as recipient dendritic cells induce a stronger immune response than EVs alone or the original EV-producing dendritic cells (Hao *et al.*, 2007; Montecalvo *et al.*, 2008; Wakim and Bevan, 2011). The differentiation state of APCs makes a significant difference in the functionality of their vesicles. Mature dendritic cell 100,000 x g EVs are 50- to 100-fold more efficient at direct T cell activation than those from immature dendritic cells *in vitro*, and only the former can stimulate T cells *in vivo* (Segura *et al.*, 2005). Recently, another group reported a novel form of antigen presentation by perivascular dendritic cells that sample the blood. These cells secrete 100,000 x g EVs loaded with circulation-derived allergens into the perivascular space, where the vesicles activate mast cells and induce anaphylaxis (Choi *et al.*, 2018). Vesicle type influences antigen-presenting activity; 100,000 x g EVs are more efficient at stimulating antigen-specific T cell activation than 10,000 x

g EVs (Wahlund *et al.*, 2017). The antigen-presenting ability of vesicles has important implications for allergy, transplantation rejection, and anti-tumor immunity (Admyre *et al.*, 2007; Segura *et al.*, 2005; Wolfers *et al.*, 2001; Zitvogel *et al.*, 1998).

EVs can also induce immune cell maturation. Mast cell exosomes induce dendritic cell maturation and acquisition of antigen-presenting capabilities (Skokos *et al.*, 2003). These EVs contain heat shock proteins hsp60 and hsc70, and blocking their receptor CD91 on recipient cells prevents dendritic cells from acquiring the ability to present antigens to T cells. Additionally, adipocytes release exosome-sized, lipid-filled EVs as an alternative pathway of lipid release (Flaherty *et al.*, 2019). These vesicles are taken up by macrophages and induce their differentiation, which could induce inflammation.

Cytokines and other immunoregulatory molecules can be released on vesicles as a non-canonical method of secretion. For example, the human THP-1 monocytic cell line releases EVs that contain active IL-1β, a proinflammatory cytokine lacking a leader sequence for canonical secretion (MacKenzie *et al.*, 2001). Additionally, similarly to cancer EVs, mouse thymic exosomes induce $Foxp3^+$ regulatory T cells and suppress proliferation of $CD4^+$ $CD25^-$ T cells (Wang *et al.*, 2008). Neutralizing TGF-β on these EVs only partially blocks these effects, suggesting that they contain other immunomodulatory contents.

Furthermore, myeloid cells and stromal cells release EVs with functional forms of membrane-bound TNF-α and its family members. Mouse macrophages treated with LPS and ATP produce microvesicles that contain membrane-bound TNF-α and cause inflammation *in vivo* (Soni *et al.*, 2019). Multiple groups have associated TNF-α with dendritic cell EV functions. Membrane-bound TNF-α on mouse dendritic cell vesicles promotes HUVEC inflammation through the NF-κB pathway (Gao *et al.*, 2016). When injected into ApoE-knockout mice, they also increase the number of atherosclerotic lesions (Gao *et al.*, 2016). Human LPS-activated dendritic cells produce EVs that contain transmembrane TNF receptors, TNFR1 and TNFR2,

and soluble TNF-α and induce epithelial cells to secrete inflammatory cytokines, including NF-κB targets IL-8 and MCP-1 (Obregon *et al.*, 2009). Dendritic cell exosomes trigger tumor cell apoptosis and enhance IL-2-activated NK cell production of IFN-γ via surface expression of TNF-α, TRAIL, and FasL (Munich *et al.*, 2012). In terms of stromal cells, synovial fibroblasts from patients with rheumatoid arthritis produce exosomes that contain active, membrane-bound TNF-α (Zhang *et al.*, 2006). These vesicles are cytotoxic to L929 cells, a line sensitive to TNF-α, and can be taken up by anti-CD3-activated T cells to activate AKT and NF-κB signaling and delay cell death. Thus, multiple cell types modulate immune cells via EVs.

Extracellular vesicle functions in other pathogenic settings

The roles of EVs in fibrosis and aging have recently been reported. For example, fibroblasts deficient in NEU1, a sialic acid processing enzyme that negatively regulates lysosomal exocytosis, have characteristics of myofibroblasts and produce large quantities of exosomes containing high levels of TGF-β and WNT signaling molecules (van de Vlekkert *et al.*, 2019). These EVs upregulate pro-fibrotic genes in normal fibroblasts and convert them into myofibroblasts, thus propagating fibrotic disease.

In terms of aging, senescent fibroblasts induce paracrine senescence via 100,000 x g EVs, a phenotype that can be partially blocked by IFITM3 depletion in the donor cells and their vesicles (Borghesan *et al.*, 2019). Together, these findings reinforce the concept that EVs have functions in a wide variety of cell types and diseases.

Extracellular vesicle functions in reproductive tissues

Given my work on the role of CTB EVs in reproduction, in this and subsequent sections, I focus on studies that employed human samples. Bodily fluids produced by reproductive organs are rich in EVs. These include semen, follicular fluid, and endometrial fluid (Campoy *et al.*,

2016; Franz *et al.*, 2016; Hoog and Lotvall, 2015). Both paternal and maternal vesicles play important roles in reproduction. In terms of the former, EVs from seminal fluid target both sperm and maternal cells. These vesicles are likely important for sperm motility, as seminal fluid EVs isolated from men with normal sperm function increases sperm motility whereas those from asthenozoospermic men do not (Murdica *et al.*, 2019). Multiple groups have described functions of these vesicles in the uterus. Human seminal fluid EVs induce endometrial stromal cell secretion of IL-6 and IL-8, two cytokines involved in implantation (Paktinat *et al.*, 2019). These EVs likely also play a role in suppressing uterine immune cells. Human seminal fluid 100,000 x g EVs inhibit proliferation of activated human peripheral blood mononuclear cells (PBMCs) (Kelly *et al.*, 1991). These vesicles are taken up by human neutrophils and monocytes, reducing their ability to phagocytose latex beads (Skibinski *et al.*, 1992). Additionally, human seminal fluid exosomes increase antigen-presenting cell production of indoleamine 2,3 deoxygenase, which is known to inhibit T cells (Vojtech *et al.*, 2019). Overall, seminal EVs improve sperm motility, promote implantation, and suppress the maternal immune system, all processes required for pregnancy.

There are only a few studies on ovarian follicle EVs and their effects on oocytes. On a practical level, obtaining follicular fluid requires a much more invasive procedure compared to collecting semen. Human follicular fluid contains EVs enriched for miRNAs that target genes that suppress follicle maturation and resumption of meiosis, suggesting that these vesicles promote oocyte development (Franz *et al.*, 2016; Santonocito *et al.*, 2014).

Uterine fluid contains EVs that likely play a role in implantation (Campoy *et al.*, 2016). Most studies have focused on endometrial epithelial cells. For example, 100,000 x g EVs from the human endometrial epithelial cell line ECC-1 contain miRNAs that target genes in pathways involved with implantation (Ng *et al.*, 2013). Multiple groups have found that these EVs promote trophectoderm adhesion and migration. ECC-1 EVs are taken up by and increase the adhesive capacity of the HTR8 trophoblast cell line (Greening *et al.*, 2016). Additionally, EEC-1 EVs

increase the invasion and adhesion of trophoblast stem cell-derived trophectoderm (Zdravkovic *et al.*, 2015) cultured as spheroids to mimic blastocysts (Evans *et al.*, 2019). In terms of primary cells, human endometrial epithelial cells secrete 120,000 x g EVs that are internalized by the trophectoderm of mouse embryos (Vilella *et al.*, 2015). These vesicles contain maternal miRNA has-miR-30d, which upregulates gene expression of adhesion molecules and increases blastocyst attachment (Vilella *et al.*, 2015). Uterine immune cells likely support implantation as well. For example, PMA-stimulated THP-1 monocyte-derived macrophage 100,000 x g EVs are taken up by the BeWo choriocarcinoma cell line and by vaginally-delivered term placental villi in an *ex vivo* explant model, in which they promote secretion of inflammatory cytokines IL-6 and IL-8 and immunosuppressive IL-10 (Holder *et al.*, 2016). Thus, a variety of EVs promote reproduction and implantation.

Placental extracellular vesicle functions in normal pregnancies

The placenta produces large numbers of EVs that increase in concentration throughout gestation (Germain *et al.*, 2007; Knight *et al.*, 1998; Salomon *et al.*, 2014; Sarker *et al.*, 2014). The component processes of human placentation have many parallels with tumorigenesis and metastasis. Cytotrophoblasts invade the uterus, breach the vasculature, and modulate the maternal immune system to promote tolerance of the feto-placental unit (Hemberger, 2013; Maltepe and Fisher, 2015). The functions of placental EVs likely mirror those of cancer vesicles, mediating a variety of physiologic and immunologic adaptations at near and distant sites in normal pregnancy.

Many studies isolate placental EVs from the maternal circulation or from immortalized cell lines. These models are problematic and have many limitations. EVs isolated from blood are contaminated by high density lipoproteins and vesicles from non-placental sources (Aatonen *et al.*, 2017; Yuana *et al.*, 2014). Placental vesicles quickly aggregate with and activate platelets, stimulating their release of EVs, which make up the majority of blood-borne vesicles (Aatonen *et*

al., 2017; Tannetta *et al.*, 2015). Functional effects observed in studies using circulating EVs could be due to placental vesicles or platelet-derived EVs influenced by placental signals.

Choriocarcinoma and immortalized placental cell lines are poor mimics of primary CTBs and STBs. In terms of epigenetics, choriocarcinoma lines JAR, JEG-3, and BeWo and transformed trophoblastic HTR-8/SVneo cells have DNA hypermethylation patterns that are more typical of cancer cells than primary CTBs (Novakovic *et al.*, 2011). Immortalized TEV-1 and SWAN71 cell lines have methylation patterns similar to each other but distinct from primary cells (Novakovic *et al.*, 2011). Choriocarcinoma and transformed trophoblast cell lines also variably express primary CTB markers. For example, JAR and HTR-8/SVneo cell lines do not express the CTB marker HLA-G, whereas BeWo cells variably express this molecule (Novakovic *et al.*, 2011). In addition, trophoblastic cell lines are functionally impaired in terms of adhesion, migration, and invasion (Hannan *et al.*, 2010). Since choriocarcinoma and transformed cell lines poorly phenocopy CTBs, the EVs they produce are less functionally relevant than primary placental vesicles.

Early studies of primary placental EVs focused on the subset generated by STBs. The authors compared vesicles collected by ultracentrifugation after generation by three methods: mechanically fractured from chorionic villi, isolated from the medium in which explants were cultured, and captured from placental perfusate (Gupta *et al.*, 2005b; Smarason *et al.*, 1993). Each method produced EVs that were morphologically similar but functionally different (Gupta *et al.*, 2005b). For example, STB EVs from all the methods inhibit HUVEC proliferation, but only those isolated by mechanical means disrupt the cells' morphology and induce apoptosis *in vitro* (Gupta *et al.*, 2005b; Smarason *et al.*, 1993).

The method by which they were generated affects the immunomodulatory activity of STB EVs. Vesicles derived mechanically and from explant cultures inhibit peripheral T cell activation, proliferation, and secretion of IL-2 and IFN-γ; EVs derived from perfusion promote T cell proliferation and increase IFN-γ secretion (Gupta *et al.*, 2005a). Explant-derived STB EVs also

carry FasL and TRAIL and induce Jurkat T cell apoptosis (Stenqvist *et al.*, 2013). Similarly, perfusion-derived STB EVs activate PBMCs, are taken up by monocytes and B cells, and stimulate production of inflammatory cytokines (Germain *et al.*, 2007; Southcombe *et al.*, 2011). Also, STBs EVs from explants and perfused placentas induce peripheral monocyte secretion of inflammatory cytokines, whereas mechanically-derived vesicles do not (Messerli *et al.*, 2010).

Of the three methods, the placental perfusion model is the most physiologically relevant and has the additional advantage of allowing for high yields of STB EVs (Dragovic *et al.*, 2015; Southcombe *et al.*, 2011). More recent studies using this method describe non-immune functions of these vesicles, such as inducing platelet activation and aggregation (Tannetta *et al.*, 2015).

Studies of primary CTB EVs have focused on those derived from term placentas. In general, the vesicles have immunomodulatory roles. For example, term cytotrophoblast exosomes confer viral resistance to recipient non-placental cells, including HUVECs, human uterine microvascular endothelial cells (HUtMVECs), placental fibroblasts, and foreskin fibroblasts (Delorme-Axford *et al.*, 2013; Ouyang *et al.*, 2016). This is likely due to miRNAs from the placenta-specific chromosome 19 cluster (C19MC), which are found in trophoblasts and their vesicles (Donker *et al.*, 2012). Transfection of this cluster into recipient cells also attenuates viral replication (Delorme-Axford *et al.*, 2013). Additionally, primary term villous cytotrophoblast 100,000 x g EVs suppress secretion of Th1 cytokines IL-2, TNF-α, and IFN-γ in activated Jurkat T cells and PBMCs; this activity is blocked by inhibition of syncytin-2 (Lokossou *et al.*, 2019). The function of CTB EVs earlier in pregnancy has not been studied.

Placental extracellular vesicle functions in complicated pregnancies

Failure of the placenta to mediate integration of the embryo/fetus with the mother results in pregnancy complications and is associated with abnormal EV production. For example,

preeclampsia, which is characterized by shallow CTB invasion and reduced maternal spiral artery remodeling (Ball *et al.*, 2006; Fisher, 2015), is associated with higher levels of circulating placental EVs (Germain *et al.*, 2007; Knight *et al.*, 1998; Lok *et al.*, 2008). Perfusion-derived STB EVs from preeclamptic and normal placentas differ in contents and function. For example, in preeclampsia, STB EVs contain increased levels of Flt-1 and the percentage of endoglin-containing vesicles decreases (Tannetta *et al.*, 2013). These anti-angiogenic molecules may contribute to the perturbation of maternal vasculature responses that is the hallmark of this pregnancy complication (Tannetta *et al.*, 2013). These EVs also contain reduced levels of the vasodilators, endothelial nitric oxide synthase and nitric oxide (Motta-Mejia *et al.*, 2017). Additionally, STB EVs have an increased ability to activate platelets (Tannetta *et al.*, 2015). Overall, it is unclear whether vesicles contribute to the pathology of the disease or are due to compensation by the placenta.

In terms of distant physiologic changes, in normal pregnancy, the mother becomes insulin resistant, which facilitates glucose transfer to the developing embryo/fetus (Lain and Catalano, 2007). To compensate, the maternal pancreas expands in size and increases insulin secretion (Baeyens *et al.*, 2018). If this organ fails to adapt, then the mother develops gestational diabetes mellitus (Rieck and Kaestner, 2010). The mechanisms remain unknown but may be due to abnormalities in placental vesicle production or contents. STB EVs contain active dipeptidyl peptidase IV (DPPIV), which breaks down GLP-1, a regulator of glucose-dependent insulin secretion (Kandzija *et al.*, 2019). In gestational diabetes, the concentration of DPPIV-containing EVs increases, which could be related to the reduced insulin secretion that characterizes this disorder (Kandzija *et al.*, 2019). Investigating maternal adaptation to normal pregnancy may provide insights into mechanisms underlying pregnancy complications.

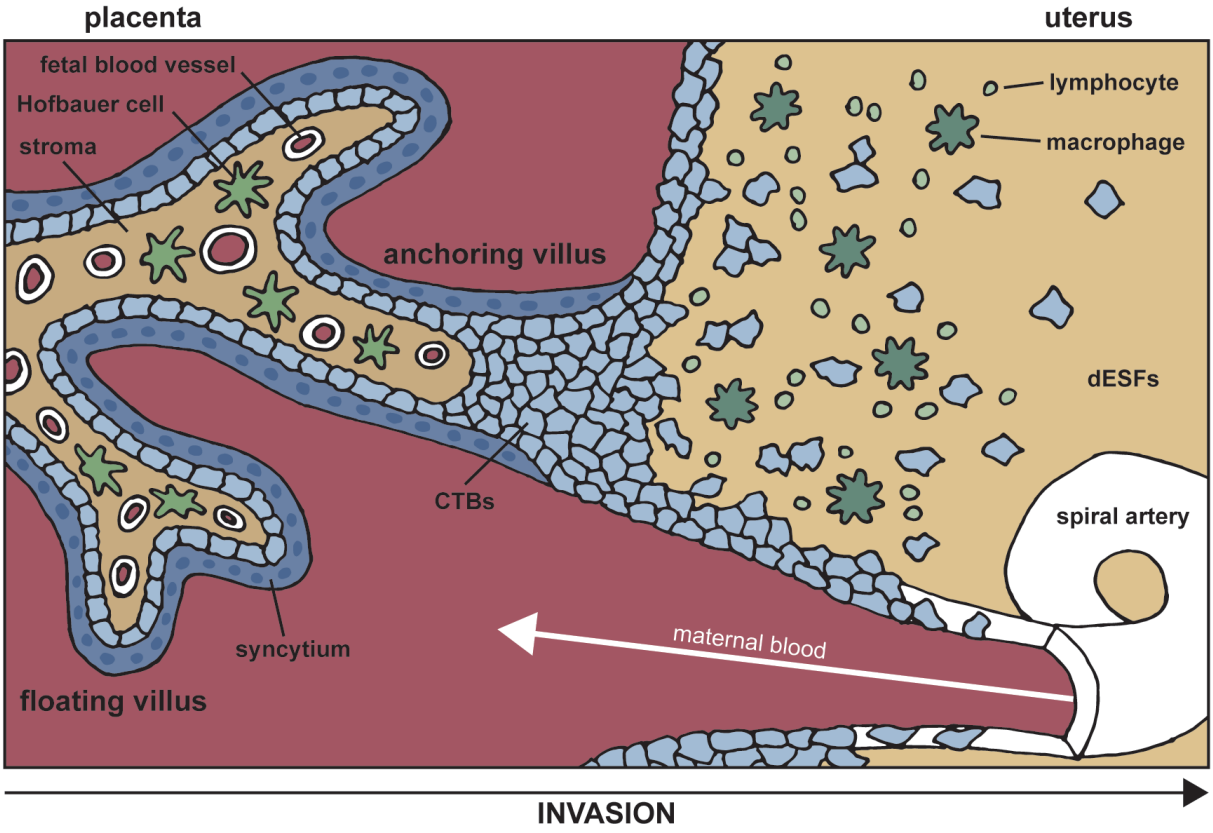

Figure 1.1 The placenta forms the maternal-fetal interface.

The placenta is composed of two types of villi, floating and anchoring. The multinucleated syncytium forms the villous surface and is bathed in maternal blood. Progenitor CTBs lie beneath the STB layer. These cells fuse to form the syncytium or invade from anchoring villi into the decidua, where they remodel spiral arteries. Invasive CTBs are in direct contact with decidual immune cells, including macrophages and lymphocytes, and uterine cells, such as decidualized endometrial stromal fibroblasts.

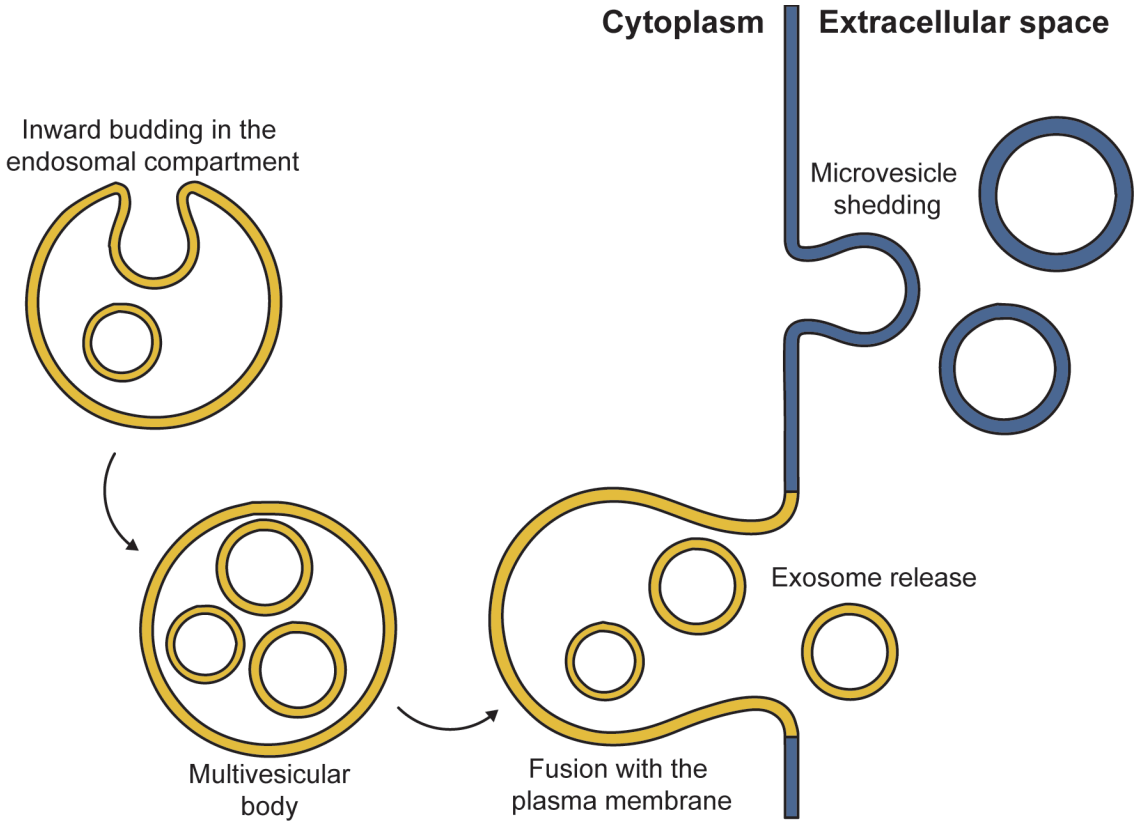

Figure 1.2 Exosomes and microvesicles originate from different cellular compartments.

Exosomes originate in the endosomal compartment, where inward budding forms multivesicular bodies (MVBs). MVBs are transported to the cell surface, where they fuse with the plasma membrane, releasing exosomes into the extracellular space. Microvesicles are formed by shedding from the plasma membrane.

Chapter 2: Characterization of cytotrophoblast extracellular vesicles

---

Sara K. Taylor[1,2,3], Joshua F. Robinson[1,2,3], Matthew J. Gormley[1,2,3], Mirhan Kapidzic[1,2,3], Elaine Y. Kwan[2], Birgit Schilling[4], Susan J. Fisher[1,2,3,5,6,7]

1. Center for Reproductive Sciences, University of California, San Francisco, California 94143
2. Department of Obstetrics, Gynecology, and Reproductive Sciences, University of California, San Francisco, California 94143
3. Eli and Edythe Broad Center for Regeneration Medicine and Stem Cell Research, University of California, San Francisco, California 94143
4. Chemistry & Mass Spectrometry, Buck Institute for Research on Aging, Novato, California 94945
5. Division of Maternal Fetal Medicine, University of California, San Francisco, California 94143
6. Department of Anatomy, University of California, San Francisco, California 94143
7. Human Embryonic Stem Cell Program, University of California, San Francisco, California 94143

Author Contributions:

S.K.T. and S.J.F. developed concepts and designed experiments. E.Y.K. and M.K. isolated CTBs. S.K.T. isolated EVs, performed experiments, and collected data. B.S. performed mass spectrometry analyses. S.K.T. and J.F.R. performed statistical analyses. S.K.T. generated schematics. S.J.F. supervised this project.

Cytotrophoblasts produce extracellular vesicles

We isolated two populations of EVs from the conditioned medium of second trimester cytotrophoblasts (CTBs) by ultracentrifugation (Figure 2.1). Because the source was primary CTBs, the limited amount of material precluded additional purification steps, such as density gradient centrifugation and/or immuno-affinity isolation. We expected the 16,500 x g EV pellet to be enriched for microvesicles and the 100,000 x g EV pellet to be enriched for exosomes. Transmission electron microscopy (TEM) revealed that the 16,500 x g pellet was comprised of a heterogenous population that included larger, crenulated vesicles and smaller exosome-like EVs (Figure 2.2). They were a heterogenous population, with 61% under 150 nm. In contrast, the 100,000 x g pellet was enriched for vesicles with a cup-like morphology typical of exosomes (Figure 2.3). These EVs were mainly smaller EVs, with 86% under 150 nm. As microvesicles and exosomes overlap in size, this heterogeneity and overlap in vesicle size was expected for EVs isolated by ultracentrifugation.

Cytotrophoblast extracellular vesicles contain exosomal and placenta-specific markers

Initially, we used immunoblotting methods to compare the protein contents of 16,500 x g and 100,000 x g EVs to CTB lysates. With regard to exosomal markers, the tetraspanin CD9, was only detected in the 100,000 x g EVs (Figure 2.4), which were also enriched for the ESCRT-0 component, HRS (Figure 2.5), compared to the 16,500 x g fraction. This was consistent with the TEM results, reinforcing the conclusion that 100,000 x g pellet was enriched for exosomes and the 16,500 x g pellet was a heterogenous population that also contained these vesicles.

With regard to placenta-specific markers, we were interested in whether these EVs contained the human trophoblast-specific nonclassical MHC class I molecule, HLA-G (McMaster *et al.*, 1995). As expected, CTB lysates primarily expressed the monomeric form (Figure 2.6), which appeared as a diffuse band due to the complex glycosylation this protein carries

(McMaster *et al.*, 1998). The 16,500 x g EVs contained both the monomer and dimer, in an approximate ratio of 3:1. In comparison, the 100,000 x g EVs were significantly enriched for both forms of the molecule compared to the lysate and 16,500 x g EVs, which were present in an approximate ratio of 3:2. Importantly, dimerized HLA-G has a higher affinity for its receptors, LILRB1 and LILRB2, suggesting enhancement of inhibitory signaling (Shiroishi *et al.*, 2006). Placenta alkaline phosphatase (PLAP) had a similar expression pattern, with significant expression in the 100,000 x g EVs versus CTB lysate (Figure 2.7).

We looked for other molecules whose functions in exosomes are relevant to the biology of pregnancy. Placental EVs contained the ECM molecule, fibronectin (Figure 2.8), whose expression was 16-fold higher in 100,000 x g EVs compared to the 16,500 x g fraction. Previous studies show that the exosomal form of this molecule promotes migration speed in an autocrine manner (Sung *et al.*, 2015; Sung and Weaver, 2017). Exosomal PD-L1 suppresses T cell activation in cancer (Poggio *et al.*, 2019). As immune evasion is critical for cancer progression and pregnancy success, we asked whether CTB EVs contained this molecule. PD-L1 was detected in CTB lysate and both populations of vesicles (Figure 2.9), suggesting that these EVs have immune function.

Global proteomic analysis of cytotrophoblast extracellular vesicles

We performed mass spectrometry profiling of the protein contents of second trimester CTB EVs. We found 811 proteins in 16,500 x g EVs and 427 proteins in 100,000 x g EVs (Figure 2.10). Of those identified, 377 were components of both vesicle types, 434 were unique to the 16,500 x g fraction, and 50 were found only in the 100,000 x g pellet. More proteins may have been identified in the 16,500 x g sample due to EV heterogeneity or the larger size of the vesicles.

Multiple exosomal markers were detected in CTB EVs: CD9 and CD81 were identified in both vesicle types, whereas CD63, TSG101, and CD82 were only found in the 100,000 x g

fraction (Raposo and Stoorvogel, 2013). In both EV populations, we identified molecules with immune functions, including CD47, CD59, CD276, lactate dehydrogenase, and Galectin-3. Additionally, HLA-G was only detected in the 100,000 x g pellet, reflecting the enrichment of this molecule observed by immunoblot (Figure 2.6). Both EV types contained multiple proteasome subunits, which process antigens for peptide presentation by HLA molecules (Vigneron *et al.*, 2017), suggesting that this process might be occurring.

Both fractions had proteins involved in iron transport, such as HLA-H, transferrin receptor protein 1, and serotransferrin (Garrick, 2011; Pascolo *et al.*, 2005). We also detected proteins previously associated with placental EVs, such as retrotransposon-derived protein PEG10, endoglin, DPPIV, and trophoblast glycoprotein (Abed *et al.*, 2019; Alam *et al.*, 2018; Kandzija *et al.*, 2019; Tannetta *et al.*, 2013). Both vesicle types contained multiple CTB adhesion-related molecules: fibronectin; Eph family members; integrins α1, α5, α6, β1, and β4; and laminin subunits (Damsky and Fisher, 1998; Red-Horse *et al.*, 2005). In other systems, these molecules are critical for vesicles homing to target cells (Hoshino *et al.*, 2015). We also detected components of prostaglandin pathways, including 15-hydroxyprostaglandin dehydrogenase, prostaglandin E synthase 3, and prostaglandin F2 receptor negative regulator. Additionally, CTB EVs contained proteins with cancer functions that reflect placental processes: neuroblast differentiation associated protein AHNAK, present in both vesicle populations, promotes tumor migration, invasion, and EV release (Shankar *et al.*, 2010; Silva *et al.*, 2016), whereas glia-derived nexin, detected in the 100,000 x g fraction, mediates tumor vascular mimicry (Wagenblast *et al.*, 2015). Overall, the EV proteome contained a multitude of proteins with diverse functions.

The proteome of each vesicle type was matched to GO terms. Significance was greater for 16,500 x g pathways compared to that of 100,000 x g, likely due to the fact they contained approximately twice the number of proteins. The top biological processes that were represented by EV contents mainly fell into 3 categories: localization and transport, viral pathways, and

metabolism (Figure 2.11). Viral processes were likely represented due to many proteins in these pathways with membrane budding functions. Vesicle-mediated transport, antigen processing and presentation, and regulation of RNA stability were also represented.

Discussion

Here we characterize second trimester CTB EVs by TEM, immunoblot, and mass spectrometry. The 16,500 x g fraction was a heterogeneous population, while the 100,000 x g fraction was enriched for vesicles with the size and morphology of exosomes. Additionally, the 100,000 x g pellet was enriched for exosomal marker CD9, and both EV populations was enriched for placental markers HLA-G and PLAP. In terms of proteome profiling, we detected a multitude of proteins with diverse functions in CTB EVs, including exosomal markers.

The interior of 100,000 x g EVs is a non-reducing environment, in which protein disulfide-isomerases catalyze formation of disulfide bonds and multimerization of molecules, which can enhance their activity (Bulleid and Ellgaard, 2011; Lynch *et al.*, 2009). As compared to the cytoplasm, these vesicles contain lower levels of glutathione, which prevents formation of these bonds (Lynch *et al.*, 2009). Other groups have found dimerized molecules in vesicles—a human EBV-transformed B cell line produces 100,000 x g EVs enriched for dimerized classical MHC class I molecules (Lynch *et al.*, 2009). Mouse neuraminidase 1-null myofibroblasts secrete exosomes containing TGF-β1 dimers (van de Vlekkert *et al.*, 2019). In the study described here, we detected multiple protein disulfide-isomerases in both CTB EV types by mass spectrometry, suggesting that they promote dimerization of vesicular proteins. Immunoblotting for HLA-G demonstrated that CTB EVs are enriched for a reactive band consistent in size with the dimeric form of this molecule (Figure 2.6). Dimerization of this CTB MHC class I molecule increases its affinity for the inhibitory receptor LILRB1 and LILRB2 and, consequently, its signaling strength (Boyson *et al.*, 2002; Kovats *et al.*, 1990; Shiroishi *et al.*, 2006; Yelavarthi *et al.*, 1991).

Furthermore, CTB HLA-G is heavily glycosylated with polylactosamine chains, which are composed of N-acetylglucosamine-galactose dimers (McMaster *et al.*, 1998). These residues are recognized by CD206, an inhibitory mannose receptor present on decidual macrophages (Co *et al.*, 2013). An individual and a first trimester placenta homozygous for a null mutant allele for HLA-G have been reported, suggesting that this MHC class I molecule is not essential for reproduction (Ober *et al.*, 1998). However, other mutations in the promoter and untranslated 3' regions of HLA-G are associated with negative pregnancy outcomes, such as miscarriage rates and preeclampsia (Ober *et al.*, 2003; Yie *et al.*, 2008). Thus, CTB EV expression of dimeric HLA-G may be one of many mechanisms that contribute to maternal tolerance to the fetus.

Materials & Methods

Tissue collection

The University of California, San Francisco (UCSF) Institutional Review Board approved this study. All donors gave informed consent. Second trimester placentas were collected immediately following elective terminations and placed in cytowash medium, containing DME/H-21, 12.5% fetal bovine serum (Hyclone), 1% glutamine plus, 1% penicillin and streptomycin, and 0.1% gentamicin. Tissue samples were placed on ice prior to dissection.

Isolation and culture of human primary cytotrophoblasts

CTBs were isolated from second trimester human placentas as previously described (Hunkapiller and Fisher, 2008). Single cells were counted using a hemocytometer and immediately plated on Matrigel (BD Biosciences)-coated 6-well plates in 1.5 ml serum-free medium containing DME/H-21, 2% Nutridoma-SP (Roche), 1% sodium pyruvate, 1% HEPES buffer, 1% glutamine plus (Atlanta Biologicals), 1% penicillin and streptomycin, and 0.1% gentamicin. CTBs were cultured at a density between $8x10^5$ and $1.5x10^6$ cells/well. CTBs were incubated at 37°C in 5% CO_2, 95% air. After 1 h, the medium with unattached immune and

other cells was removed and replaced with another 3 ml serum-free medium before returning the cells to the incubator.

Isolation of extracellular vesicles

EVs were isolated by differential centrifugation at 4°C by using published methods (Thery *et al.*, 2006). After culturing for 36-38 h, conditioned medium was centrifuged at 400 x g for 5 min to pellet the cells. The supernatant was sequentially centrifuged at 2,000 x g and 16,500 x g*,* each for 20 min. The liquid fraction was passed through a 0.22 µm filter prior to ultracentrifugation at 100,000 x g for 70 min. The supernatant was removed by aspiration. The 16,500 x g and 100,000 x g pellets were resuspended in 35 ml phosphate buffered saline (PBS) and re-centrifuged under the original conditions with which they were collected. The pellet was isolated by aspiration of the liquid phase. Typically, 5 µl were aliquoted to determine the protein concentration and the remaining 70 µl were used in experiments. Both aliquots were stored at -80°C. Samples for protein determinations were lysed in an equivalent volume of buffer containing 100 mM ammonium bicarbonate and 0.2% SDS. Quantitation was accomplished by using a Micro BCA Protein Assay kit (Thermo Scientific Pierce).

Transmission electron microscopy

Transmission electron microscopy (TEM) was performed as previously described (Thery *et al.*, 2006). In brief, EVs were adsorbed onto a glow discharged 400 mesh Formvar-coated copper grid (Electron Microscopy Sciences) for 1 min. Samples were negatively stained by dipping four times in 1% aqueous uranyl acetate. Excess liquid was blotted with filter paper. Grids were air dried and imaged in a Tecnai 12 transmission electron microscope (Field Electron and Ion Company). EV diameter was measured using ImageJ.

Immunoblotting

EVs or cell lysates were lysed as described above. For all targets, 2 µg protein was dissolved under non-reducing conditions with NuPAGE LDS Sample Buffer (Invitrogen). Samples were boiled for 10 min, separated on a NuPAGE 4-12% Bis-Tris gel (Invitrogen), and

transferred to a 0.45 µm nitrocellulose membrane (Bio-Rad). Blocking was accomplished with 5% powdered nonfat dry milk reconstituted in PBS-T (0.1% Tween in PBS). Membranes were incubated in primary antibody diluted in blocking buffer at 4°C overnight. The isotype, dilution, and source for each of the primary and secondary antibodies are summarized in Table 2.1. Immunoreactive bands were visualized with ECL2 Western blotting substrate (Thermo Scientific Pierce) and Amersham Hyperfilm ECL (GE Healthcare).

Proteomics

EV samples were lysed as described above. Lysates were prepared that contained a minimum of 25 µg protein, sometimes achieved by pooling samples. Samples were reduced with tris(2-carboxyethyl) phosphine hydrochloride (TCEP) added to a final concentration of 5 mM in lysis buffer at 60°C for 1 h and immediately alkylated with freshly prepared iodoacetamide (IAA) at a final concentration of 10 mM for 15 min at room temperature. Digestion was performed by incubating samples overnight with 3 µg sequencing grade trypsin (Promega) at 37°C. SDS was removed with 2 ml Detergent Removal Columns (Pierce).

Sequential Window Acquisition of All Theoretical Mass Spectra (SWATH-MS) was performed as previously described (Collins *et al.*, 2017). Peptides were separated by reversed phase nanoLC (Sciex) immediately followed by mass spectrometry analysis on a TripleTOF 5600 (Sciex) using data-independent acquisition.

Proteins were identified and quantified using Spectronaut and the pan-human spectral library. Redundancies were collapsed according to number of total peptides. We used DAVID to perform functional enrichment of Gene Ontology (GO) Biological Processes (Level 4) of the EV proteomes as defined by gene symbols (Huang *et al.*, 2007).

Statistics

Statistical analyses were performed using SPSs version 24 (IBM). Immunoblot densitometry measurements were analyzed using a one-way ANOVA with Dunnett's test.

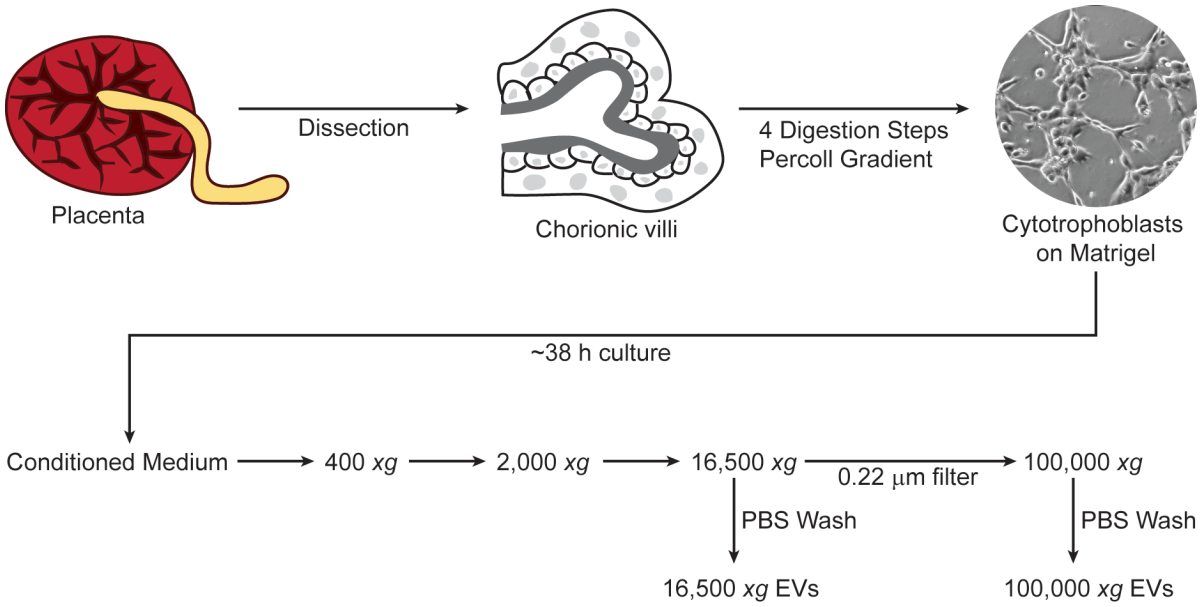

Figure 2.1 Schematic of primary human cytotrophoblast (CTB) and EV isolation

Each placenta was mechanically dissected into chorionic villi. Cells were separated from the tissue by 4 enzymatic digestion steps. A Percoll density gradient enriched for CTBs, which were plated on Matrigel in a 6-well plate with serum-free medium. Medium was changed after 1 h to remove dead or non-adherent cells. After ~38 h cell culture, the conditioned medium was removed for EV isolation by differential (ultra)centrifugation. Dead cells were pelleted at 400 x g. The supernatant was centrifuged at 2000 x g to remove apoptotic bodies. EVs were pelleted from the supernatant at 16,500 x g. After filtering with a 0.22 μm filter, the supernatant was ultracentrifuged at 100,000 x g to collect another population of EVs. Both sets of vesicles were resuspended in PBS and re-pelleted at the original isolation speeds.

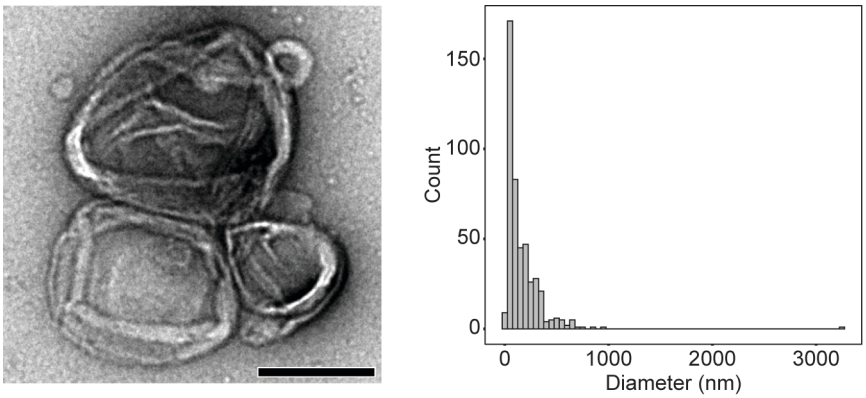

Figure 2.2 TEM of the CTB 16,500 x g pellet revealed a heterogenous vesicle population.

Transmission electron microscopy (TEM) of the 16,500 x g fraction demonstrated that they are a heterogeneous population comprised of a heterogenous population that included larger, crenulated vesicles and smaller exosome-like EVs (left panel; scale bar = 200 nm). A histogram of CTB 16,500 x g EV sizes showed a range of sizes, with most vesicles (61%) under 150 nm (right panel). n=3 biological replicates, 2 independent experiments.

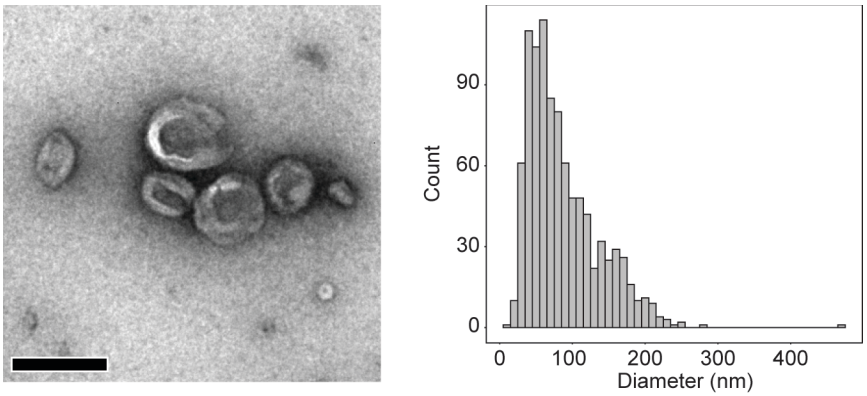

Figure 2.3 The CTB 100,000 x g fraction was enriched for EVs with exosomal size and morphology by TEM.

TEM revealed that the 100,000 x g pellet was enriched for vesicles with a cup-like morphology typical of exosomes (left panel; scale bar = 200 nm). A histogram of this fraction showed that it was composed of mainly smaller EVs, with the majority (86%) under 150 nm (right panel). n=3 biological replicates, 2 independent experiments.

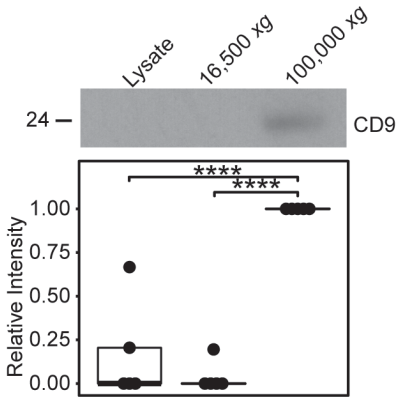

Figure 2.4 CTB 100,000 x g EVs were enriched for CD9.

Immunoblots comparing CTB lysate, 16,500 x g EVs, and 100,000 x g EVs were stained for the exosomal marker CD9. A representative blot is shown. Relative intensity was measured by densitometry. The 100,000 x g fraction was enriched for CD9. n=5 biologic replicates, each performed independently. **** $p<0.001$.

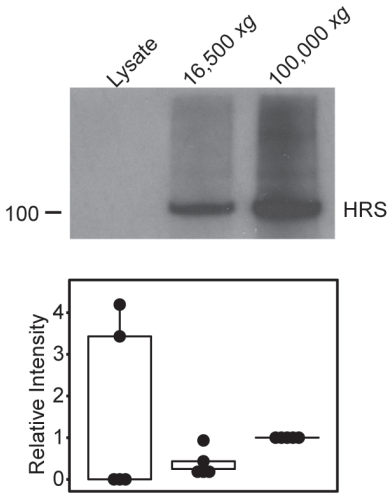

Figure 2.5 CTB EVs contained HRS.

Immunoblots comparing CTB lysate, 16,500 x g EVs, and 100,000 x g EVs were stained for the ESCRT-0 component HRS. A representative blot is shown. Relative intensity was measured by densitometry. n=5 biologic replicates, each performed independently. No significant difference in expression was calculated.

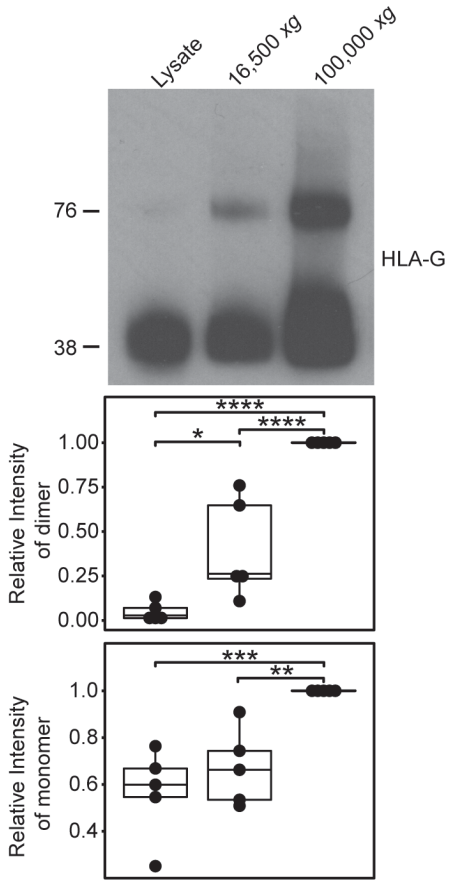

Figure 2.6 CTB 100,000 x g EVs were enriched for monomeric and dimeric HLA-G.

Immunoblots comparing CTB lysate, 16,500 x g EVs, and 100,000 x g EVs were stained for HLA-G, a CTB marker. Two bands were detected, consistent in size with the monomeric and dimeric forms of the molecule. A representative blot is shown. Relative intensities were measured by densitometry. The 16,500 x g pellet was enriched for the dimer compared to cell lysate. The 100,000 x g fraction was enriched for both forms of the molecule. n=5 biologic replicates, each performed independently. * $p<0.05$, ** $p<0.01$, *** $p<0.005$, **** $p<0.001$.

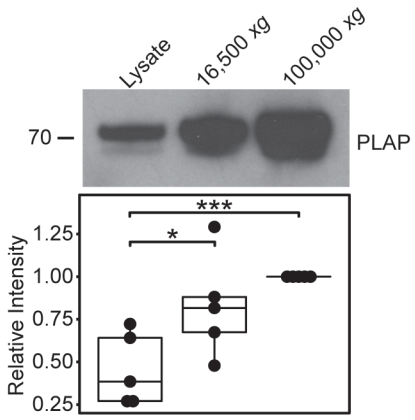

Figure 2.7 CTB EVs were enriched for placental alkaline phosphatase (PLAP).

Immunoblots comparing CTB lysate, 16,500 x g EVs, and 100,000 x g EVs were stained for the placental marker PLAP. A representative blot is shown. Relative intensity was measured by densitometry. Both EV populations were enriched for PLAP. n=5 biologic replicates, each performed independently. * $p<0.05$, *** $p<0.005$.

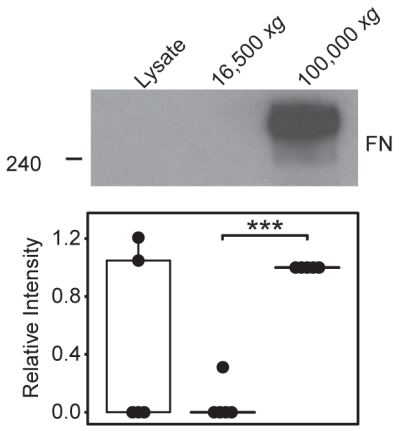

Figure 2.8 CTB 100,000 x g EVs were enriched for fibronectin (FN) compared to the 16,500 x g fraction.

Immunoblots comparing CTB lysate, 16,500 x g EVs, and 100,000 x g EVs were stained for FN. A representative blot is shown. Relative intensity was measured by densitometry. The 100,000 x g fraction was enriched for FN compared the 16,500 x g pellet. n=5 biologic replicates, each performed independently. *** $p<0.005$.

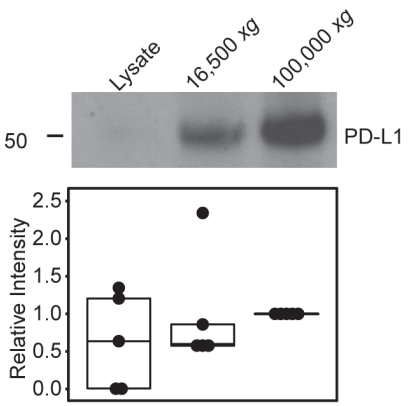

Figure 2.9 CTB EVs contained PD-L1.

Immunoblots comparing CTB lysate, 16,500 x g EVs, and 100,000 x g EVs were immunostained for PD-L1. A representative blot is shown. Relative intensity was measured by densitometry. PD-L1 was detected in CTB EVs. n=5 biologic replicates, each performed independently.

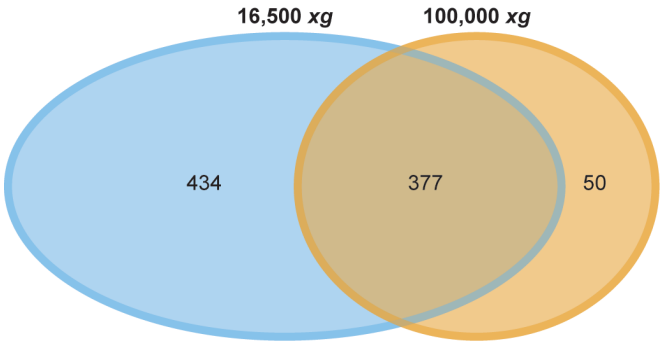

Figure 2.10 Venn diagram of proteins identified by mass spectrometry profiling showed that CTB EV contents overlapped.

Mass spectrometry profiling detected 811 proteins in CTB 16,500 x g EVs and 427 proteins in CTB 100,000 x g EVs. Of the identified proteins, 377 were shared between both populations, 434 were unique to the 16,500 x g pellet, and 50 were only found in the 100,000 x g fraction.

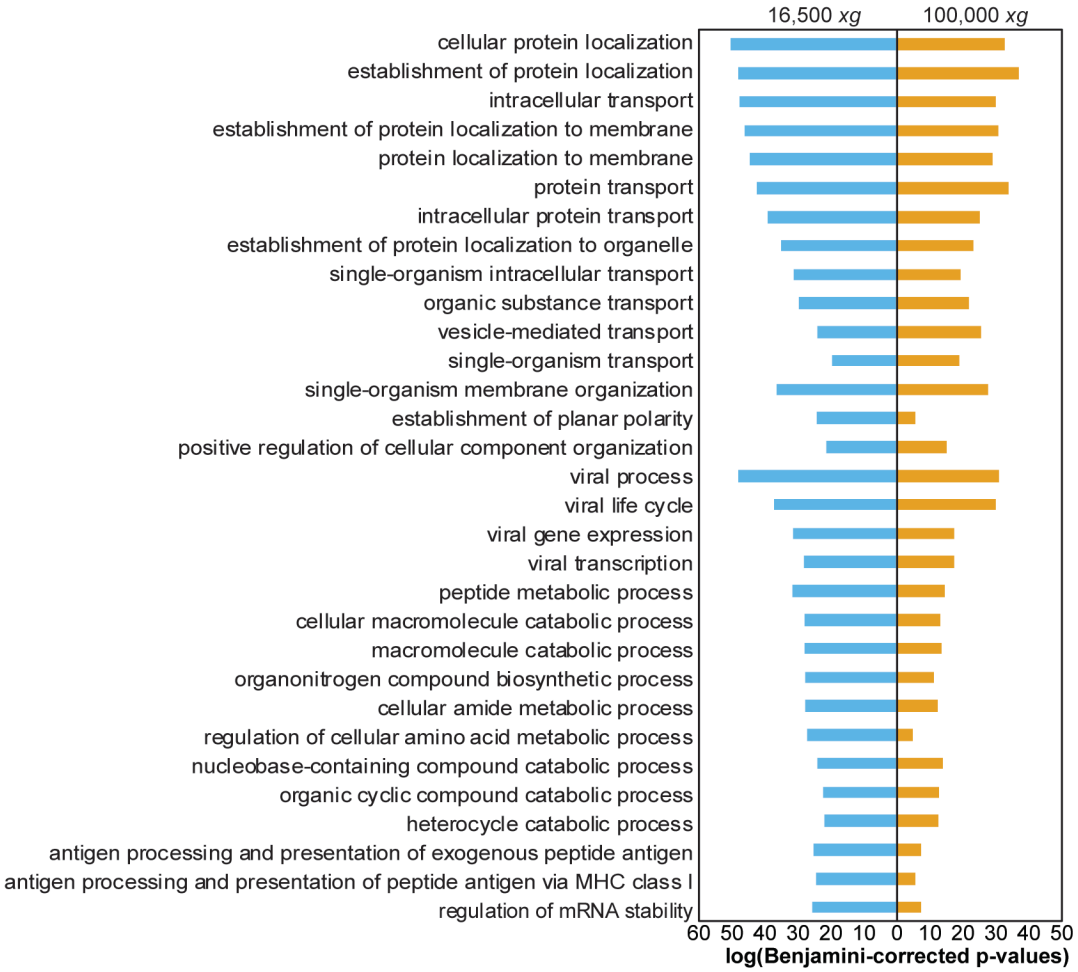

Figure 2.11 CTB EV proteomes were enriched for proteins in a variety of GO Biological Processes.

The proteome of each vesicle type was matched to GO terms. The most significant 25 Biological Processes for each EV type are presented here and mainly fell into 3 categories: localization and transport, viral pathways, and metabolism. Cellular organization, antigen processing and presentation, and regulation of RNA stability were also represented.

Table 2.1 Antibodies for immunoblotting

Primary Antibodies						Secondary Antibodies			
Target	**Clone**	**Supplier**	**Catalog #**	**Host**	**Dilution**	**Antibody**	**Conjugate**	**Supplier**	**Dilution**
CD9	KMC8	BD Biosciences	BDB553758	rat	1:250	Donkey anti-rat	Peroxidase	Jackson ImmunoResearch Labs, Inc.	1:5000
FN	Clone 10/ Fibronectin	BD Biosciences	610077	mouse	1:1000	Donkey anti-mouse	Peroxidase	Jackson ImmunoResearch Labs, Inc.	1:5000
HLA-G	4H84	Laboratory of S.J. Fisher	N/A	mouse	1:250	Donkey anti-mouse	Peroxidase	Jackson ImmunoResearch Labs, Inc.	1:5000
HRS	D7T5N	Cell Signaling Technology	15087	rabbit	1:1000	Donkey anti-rabbit	Peroxidase	Jackson ImmunoResearch Labs, Inc.	1:5000
PD-L1	E1L3N	Cell Signaling Technology	13684	rabbit	1:1000	Donkey anti-rabbit	Peroxidase	Jackson ImmunoResearch Labs, Inc.	1:5000
PLAP	EPR6141	Millipore Sigma	MABC644	rabbit	1:750	Donkey anti-rabbit	Peroxidase	Jackson ImmunoResearch Labs, Inc.	1:5000

Chapter 3: Cytotrophoblast extracellular vesicles increase decidual cell secretion of immune modulators via TNF-α

Sara K. Taylor[1,2,3], Sahar Houshdaran[1,2], Joshua F. Robinson[1,2,3,] Elaine Y. Kwan[2], Mirhan Kapidzic[1,2,3], Linda C. Giudice[2], Susan J. Fisher[1,2,3,4,5,6]

1. Center for Reproductive Sciences, University of California, San Francisco, California 94143
2. Department of Obstetrics, Gynecology, and Reproductive Sciences, University of California, San Francisco, California 94143
3. Eli and Edythe Broad Center for Regeneration Medicine and Stem Cell Research, University of California, San Francisco, California 94143
4. Division of Maternal Fetal Medicine, University of California, San Francisco, California 94143
5. Department of Anatomy, University of California, San Francisco, California 94143
6. Human Embryonic Stem Cell Program, University of California, San Francisco, California 94143

Author Contributions:

S.K.T., S.H., L.C.G., and S.J.F. developed concepts and designed experiments. E.Y.K. and M.K. isolated CTBs. E.Y.K. performed immunofluorescence experiments. S.K.T. isolated EVs. S.H. and S.K.T. cultured endometrial cells. S.K.T. performed EV functional experiments and collected data. S.K.T. and J.F.R. performed statistical analyses. S.K.T. generated schematics.

Cytotrophoblast 100,000 x g extracellular vesicles contain TNF-α

Given that proteins with immune functions were represented in CTB EVs, we performed a cytokine array (Luminex High Sensitivity T Cell panel) to identify cargo that may be present at biologically active concentrations too low to be detected by mass spectrometry. In these experiments, we compared the contents of CTB 16,500 x g and 100,000 x g EVs. As a control for placenta-specific vesicle functions, we included 100,000 x g EVs from the K562 erythroleukemic cell line, which have been shown to abundantly produce vesicles (Rivoltini *et al.*, 2016; Savina *et al.*, 2002). Most analytes were below the threshold of detection, but low levels of IL-6 (~0.2 pg/μg; $p<0.05$) and MIP-3a (~1 pg/μg; $p<0.001$) were detected in the 100,000 x g EV fraction (Figure 3.1). In contrast, only the CTB 100,000 x g EVs contained relatively high levels of TNF-α (~5 pg/μg protein; $p<0.001$; Figure 3.2).

To confirm this finding, we immunoblotted CTB EVs with anti-TNF-α. The 100,000 x g fraction had a band with an estimated molecular weight of 70 kDa (Figure 3.3), which was consistent with the trimeric membrane form of this molecule (Kriegler 1988; Tang, 1996). Previous studies have shown that this multimer has the highest activity (Tang, 1996). We also examined CTB TNF-α expression *in situ*. Immunolocalization at the maternal-fetal interface showed expression among cytokeratin-positive CTBs in both villous (data not shown) and invasive cells (Figure 3.4).

Cytotrophoblast extracellular vesicles induce decidual cell transcription and secretion of cytokines

Previous work showed CTB conditioned medium amplifies decidual cell expression and secretion of angiogenic and immune-modulating factors (Hess *et al.*, 2007). Specifically, gene ontology suggested the mechanism involved activation of the NF-κB cascade. The consequences included increased decidual cell secretion of downstream targets *CXCL1*/GRO1

and *CXCL8*/IL-8. Given that exosomal TNF-α activates NF-κB signaling in target cells, including fibroblasts and T cells (Zhang *et al.*, 2006), we asked whether TNF-α-containing CTB 100,000 x g EVs induced expression and secretion of NF-κB targets in decidualized endometrial stromal fibroblasts (dESFs) over a 24 h culture period (Figure 3.5). As in the cytokine analyses above, 100,000 x g EVs from the K562 cell line were used as a control.

Changes in gene expression were measured with a chip-based qRT-PCR method (Fluidigm). Of the target genes measured, 12 mRNAs were significantly upregulated by CTB 100,000 x g EVs compared to PBS over the course of the experiment with the most significant changes at 3 h (Figure 3.6). Upregulated genes included *CXCL8 (IL-8)*, *IL6, CXCL1 (GRO), CCL2 (MCP-1), CSF1, ICAM1, NFKB1, NFKB2, RELB, TNFAIP2*, and *TNFAIP3*, which are known targets of NF-κB activation (Anisowicz *et al.*, 1991; Brach *et al.*, 1991; Bren *et al.*, 2001; Hohensinner *et al.*, 2007; Kang *et al.*, 2007; Kunsch and Rosen, 1993; Libermann and Baltimore, 1990; Lombardi *et al.*, 1995; Son *et al.*, 2008; Ten *et al.*, 1992; Ueda *et al.*, 1994; van de Stolpe *et al.*, 1994; Zhou *et al.*, 2003). Compared to the PBS control, treatment with CTB 100,000 x g EVs increased mRNA levels of *CXCL8* by 4.8-fold (Figure 3.7), *IL6* by 2.8-fold (Figure 3.8), *CXCL1* by 5.2-fold (Figure 3.9), and *CCL2* by 5.4-fold (Figure 3.10) at the 3 h time point. CTB 16,500 x g EV treatment increased mRNA levels of *LIF* and most NF-κB targets upregulated by the 100,000 x g fraction at 3h. K562 100,000 x g EVs did not significantly change mRNA levels of target genes. Transcription returned to levels not significantly different from PBS control at 12 and 24 h.

We calculated that EVs in the above experiments contained ~10 pg of TNF-α based on the data shown in Figure 3.2. To determine whether this cytokine alone could recapitulate the effects of CTB 100,000 x g EVs, we treated dESFs with the recombinant version of this molecule (rhTNF-α) at an equivalent concentration and a 10-fold lower amount over the course of 24 h. A 10-fold higher concentration was omitted due to obvious cell death. The

transcriptional response was similar to that of CTB 100,000 x g EV treatment, but upregulation of NF-κB target genes was sustained at each time point (Figure 3.11). In particular, rhTNF-α increased mRNA levels of NF-κB targets *CXCL8* (Figure 3.12), *IL6* (Figure 3.13), *CXCL1* (Figure 3.14), *CCL2* (Figure 3.15), *CSF1, ICAM1, NFKB1, NFKB2, RELB, TNFAIP2, TNFAIP3, EGFR*, and *JUNB*. There was no significant difference between the two doses of rhTNF-α studied. Overall, the number, magnitude, and duration of transcriptional changes were greater in dESFs treated with an equivalent concentration of rhTNF-α compared to CTB EV treatment, likely because these vesicles contain other molecules that constrain the response to this cytokine.

To extend the RNA data, we performed a Luminex cytokine array for upregulated targets. Compared to PBS controls, CTB 100,000 x g EVs increased dESF secretion of a number of chemokines and cytokines. However, the kinetics were different for each analyte. Levels of CXCL8/IL-8 increased at each time point, with the most significant effects at 3 and 12 h (Figure 3.16). Similarly, CTB 100,000 x g EVs increased CXCL1/GRO secretion, particularly at 3 h (Figure 3.17). In contrast, their effects on CCL2/MCP-1 peaked at 12 h (Figure 3.18). EV-induced IL-6 secretion did not significantly change at any individual time point, but, in the aggregate, the EVs had a significant positive effect (Figure 3.19). Likewise, a generalized linear model showed that CTB 100,000 x g EVs increased dESF secretion of the other three factors over the 24-h course of the experiment ($p<0.001$).

Next, we asked whether the CTB 100,000 x g EV effects on dESFs were unique. Compared to the PBS control, CTB 16,500 x g EVs had a similar effect on dESF secretion of the chemokines and cytokines we analyzed. All four factors significantly increased over the course of the experiment by a generalized linear model. However, with the exception of CXCL1/GRO, the observed increases were smaller in magnitude and for the most part the kinetics differed (Figures 3.16-3.19). K562 100,000 x g EVs did not significantly increase

secretion of the four factors compared to PBS control treatment at any individual time point, but CXCL8/IL-8 secretion was increased over the course of the experiment as determined by the generalized linear model.

Finally, we asked if the addition of rhTNF-α at a concentration comparable to that of CTB 100,0000 *xg* EVs could mimic their effects at the protein level. Here, we focused on CXCL8/IL-8, the dESF chemokine with the most robust response to CTB EVs. The addition of rhTNF-α induced dESF secretion of CXCL8/IL-8 in a dose-dependent manner as measured by ELISA (Figure 3.20). This increase was much greater than that induced by the CTB 100,000 x g EV treatment, possibly because they contain other immunomodulatory contents that may constrain the inflammatory and angiogenic response to TNF-α.

TNF-α in cytotrophoblast 100,000 x g extracellular vesicles increases dESF IL-8 secretion

Since CTB 100,000 x g EVs contain TNF-α, we tested whether this cytokine is necessary for increased dESF secretion of NF-κB targets. Initially, we used neutralizing anti-TNF-α antibodies, but those experiments were unsuccessful (data not shown). The placenta is known to express a variety of Fc receptors, which bind to the Fc region of antibodies (Saji *et al.*, 1999; Simister *et al.*, 1996). Immunoblotting revealed that CTB 100,000 x g EVs are reactive with an antibody against the neonatal Fc receptor (FcRn) at a size consistent with the molecule (Figure 3.21)(Simister and Mostov, 1989).

As an alternative to neutralizing antibodies, we asked whether a soluble form of the TNF-α receptor TNFR1 (sTNFR1) could inhibit the effects of CTB 100,000 x g EVs on dESF IL-8 secretion (Figure 3.22). Because the vesicles were isolated from primary CTBs and their quantity was limited, we focused on the 12 h time point. CTB 100,000 x g EV treatment increased IL-8 secretion by 2.1-fold compared to PBS ($p<0.05$), whereas pre-incubating the

vesicles with sTNFR1 returned IL-8 secretion to baseline ($p<0.005$; Figure 3.23). Thus, the observed effects of CTB 100,000 x g EVs on dESF IL-8 secretion were attributable to TNF-α.

Discussion

Here, we investigate the function of CTB EVs in the uterus. We report the discovery of TNF-α in CTB 100,000 x g EVs. These vesicles increased decidual cell transcription and secretion of NF-κB target cytokines: CXCL8/IL-8, IL-6, CCL2/MCP-1, and CXCL1/GRO. However, not all targets upregulated by CTB-conditioned medium were significantly increased by EVs (Hess *et al.*, 2007). rhTNF-α mimicked the ability of EVs to enhance transcription of NF-κB target genes and secretion of IL-8. A soluble form of the TNF-α receptor inhibited the ability of CTB 100,000 x g EVs to increase dESF secretion of IL-8, linking TNF-α with decidual cell release of this molecule.

TNF-α was only detected in the 100,000 x g pellet, but both EV populations enhanced dESF transcription and secretion of NF-κB targets. Two possibilities could explain this discrepancy. First, the 16,500 x g pellet was a heterogenous population and many vesicles overlapped in size with the 100,000 x g fraction (Figures 2.2 and 2.3). It is possible that TNF-α was present in the 16,500 x g pellet at a concentration sufficient to drive NF-κB signaling but too low for detection by cytokine array. Second, stimuli other than TNF-α can activate the NF-κB pathway (Oeckinghaus and Ghosh, 2009). The 16,500 x g fraction could contain a different NF-κB activator. Additional experiments using sTNFRI to block TNF-α on 16,500 x g EVs may clarify whether the mechanism driving enhanced dESF transcription and secretion of NF-κB targets is the same between both EV populations.

Soluble TNF-α trimers are unstable at bioactive concentrations (Corti *et al.*, 1992). The trimeric form of the cytokine is stable at high concentrations, but at 3.12 ng/ml, half of the molecules dissociate into monomers after 72 h (Corti *et al.*, 1992). Packaging this molecule into

EVs may stabilize the molecule at low concentrations and allow for delivery with other immunomodulatory molecules.

TNF-α, CXCL8/IL-8, CCL2/MCP1, CXCL1/GRO, and their receptors are present at the maternal-fetal interface at early and mid-gestation in humans, bolstering the *in vivo* relevance of this study. Anti-TNF-α staining localizes to first and second trimester invasive and endovascular CTBs and decreases to only weak staining in spiral arteries at term (Pijnenborg *et al.*, 1998). *In situ* hybridization revealed that the decidual stroma uniformly expresses *CXCL1*/Gro-a, while *CCL2*/MCP-1 localizes strongly to isolated patches of these cells and at a lower level (Red-Horse *et al.*, 2001). In terms of receptors, CTBs immunostain with anti-CXCR1 (CXCL8/IL-8 receptor) by immunohistochemistry and variably express mRNAs for *CXCR2* (CXCL8/IL-8 and CXCL1/GRO-a receptor) and *CCR2* (CCL2/MCP-1 receptor), indicating that dESF cytokines may be part of a network of paracrine signals that can influence CTBs (Drake *et al.*, 2004; Hanna *et al.*, 2006). Decidual leukocytes express mRNAs for *CCR4* (CCL2/MCP-1 receptor) consistently and for *CXCR1* and *CXCR2* variably (Red-Horse *et al.*, 2001), suggesting a role for recruitment of immune cells to the maternal-fetal interface.

CTB EV-induced dESF cytokine secretion may play important roles in CTB migration and recruitment of immune cells to the decidua. IL-8 increases first trimester primary CTB migration, whereas MCP-1 has no effect (Hanna *et al.*, 2006). Another study found that IL-6 secreted by endometrial cells is partially responsible for promoting migration of trophoblast cell lines *in vitro* (Dominguez *et al.*, 2008). MCP-1 is a chemoattractant for monocytes, NK cells, and T cells (Allavena *et al.*, 1994; Carr *et al.*, 1994; Matsushima *et al.*, 1989; Valente *et al.*, 1988). Thus, the CTB EV-dESF interactions have effects on other types of cells that play important roles in pregnancy outcome.

Based on studies of the biological activities of CTB-conditioned medium, EVs likely have broader functional effects on the uterine environment. CTBs secrete factors that promote

lymphangiogenesis via a mechanism that partially depends on TNF-α (Red-Horse *et al.*, 2006). First trimester CTB-conditioned medium induces peripheral monocyte differentiation into macrophages and alters their ability to secrete cytokines (Aldo *et al.*, 2014). CTB secreted factors induce apoptosis of smooth muscle cells in spiral arteries via Fas ligand, a transmembrane protein that has been identified on CTB EVs (Abrahams *et al.*, 2004; Harris *et al.*, 2006). Thus, although we focused on the function of TNF-α in the context of CTB EVs, we believe that this molecule is one of many that can play important roles in modulation of the uterine environment, with possible systemic effects.

In the gray short-tailed opossum, a marsupial whose pregnancy is much shorter than eutherian mammals, trophoblast contact with the uterus is correlated with transcription of *TNF, IL6, CXCL8 (IL-8)*, and other cytokines, indicating conservation of an inflammatory response at implantation across mammalian species (Griffith *et al.*, 2017). However, inhibition of most cytokines does not prevent implantation in mice and humans, suggesting redundant pathways. Individual genetic deletions of *TNF, IL6, CXCL1 (GRO), or CCL2 (MCP-1)* result in fertile mice with normal litter sizes (Boisvert *et al.*, 2006; Lu *et al.*, 1998; Marino *et al.*, 1997; Pasparakis *et al.*, 1996; Robertson *et al.*, 2010). However, suppression of uterine NF-κB activity with an inhibitory subunit of the complex delays implantation by one day in mice (Nakamura *et al.*, 2004). TNF-α and IL-6 inhibitors are prescribed to treat human autoimmune disease, and women on these biologic therapies have live births. However, even transient treatment with TNF-α inhibitors during pregnancy may increase the risk of birth defects and preterm labor, but it is difficult to separate TNF-α effects and those of the underlying maternal disease (Johansen *et al.*, 2018). Data on IL-6 inhibition during pregnancy is more limited and drawn from smaller sample sizes. Results to date suggest an increased risk of preterm birth but not fetal anomalies (Hoeltzenbein *et al.*, 2016). Overall, these findings suggest redundant mechanisms;

simultaneous blockade of multiple cytokines may be required to negatively impact implantation and maintenance of pregnancy.

In addition to implantation, parturition is associated with an inflammatory response across species. Genetic deletion of *IL6* in mice results in a 24 h delay in delivery, which is restored to normal with administration of recombinant IL-6 (Robertson *et al.*, 2010). In humans, CXCL8/IL-8 is upregulated at parturition in the myometrium and the decidua, where it localizes to the stroma and may have a role in cervical dilation (Osmers *et al.*, 1995; Sakamoto *et al.*, 2004). Microarray analyses showed that labor increases term decidual expression of *TNFAIP3, IL6, NFKBIA*, and other NF-κB targets (Rinaldi *et al.*, 2017). Additionally, labor increases decidual expression of *CXCL8* while decreasing that of *CCL2* (El-Azzamy *et al.*, 2017). Thus, the ability of CTB EVs to modulate the expression of NF-κB targets across gestation could have important effects at many stages of pregnancy.

Pregnancy requires a balance between inflammatory and tolerizing mechanisms. How do TNF-α-containing CTB EVs avoid immune activation and pregnancy rejection? The NF-κB complex regulates hundreds of genes and it is unlikely that pregnancy affects every target (Cookson and Chapman, 2010). In mice, epigenetic silencing inhibits decidual stromal cell production of inflammatory chemokines CXCL9, CXCL10, and CCL5, thus preventing T cell accumulation in the uterus (Nancy *et al.*, 2012). A similar mechanism likely exists in humans that constrains the NF-κB response, but allows for the production of specific TNF-α-induced cytokines and chemokines.

Preeclampsia increases circulating levels of placental EVs (Germain *et al.*, 2007; Knight *et al.*, 1998; Lok *et al.*, 2008). Perfusion-derived STB EVs from preeclamptic and normal placentas differ in contents and function. For example, in preeclampsia, STB EVs contain increased levels of Flt-1 and the percentage of endoglin-containing vesicles decreases (Tannetta *et al.*, 2013). These anti-angiogenic molecules may contribute to the perturbation of

maternal vasculature responses that is the hallmark of this pregnancy complication (Tannetta *et al.*, 2013). These EVs also contain reduced levels of endothelial nitric oxide synthase and nitric oxide (Motta-Mejia *et al.*, 2017). Additionally, STB EVs have an increased ability to activate platelets (Tannetta *et al.*, 2015). Overall, it is unclear whether vesicles contribute to the pathology of the disease or are due to compensation by the placenta.

In this work, we identified CTB EV function in the uterus. Since CTBs are in direct contact with maternal blood, they likely secrete EVs into circulation to mediate pregnancy-associated changes throughout the mother's body. For example, many organs enlarge during pregnancy. Blood volume expands by almost 50% (Hytten, 1985). The liver increases in size to meet the enhanced demands of the embryo/fetus (Hollister *et al.*, 1987). In mice, pregnancy stimulates neurogenesis in the maternal olfactory bulb via a prolactin-mediated mechanism (Medina and Workman, 2018; Shingo *et al.*, 2003). Pregnant women develop insulin resistance, increasing glucose availability for the growing embryo/fetus and requiring the maternal pancreas to secrete higher levels of insulin (Lain and Catalano, 2007). The mechanism underlying pancreatic adaptation to pregnancy is unknown. Thus, placental EVs may play a role in a subset of these maternal responses to pregnancy. Additional studies will focus on a role for CTB EVs in mediating distant physiological changes required for reproductive success.

Materials & Methods

Placental tissue, CTB isolation and culture, and EV preparation

Tissue was collected, CTBs were isolated, and EVs were prepared as described in the Materials & Methods section of Chapter 2.

K562 cell culture

Erythroleukemic K562 cell cultures were seeded with $1x10^5$ cells per ml Iscove's Modified Dulbecco's Medium modified with 10% fetal bovine serum (FBS) and 1% penicillin and streptomycin. They were grown in 15 cm dishes at 37°C in 5% CO_2/95% air. For EV isolation,

K562 cells were pelleted at 400 x g and resuspended ($1x10^5$ cells/ml) in AIM-V serum-free medium (Gibco).

Profiling EV cytokines

To identify cytokine contents, 2 µg of EV protein was diluted to 1 ml with ESF medium containing 2% charcoal-stripped FBS, DMEM, insulin 0.5%, and MCDB 105 medium (Sigma-Aldrich). The samples were profiled with the MILLIPLEX $_{MAP}$ Human High Sensitivity T Cell Panel (Millipore, #HSTCMAG-28SK) on a Luminex LX 200 analyzer (Luminex) using Bio-Plex manager software 6.1.1 (Bio-Rad).

Immunoblotting and immunofluorescence

EVs or cell lysates were lysed as described in Chapter 2. For FcRn immunoblotting, 10 µg protein was solubilized in NuPAGE LDS Sample Buffer containing 0.1 M dithiothreitol (DTT). For TNF-α immunoblots, 10 ug protein was concentrated to near dryness with a CentriVap (LabConco) and reconstituted with 8 M urea buffer (pH 5.9). 1M DTT and 4x NuPAGE LDS Sample Buffer were added to final concentrations of 0.1 M and 1x, respectively. Samples were boiled for 10 min, separated on a NuPAGE 4-12% Bis-Tris gel (Invitrogen), and transferred to a 0.45 µm nitrocellulose membrane (Bio-Rad). Blocking was accomplished with 5% powdered nonfat dry milk reconstituted in PBS-T (0.1% Tween in phosphate buffered saline). Membranes were incubated in primary antibody diluted in blocking buffer at 4°C overnight. The isotype, dilution, and source for each of the primary and secondary antibodies is summarized in Table 3.1. Immunoreactive bands were visualized with ECL2 Western blotting substrate (Thermo Scientific Pierce) and Amersham Hyperfilm ECL (GE Healthcare).

Immunofluorescence was performed as previously described (Robinson *et al.*, 2017). Briefly, tissue was fixed in 4% paraformaldehyde and dehydrated by passing through sequential solutions containing increasing sucrose concentrations before embedding in OCT (Thermo Fisher Scientific). Sections (15 µm) were incubated with rat anti-human cytokeratin 7 (Damsky *et al.*, 1992) to label CTBs and mouse anti-human TNF-α diluted at 1:100 (vol/vol) in blocking

buffer (PBS with 3% bovine serum albumin) for 1 h at room temperature. Primary antibodies were detected with species-specific secondary antibodies; details on these antibodies and their sources are described in Table 3.2. Sections were washed in PBS and mounted with Vectashield containing 4′6-diamidino-2-phenylindole (Vector Bio-Laboratories). Samples were visualized with a Leica SP5 confocal microscope or a Leica DM5000 B inverted microscope. Tissue sections from 3 placentas were evaluated.

Endometrial stromal fibroblast culture and decidualization

Human endometrial samples were collected from the UCSF/NIH Human Endometrial Tissue and DNA Bank after written informed consent. Endometrial stromal fibroblasts (ESFs) were isolated from endometrial biopsies (n=20). They were washed in PBS and digested with collagenase IV for 1 h at 37ºC with constant shaking. The digests were size fractionated by passing through a 40 μm filter. The primary cells present in the filtrate and subsequent passages were cultured in stromal cell medium (SCM): 10% charcoal-stripped fetal bovine serum-containing medium, DMEM, 1 mM sodium pyruvate, 5 μg/ml final concentration insulin, and MCDB 105 (Irwin *et al.*, 1989). Only morphologically homogenous ESF cell cultures as determined by microscopic examination were used in experiments. Prior to decidualization, cultured ESFs were serum-starved for 24 h in 2% charcoal-stripped fetal bovine serum-containing medium without insulin. Then they were treated with 10 nM E2 and 1 μM P4 in ESF medium (E2P4 medium) or the vehicle control for 14-21 days (Houshdaran *et al.*, 2014). Decidualization was assessed by using an ELISA to quantify IGFBP1 secretion into the medium (Alpha Diagnostic International Inc., #0900) and by assessing microscopic examination to assess morphologic changes. The 3 ESF cell lines exhibiting the most robust decidualization were used in the initial screens. The subsequent functional assays also employed the same 3 ESF lines, which were frozen, thawed, and decidualized for each set of experiments.

EV effects on the ESF secretome and the role of TNF-α

The effects of EVs from 3 CTB cultures established from different placentas were analyzed. A portion of each EV fraction that was aliquoted in PBS was added to the hormone-containing ESF medium to a final concentration of 2 µg per ml. Typically, 10 ml batches were prepared. A portion (500 µl) was reserved as a control for downstream analyses and 1 ml was added to each decidualized ESF (dESF) well. The cells were cultured for 3, 12, or 24 h, at which point conditioned medium was collected and centrifuged at 400 x g. The supernatant was stored at -80ºC. The cells were washed with PBS, detached from the plate by treatment with 0.25% trypsin with EDTA in PBS (Ca^{++}/Mg^{++}-free), and pelleted by centrifugation at 400 x g. The pellets were flash frozen in a dry ice-ethanol slush and stored (-80ºC).

Samples of dESF RNA were prepared for analysis by a chip-based method of qRT-PCR using a 96.96 Dynamic Array integrated fluidic circuit (IFC; Fluidigm) according to the manufacturer's protocol. Total RNA was isolated from frozen cell pellets with a NucleoSpin RNA isolation kit (Machery-Nagel). The concentration and quality were estimated using a Nanodrop spectrophotometer (Thermo Fisher Scientific). cDNA libraries were prepared with 150 ng RNA using Reverse Transcription Master Mix (Fluidigm) and pre-amplified with Preamp Master Mix (Fluidigm) and pooled delta gene assay mix (500 nm; Fluidigm). The samples were digested with exonuclease I (New England BioLabs), and diluted 1:10 (vol/vol) in 1x DNA suspension buffer (TEKnova). Delta gene assay primer sequences are listed in Table 3.3. Samples were prepared with 2x SsoFast EvaGreen Supermix with low ROX (Bio-Rad) and 20x DNA Binding Dye (Fluidigm). Primer mixes contained 2x Assay Loading Reagent (Fluidigm), 1x DNA Suspension Buffer, and Delta gene assay combined forward and reverse primers (100 µM). After priming and loading the 96.96 chip using an IFC Controller HX (Fluidigm), qRT-PCR data were collected on a Biomark instrument (Fluidigm). Statistics were performed on dCt values calculated as the difference in Ct values between the gene of interest and the average of two housekeeping genes: *HSP90AB1* and *G6PD*. Differential expression between EV treatments

and controls was calculated via the ΔΔCT method: normalized to the mean of housekeeping genes and adjusted to the PBS control for each ESF line, EV batch, and time point.

We measured changes in dESF NF-κB target secretion in response to EV treatment using a custom MILLIPLEX $_{MAP}$ Human Cytokine/Chemokine Magnetic Bead Panel (Millipore, # HCYTOMAG-60K) to assay conditioned medium for IL-8 (CXCL8), IL-6, MCP-1 (CCL2), and GRO. These experiments employed a Luminex LX 200 analyzer (Luminex) and the data were generated by using Bio-Plex manager software 6.1.1 (Bio-Rad).

To determine the effects of recombinant human TNF-α (rhTNF-α), the lyophilized, *E. coli*-derived protein (R&D Systems, #210-TA) was reconstituted in PBS to a concentration of 0.1 mg/ml. This working solution was serially diluted to a final concentration of 1 pg/ml, 10 pg/ml, or 100 pg/ml in E2P4 medium. rhTNF-α-containing medium (1 ml) was added to each well of dESFs. As a control, some wells contained E2P4 medium alone. Conditioned medium and cell pellets for RNA isolation were collected after 3, 12, or 24 h of culture as described above.

IL-8 levels were measured with a Quantikine ELISA Kit (R&D Systems, #S8000C) according to manufacturer's instructions. Samples were diluted 1:20 in calibrator diluent RD5P. According to the manufacturer's instruction, a face mask was worn during the assay to prevent IL-8 contamination from saliva.

For TNF-α inhibition experiments, sTNFR1 (R&D Biosystems, #636-R1-025) was reconstituted in PBS. EVs diluted in E2P4 medium as described above were incubated with or without sTNFR1 (1 μg/ml) for 20 min at 37ºC. An aliquot (1 ml) was added to each dESF well. After 12 h, conditioned medium was collected as described above.

Statistics

Statistical analyses were performed using SPSs version 24 (IBM). The high sensitivity T cell cytokine array and mRNA data were analyzed using a one-way ANOVA with Bonferroni correction. The ESF cytokine array data at individual time points and the IL-8 ELISAs were

analyzed using a one-way ANOVA with Dunnett's test. We also generated a generalized linear model of cytokine secretion for the time course experiment with time, cell line, EV batch, and treatment as independent variables.

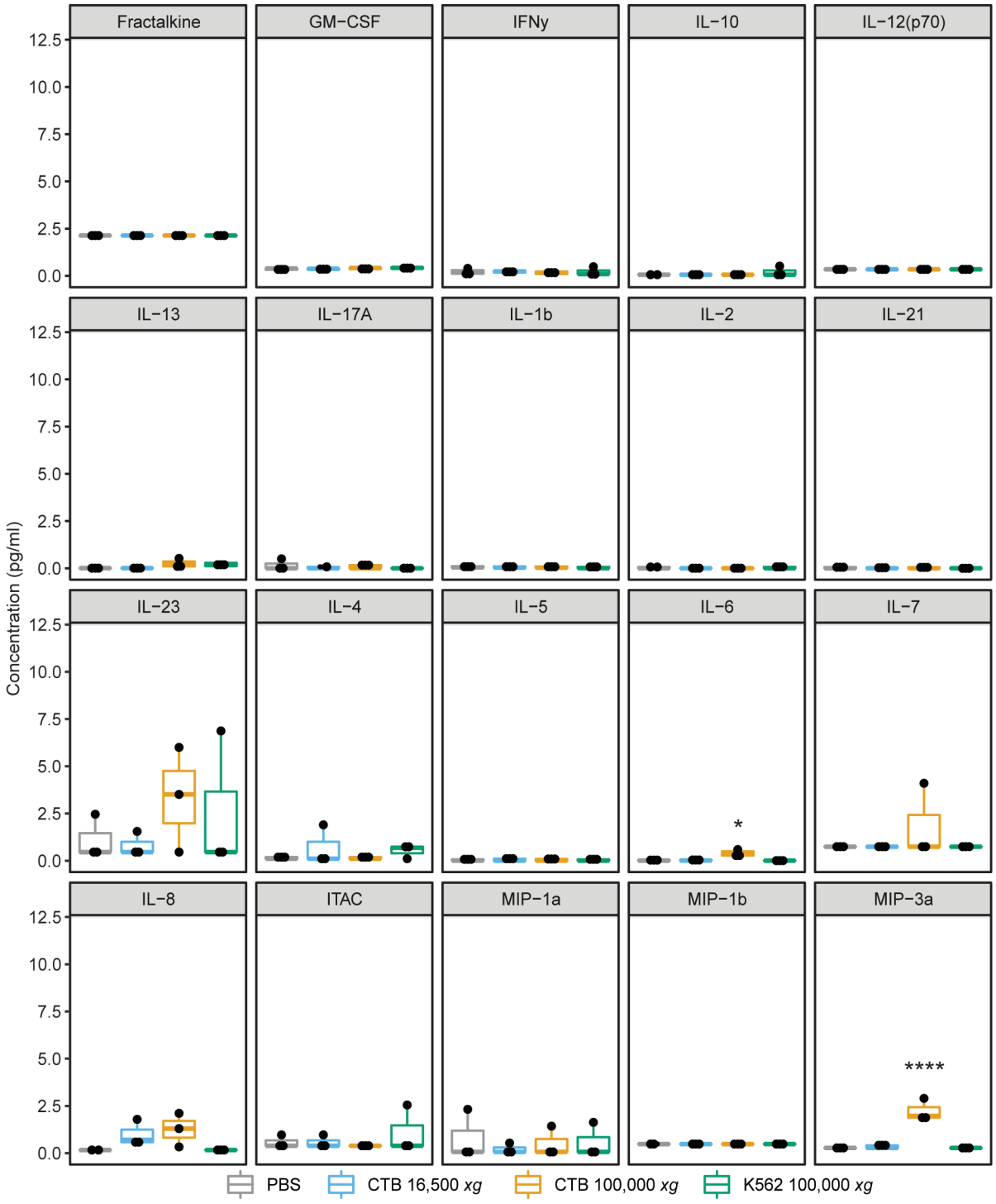

Figure 3.1 CTB EVs lacked detectable levels of most analytes measured by cytokine array.

EVs (2 µg) were analyzed by a high sensitivity cytokine array. Most analytes were below the threshold of detection. In the CTB 100,000 x g pellet, IL-6 was present at ~0.2 pg/µg and MIP-3a was detected at ~1 pg/µg. n=3 biological replicates. * $p<0.05$, **** $p<0.001$.

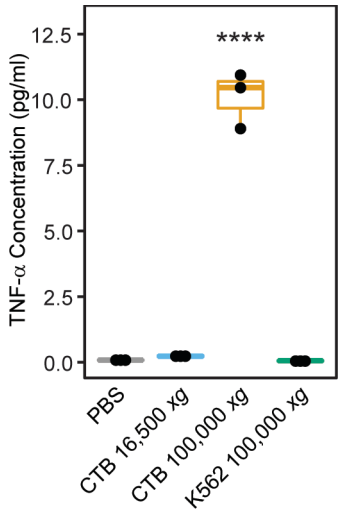

Figure 3.2 CTB 100,000 x g EVs contained TNF-α.

As measured by a high sensitivity cytokine array, CTB 100,000 x g EVs contained ~5 pg TNF-α per 1 µg total protein (10 pg per 2 µg protein). n=3 biological replicates. **** p<0.001.

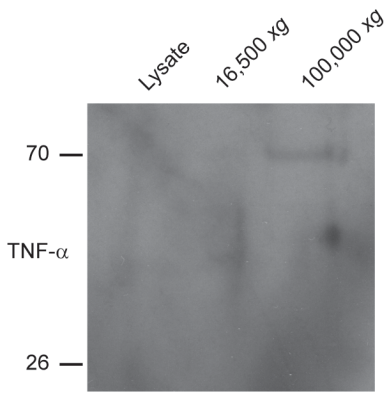

Figure 3.3 CTB EVs immunoblotted for anti-TNF-α at a size consistent with the trimeric membrane form.

Immunoblotting for TNF-α was used to compare CTB lysate, 16,500 x g EVs, and 100,000 x g EVs. The 100,000 x g fraction was immunoreactive for a faint band at ~70kDa, consistent in size with the trimeric membrane form of the cytokine. n=2.

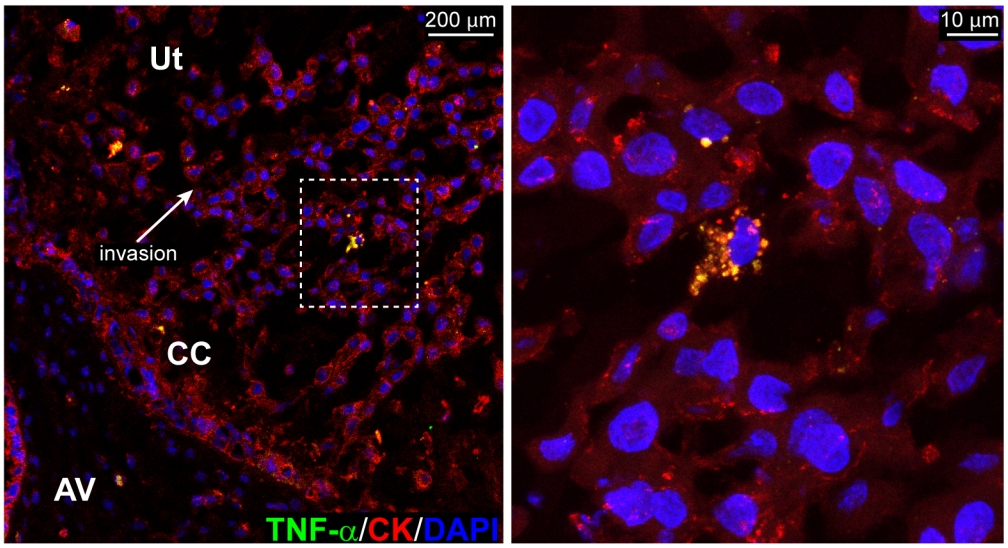

Figure 3.4 Cytokeratin-positive CTBs express TNF-α *in situ*.

Sections of basal plate were stained for CTB-marker cytokeratin (CK, red), TNF-α (green), and DAPI (blue), followed by imaging at 20x (left panel, scale=200 µm) and 63x (right panel, scale=10 µm). TNF-α was present in cytokeratin-positive CTBs in a vesicular pattern. n=3 biological replicates.

AV, anchoring villi; CC, cell column; Ut, uterus.

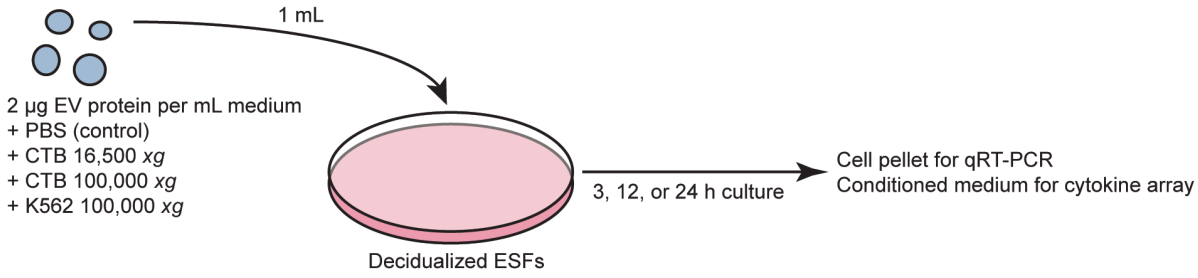

Figure 3.5 Schematic of functional assay of CTB EVs on decidualized endometrial stromal fibroblasts (dESFs).

Three sets of human primary dESFs were treated with three batches of CTB 16,500 x g EVs, CTB 100,000 x g EVs, K562 100,000 x g EVs or PBS. EVs were added to dESF medium to a final concentration of 2 µg/mL and 1 mL was added to each well. The cells were cultured 3, 12, or 24 h, at which point conditioned medium was collected for a cytokine array and cell pellets were harvested for RNA analysis.

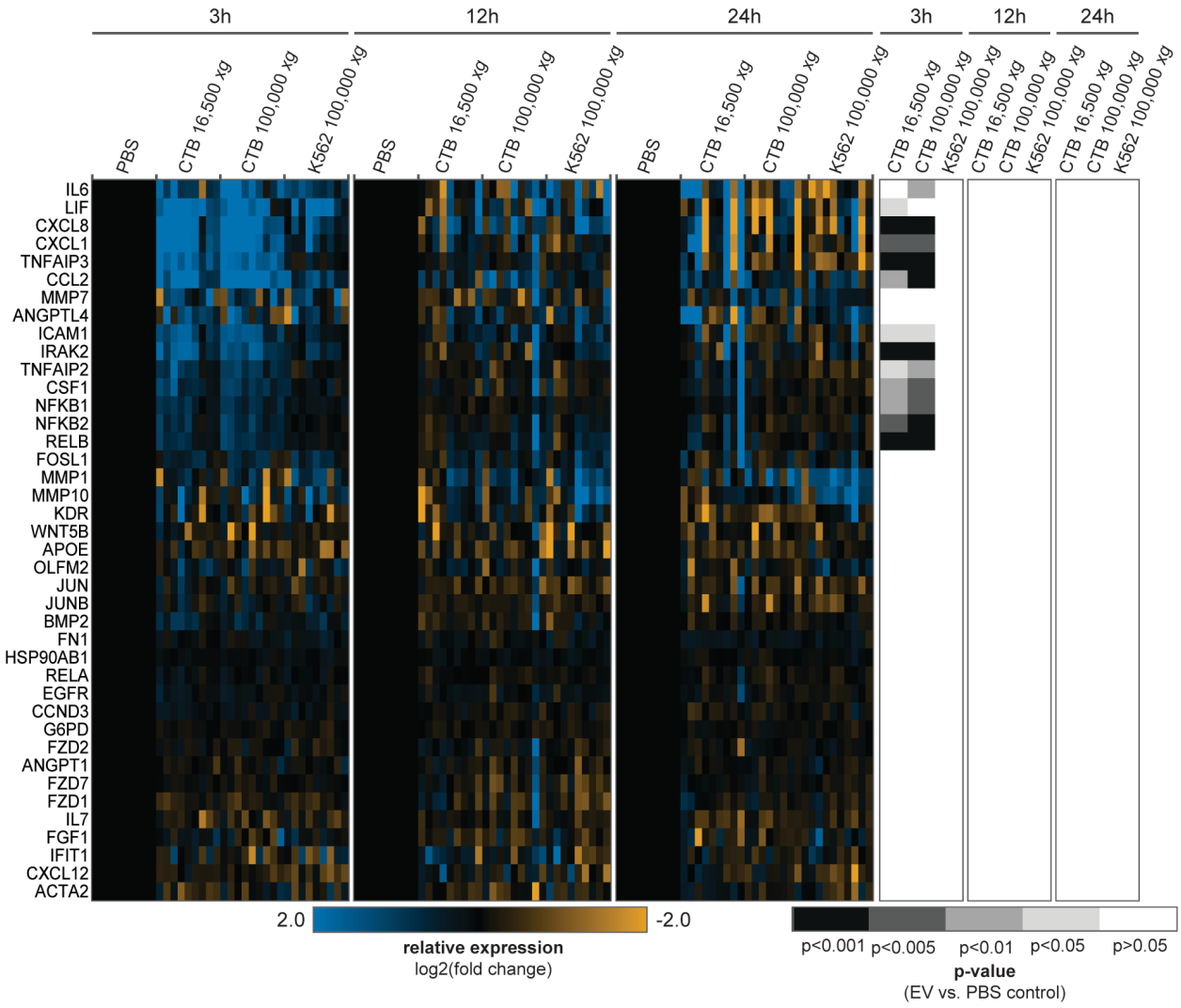

Figure 3.6 CTB EVs increased dESF transcription of NF-κB targets.

Heat maps of gene expression changes in dESFs as measured by a Fluidigm 96.96 Dynamic Array (left) and p-values compared to the PBS control (right). CTB EVs transiently increased transcription of NF-κB target genes at 3 h. n=3 biological replicates (each point is the result of a matrix of 3 dESF lines treated with 3 EV batches), each EV batch was performed as an independent experiment.

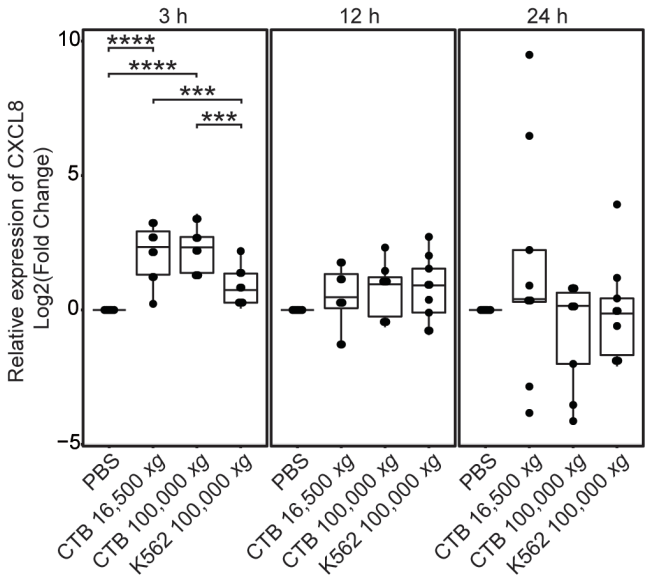

Figure 3.7 CTB EVs increased dESF transcription of NF-κB target *CXCL8*.

Both CTB EV populations increased dESF transcription of *CXCL8* (*IL-8*) at 3 h compared to both PBS and K562 100,000 x g EVs as measured by a Fluidigm 96.96 Dynamic Array IFC. There were no significant differences at 12 or 24 h. n=3 biological replicates (each point is the result of a matrix of 3 dESF lines treated with 3 EV batches), each EV batch was performed as an independent experiment. *** $p<0.005$, **** $p<0.001$.

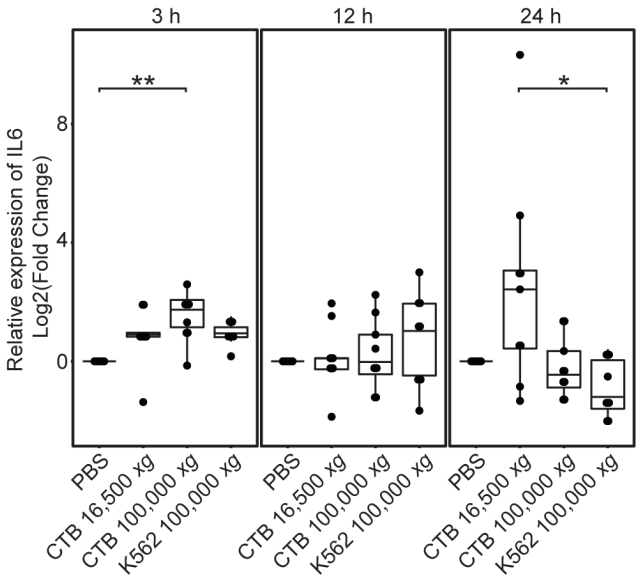

Figure 3.8 CTB 100,000 x g EVs increased dESF transcription of NF-κB target *IL6*.

Compared to PBS control, CTB 100,000 x g EVs increased dESF transcription of *IL6* at 3 h. CTB 16,500 x g EVs increased expression of this RNA at 24 h as measured by a Fluidigm 96.96 Dynamic Array IFC. n=3 biological replicates (each point is the result of a matrix of 3 dESF lines treated with 3 EV batches), each EV batch was performed as an independent experiment. * $p<0.05$, ** $p<0.01$.

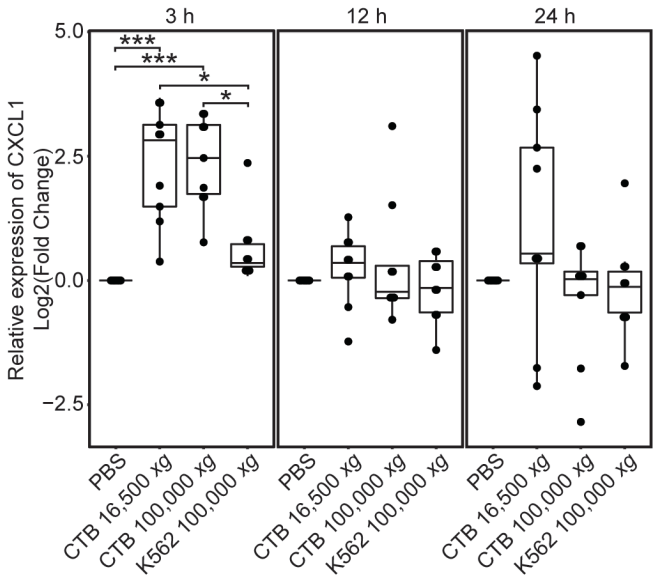

Figure 3.9 CTB EVs increased dESF transcription of NF-κB target *CXCL1*.

Both CTB EV fractions increased dESF transcription of *CXCL1* (GRO) at 3 h compared to the PBS and K562 100,000 x g controls as measured by a Fluidigm 96.96 Dynamic Array IFC. n=3 biological replicates (each point is the result of a matrix of 3 dESF lines treated with 3 EV batches), each EV batch was performed as an independent experiment. * $p<0.05$, *** $p<0.005$.

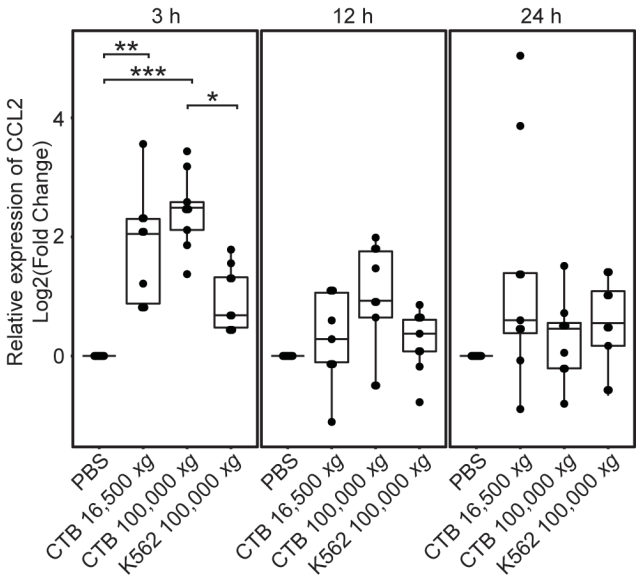

Figure 3.10 CTB EVs increased dESF transcription of NF-κB target *CCL2*.

CTB 100,000 x g EVs increased dESF transcription of *CCL2 (MCP-1)* at 3h compared to the PBS and K562 100,000 x g controls as measured by a Fluidigm 96.96 Dynamic Array IFC. CTB 16,500 x g EVs also increased expression of this gene compared to PBS at 3h. n=3 biological replicates (each point is the result of a matrix of 3 dESF lines treated with 3 EV batches), each EV batch was performed as an independent experiment. * $p<0.05$, ** $p<0.01$, *** $p<0.005$.

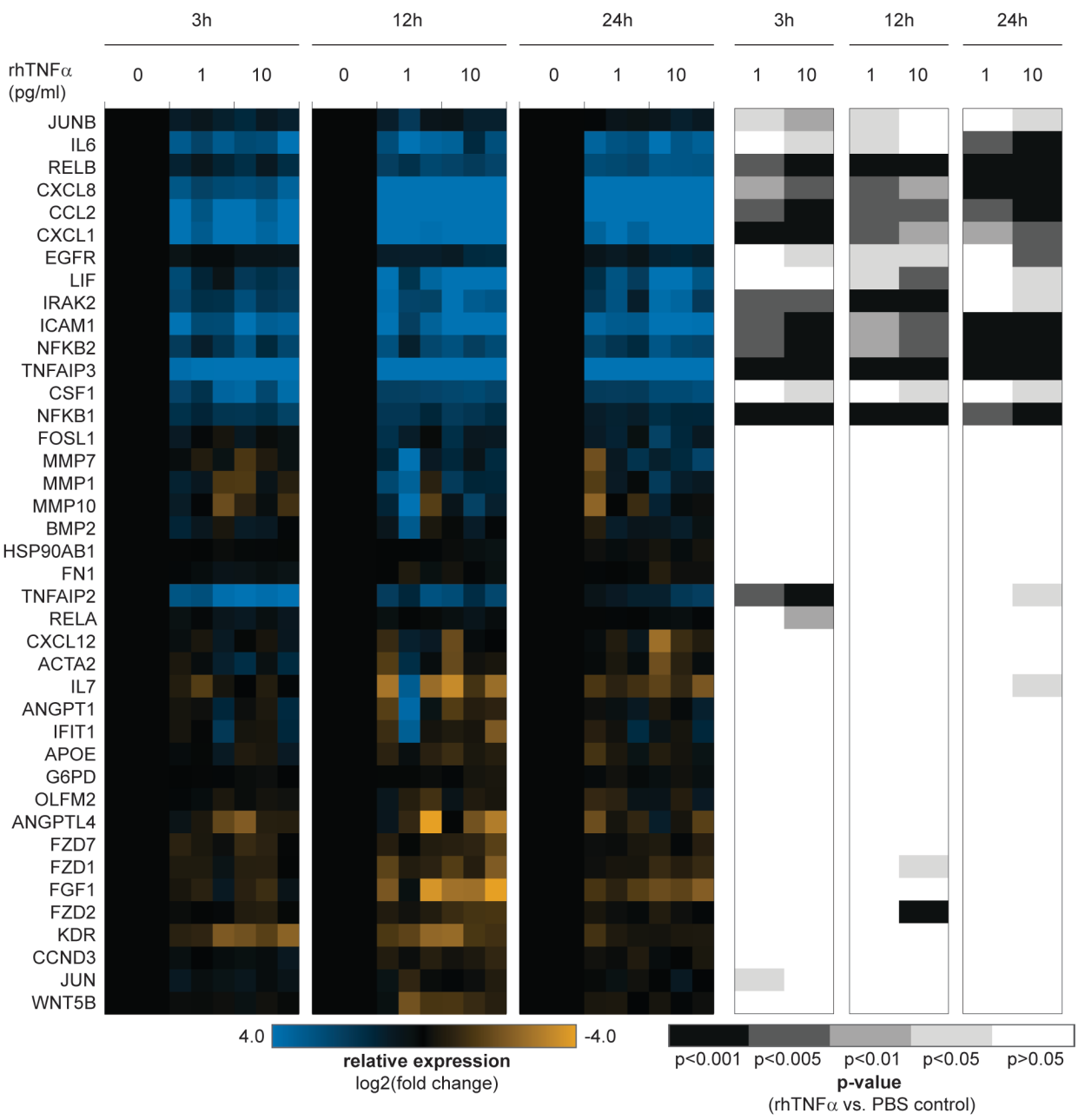

Figure 3.11 Recombinant human TNF-α (rhTNF-α) sustained increased dESF expression of NF-κB targets for the duration of the 24 h time course.

Heat maps of gene expression changes measured by Fluidigm 96.96 Dynamic Array IFC (left) and p-values (right) compared to PBS control. Treatment with rhTNF-α increased transcription of NF-κB targets that was sustained over the course of the experiment. n=3 biological replicates (dESFs), 2 independent experiments.

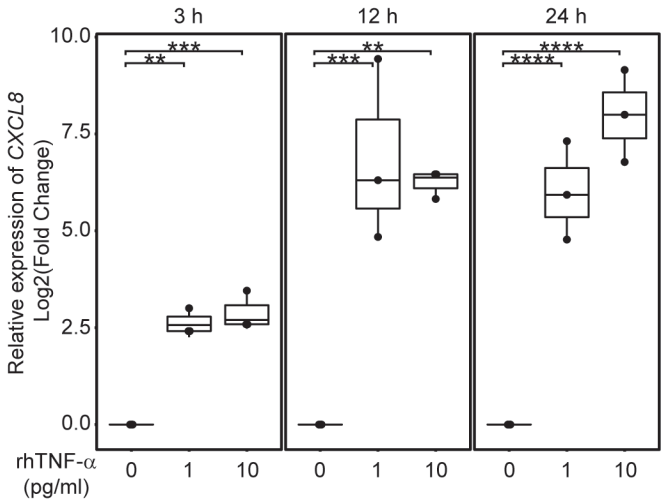

Figure 3.12 rhTNF-α increased dESF transcription of NF-κB target *CXCL8* over 24 h.

Compared to the PBS control, both concentrations of rhTNF-α (1 pg/ml and 10 pg/ml) increased transcription of *CXCL8 (IL-8)* at each time point studied as measured by a Fluidigm 96.96 Dynamic Array IFC. n=3 biological replicates (dESFs), 2 independent experiments. ** $p<0.01$, *** $p<0.005$, **** $p<0.001$.

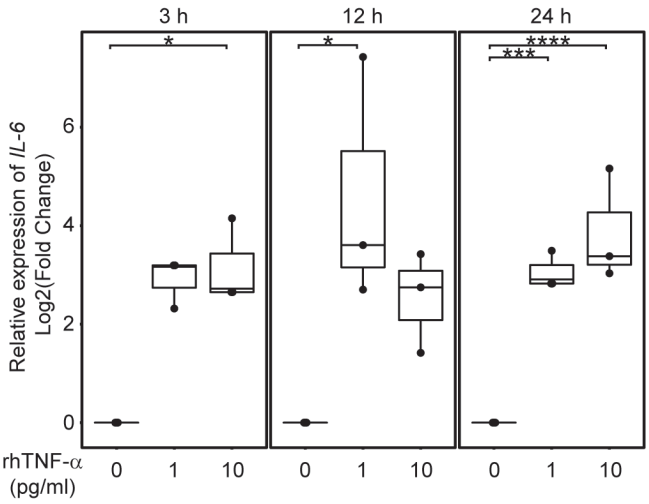

Figure 3.13 rhTNF-α increased dESF transcription of NF-κB target *IL6* over 24 h.

Both concentrations of rhTNF-α (1 pg/ml and 10 pg/ml) increased transcription of *IL6* compared to the PBS control. Changes in gene expression were measured with a Fluidigm 96.96 Dynamic Array IFC. n=3 biological replicates (dESFs), 2 independent experiments. * $p<0.05$, *** $p<0.005$, **** $p<0.001$.

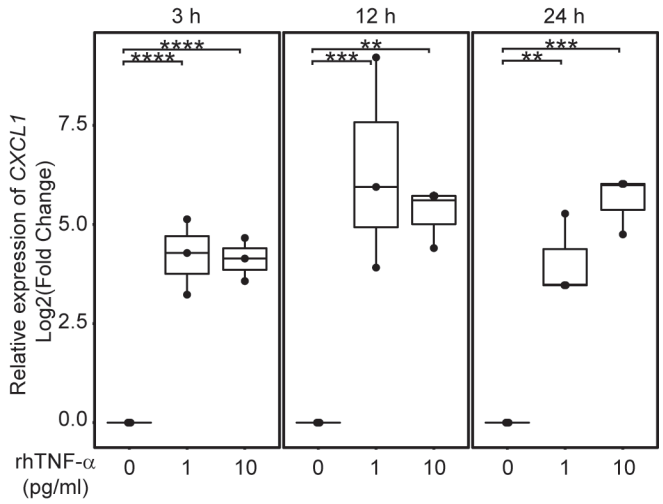

Figure 3.14 rhTNF-α increased dESF transcription of NF-κB target *CXCL1* over 24 h.

Compared to the PBS control, both concentrations of rhTNF-α (1 pg/ml and 10 pg/ml) increased RNA expression of *CXCL1* (*GRO*) at each time point studied as measured with a Fluidigm 96.96 Dynamic Array IFC. n=3 biological replicates (dESFs), 2 independent experiments. ** p<0.01, *** p<0.005, **** p<0.001.

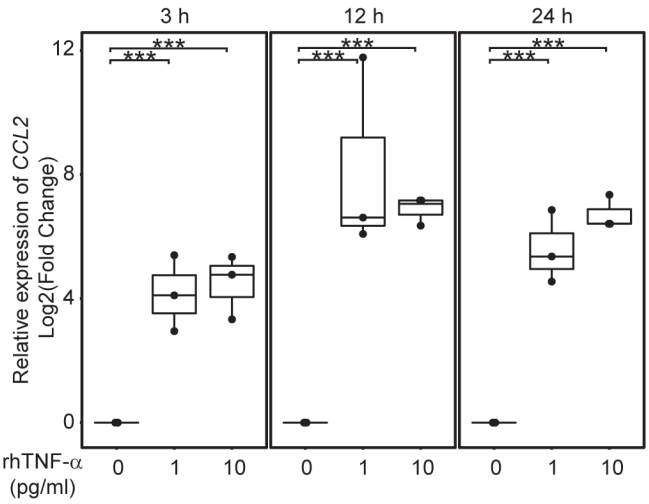

Figure 3.15 rhTNF-α increased dESF transcription of NF-κB target *CCL2* over 24 h.

Both concentrations of rhTNF-α (1 pg/ml and 10 pg/ml) increased transcription of *CCL2* (*MCP-1*) compared to the PBS control at each time point analyzed with a Fluidigm 96.96 Dynamic Array IFC. n=3 biological replicates (dESFs), 2 independent experiments. *** $p<0.005$.

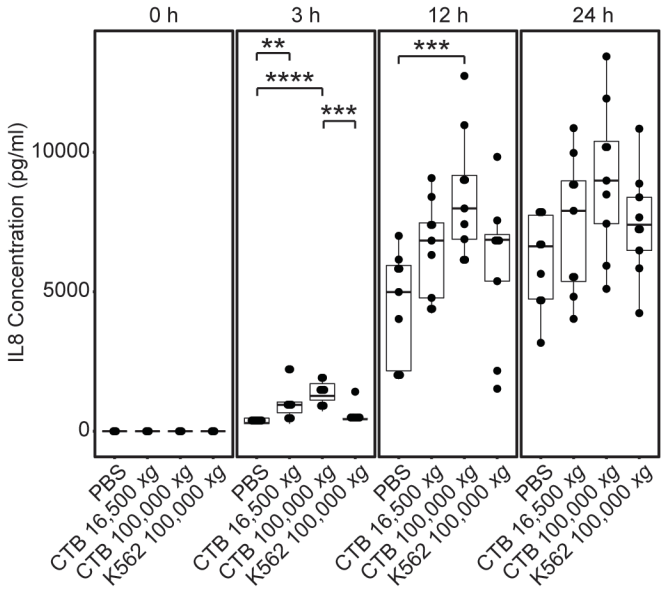

Figure 3.16 CTB 100,000 x g EVs increased secretion of NF-κB target CXCL8/IL-8.

Conditioned medium from primary dESF lines treated with CTB 100,000 x g EVs, CTB 16,500 x g EVs, K562 100,000 x g EVs, or PBS collected at 0, 3, 12, and 24 h was analyzed by cytokine array. CTB 100,000 x g EVs significantly increased dESF CXCL8/IL-8 secretion at 3 and 12 h and overall compared to the PBS control. CTB 16,500 x g vesicles significantly increased this cytokine at 3 h. n=3 biological replicates (each point is the result of a matrix of 3 dESF lines treated with 3 EV batches), EV batches were performed as independent experiments. ** $p<0.01$, *** $p<0.005$, **** $p<0.001$.

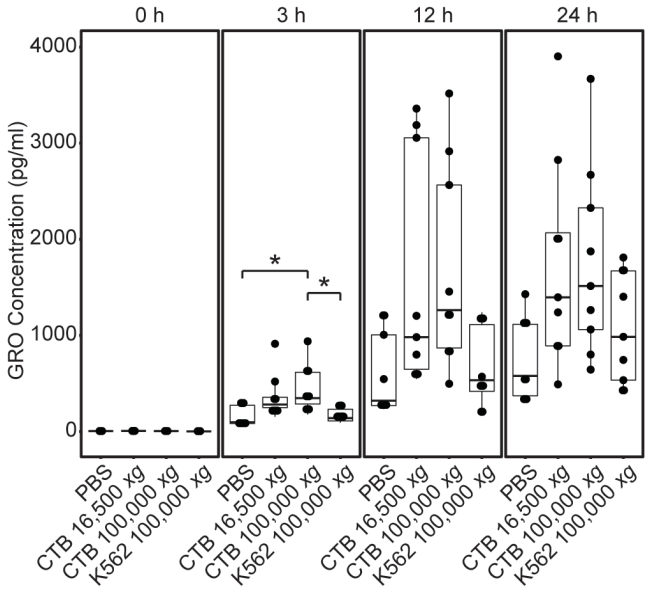

Figure 3.17 CTB 100,000 x g EVs increased secretion of NF-κB target CXCL1/GRO.

Conditioned medium from primary dESF lines treated with CTB 100,000 x g EVs, CTB 16,500 x g EVs, K562 100,000 x g EVs, or PBS collected at 0, 3, 12, and 24 h was analyzed by cytokine array. CTB 100,000 x g EVs significantly increased dESF secretion of CXCL1/GRO at 3h compared to the PBS and K562 100,000 x g controls. n=3 biological replicates (each point is the result of a matrix of 3 dESF lines treated with 3 EV batches), EV batches were performed as independent experiments. * $p<0.05$.

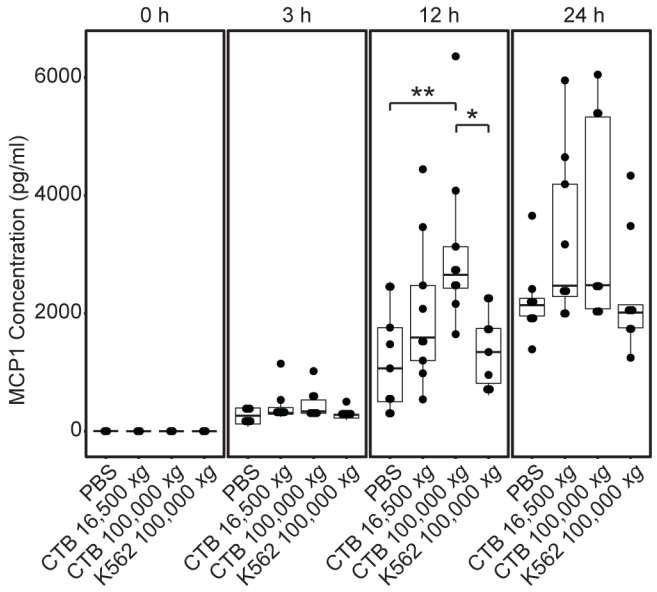

Figure 3.18 CTB 100,000 x g EVs increased secretion of NF-κB target CCL2/MCP-1.

Conditioned medium from primary dESF lines treated with CTB 100,000 x g EVs, CTB 16,500 x g EVs, K562 100,000 x g EVs, or PBS collected at 0, 3, 12, and 24 h was analyzed by cytokine array. CTB 100,000 x g EVs enhanced dESF release of CCL2/MCP-1 at 12 h compared to the PBS K562 100,000 x g controls. n=3 biological replicates (each point is the result of a matrix of 3 dESF lines treated with 3 EV batches), EV batches were performed as independent experiments. * $p<0.05$, ** $p<0.01$.

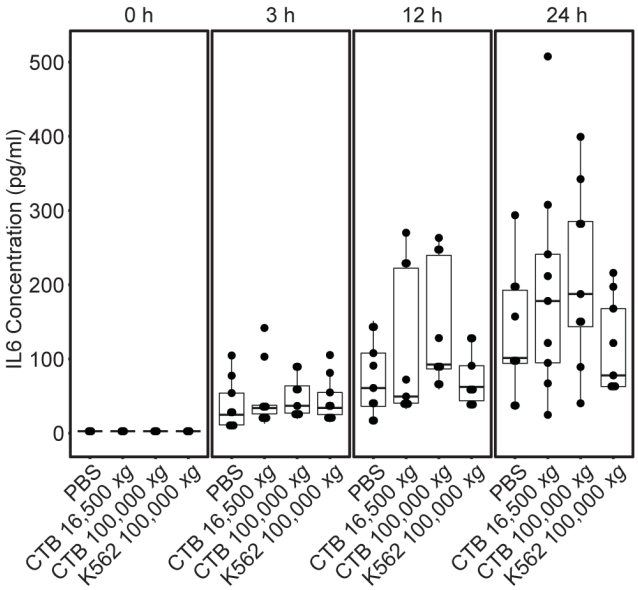

Figure 3.19 CTB 100,000 x g EVs increased secretion of NF-κB target IL-6.

Conditioned medium from primary dESF lines treated with CTB 100,000 x g EVs, CTB 16,500 x g EVs, K562 100,000 x g EVs, or PBS collected at 0, 3, 12, and 24 h was analyzed by cytokine array. IL-6 levels were not significantly different at any individual time point. n=3 biological replicates (each point is the result of a matrix of 3 dESF lines treated with 3 EV batches), EV batches were performed as independent experiments.

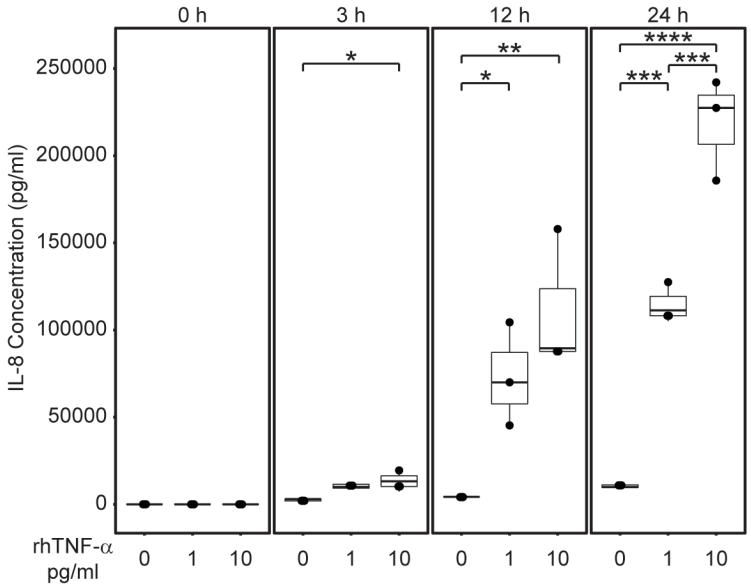

Figure 3.20 rhTNF-α recapitulated increased dESF *CXCL8*/IL-8 secretion.

rhTNF-α treatment induced dESF secretion of IL-8 in a dose-dependent manner as measured by ELISA. One pg/ml rhTNF-α treatment increased IL-8 secretion by 4.5-fold at 3 h, 17.4-fold at 12 h, and 10.9-fold at 24 h. Ten pg/ml rhTNF-α treatment increased IL-8 secretion by 5.7-fold at 3 h, 26.4-fold at 12 h, and 20.7-fold at 24 h. n=3 biological replicates (dESFs), performed as 2 independent experiments. * $p<0.05$, ** $p<0.01$, *** $p<0.005$, **** $p<0.001$.

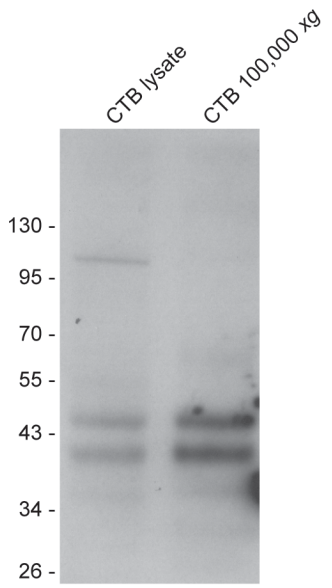

Figure 3.21 CTBs and 100,000 x g EVs contained the neonatal Fc receptor (FcRn).

Immunoblotting methods revealed that CTB lysate and 100,000 x g EVs were reactive with anti-FcRn at ~45 kDa, a size consistent with the molecule. n=1.

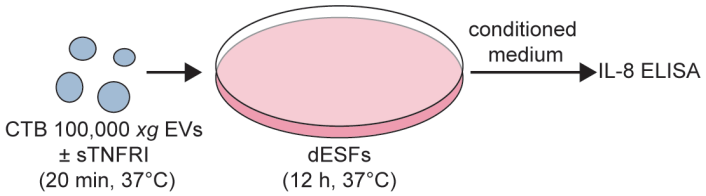

Figure 3.22 Schematic of TNF-α inhibition on EVs and dESF secretion of IL-8.

CTB 100,000 x g EVs were pre-incubated with a soluble form of the TNF-α receptor (sTNFRI) for 20 m at 37°C before addition to dESFs. After 12 h culture, conditioned medium was collected and analyzed by an ELISA for IL-8.

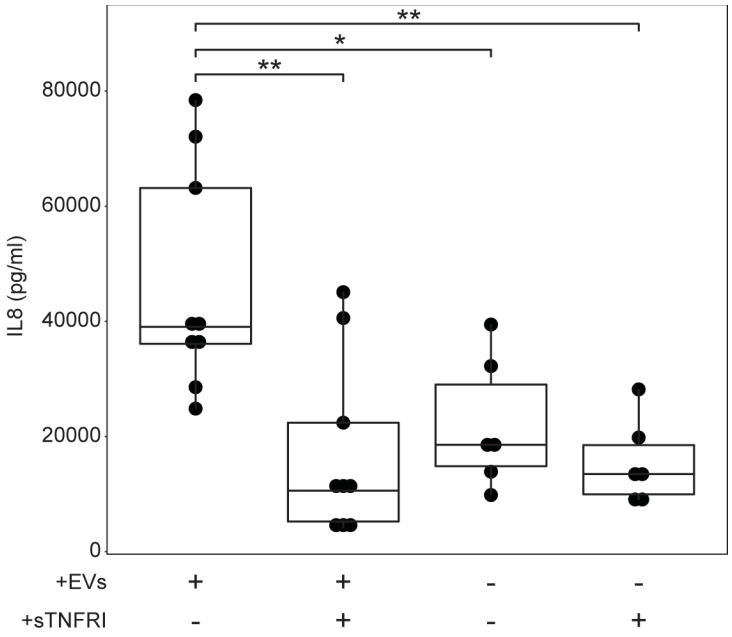

Figure 3.23 TNF-α inhibition attenuated increased dESF IL-8 secretion induced by CTB 100,000 x g EVs.

sTNFRI pre-treatment of CTB 100,000 x g EVs returned dESF IL-8 secretion to baseline after 12 h of culture as measured by ELISA. n=3 biological replicates (each point is the result of a matrix of 3 dESF lines treated with 3 EV batches), performed as 1 experiment. * $p<0.05$, ** $p<0.005$

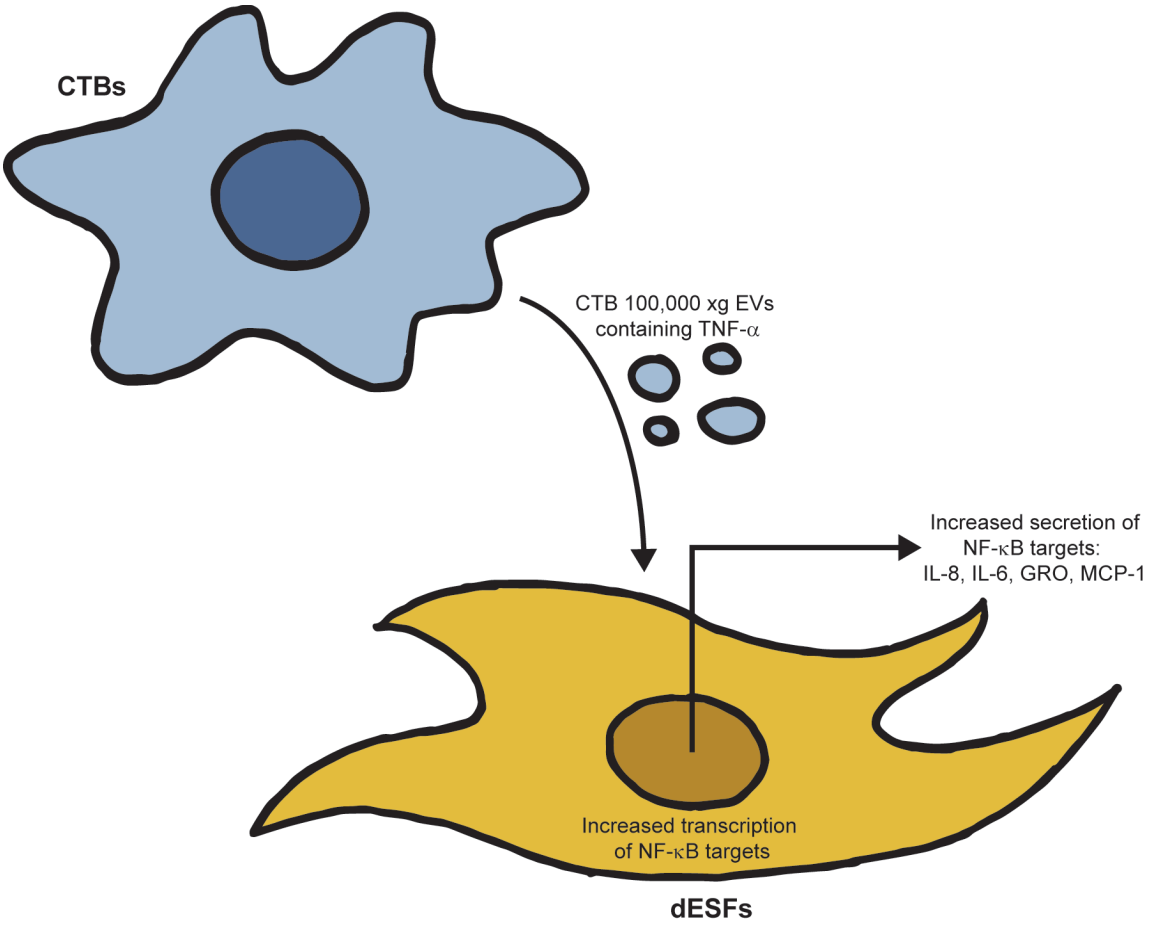

Figure 3.24 Proposed model of CTB communication with dESFs via EVs.

CTBs released 100,000 x g EVs containing TNF-α, which increased dESF transcription and secretion of NF-κB targets.

Table 3.1 Antibodies for immunoblotting

Primary Antibodies						Secondary Antibodies			
Target	**Clone**	**Supplier**	**Catalog #**	**Host**	**Dilution**	**Antibody**	**Conjugate**	**Supplier**	**Dilution**
FcRn	Polyclonal	Laboratory of N.E. Simister	N/A	mouse	1:200	Donkey anti-mouse	Peroxidase	Jackson ImmunoResearch Labs, Inc.	1:5000
TNF-α	2C8	Abcam	ab8348	mouse	1:500	Donkey anti-mouse	Peroxidase	Jackson ImmunoResearch Labs, Inc.	1:5000

Table 3.2 Antibodies for immunofluorescence

Primary Antibodies						Secondary Antibodies			
Target	**Clone**	**Supplier**	**Catalog #**	**Host**	**Dilution**	**Antibody**	**Conjugate**	**Supplier**	**Dilution**
CK	7D3	Laboratory of S.J. Fisher	N/A	rat	1:100	Donkey anti-rat	Rhodamine	Jackson ImmunoResearch Labs, Inc.	1:100
TNF-α	2C8	Abcam	ab8348	mouse	1:100	Donkey anti-mouse	FITC	Jackson ImmunoResearch Labs, Inc.	1:100

Table 3.3 qRT-PCR primers

Target	Forward Primer	Reverse Primer
ACTA2	AAGGCCAACCGGGAGAAAA	CGCCTGGATAGCCACATACA
ANGPT1	TCCAAAGAGGCTGGAAGGAA	CCTCTGACTGGTAATGGCAAAA
ANGPTL4	TCCACTTGGGACCAGGATCA	AATGGCTGCAGGTGCCAAA
APOE	CCCAGGTCACCCAGGAAC	TGTTCCTCCAGTTCCGATTTGTA
BMP2	ACTGTGCGCAGCTTCCA	ACTCCTCCGTGGGGATAGAA
CCL2	TAGCAGCCACCTTCATTCCC	CCTCTGCACTGAGATCTTCCTA
CCND3	CGACAGGCCTTGGTCAAAA	ATCATGGATGGCGGGTACA
CSF1	GGAGACCTCGTGCCAAATTA	TGCCTTCTTAAGGTAGCACAC
CXCL1	CTTGCCTCAATCCTGCATCC	AGCCACCAGTGAGCTTCC
CXCL12	GCTGGTCCTCGTGCTGAC	GAATCGGCATGGGCATCTGTA
CXCL8	ACACTGCGCCAACACAGAAA	CAGTTTTCCTTGGGGTCCAGAC
EGFR	AGTGTAAGAAGTGCGAAGGG	TCGTAGCATTTATGGAGAGTGAG
FGF1	TCTGCCTCCAGGGAATTACA	CCTGTCCCTTGTCCCATCC
FN1	GTGTGTGTGTCTTGGTAATGGAAA	AGTCCCAGCAGCATGATCAA
FOSL1	ATTGAGGAGCTGCAGAAGCA	CCCTCCTTGGCTCCTTCC
FZD1	GCTTCGTGGGGCTTAACAAC	ACGTGCCGATAAACAGGTACA
FZD2	CCTTCTTCACTGTCACCACGTA	TGTAGCAGCCCGACAGAAAA
FZD7	TCCGCACCATCATGAAACAC	GTGTAGAGCACGCTGAAGAC
G6PD	GCCGTCACCAAGAACATTCA	CTCCCGAAGGGCTTCTCC
HSP90AB1	TCCTTCGGGAGTTGATCTCTA	GGGTCTGTCAGGCTCTCATA
ICAM1	CCCCTACCAGCTCCAGACC	TGCGTGTCCACCTCTAGGAC
IFIT1	AGGCTGTCCGCTTAAATCCA	TCAGCTTCCTGTCCTTCATCC
IL6	AGAGCTGTGCAGATGAGTACAA	GTTGGGTCAGGGGTGGTTA
IL7	ATTGAAGGTAAAGATGGCAAACA	TCATTATTCAGGCAATTGCTACC
IRAK2	GTCTGGAGATCATCCACAGCAA	TGAGCCATTGGGTGAGCAA
JUN	AAGAACTCGGACCTCCTCAC	TGGATTATCAGGCGCTCCA
JUNB	TGGCCCAGCTCAAACAGAA	AGAAGGCGTGTCCCTTGAC
KDR	AGTGGGCTGATGACCAAGAA	CCATGCCACTTCCAAAAGCA
LIF	CTCGGGTAAGGATGTCTTCCA	ACACGGCGATGATCTGCTTA
MMP1	CACCTTCAGTGGTGATGTTCA	GCTGGACAGGATTTTGGGAA
MMP10	TGAGCCTAAGGTTGATGCTGTA	GGCATTGGGGTCAAACTCAA
MMP7	TGTATGGGGAACTGCTGACA	ATGAGCCAGCGTGTTTCC
NFKB1	CTACCTGGTGCCTCTAGTGAAA	ACCTTTGCTGGTCCCACATA
NFKB2	TACCTGGTGATCGTGGAACA	GCCTTCACAGCCATATCGAA
OLFM2	GGCTCCTGGATGACTGACA	GGCGGCCTTTGTAATAGCC
RELA	GCATCCAGACCAACAACAACC	AGAGCCGCACAGCATTCA
RELB	TGCTTTCCGAGCCCGTCTA	CGGCCCGCTTTCCTTGTTAA
TNFAIP2	AAGAGCCACGGCTTTGACA	GTGTGCGTGAACCTCTTGAAC
TNFAIP3	GAAGCTTGTGGCGCTGAAAA	CCTGAACGCCCCACATGTA
WNT5B	ATTGCAGCACAGCGGACAA	CTCACCGCGTGGGTGAA

Chapter 4: Cytotrophoblast extracellular vesicles promote pancreatic β-cell adaptation to pregnancy

---

Luc Baeyens[1,2], **Sara K. Taylor**[1,3,4], Matthew Gormley[4], Mirhan Kapidzic[1,3,4], Elaine Y. Kwan[4], Susan J. Fisher[1,3,4,5,6,7], Mike S. German[1,2,8]

1. Eli and Edythe Broad Center for Regeneration Medicine and Stem Cell Research, University of California, San Francisco, California 94143
2. Diabetes Center, University of California San Francisco, San Francisco.
3. Center for Reproductive Sciences, University of California, San Francisco, California 94143
4. Department of Obstetrics, Gynecology, and Reproductive Sciences, University of California, San Francisco, California 94143
5. Division of Maternal Fetal Medicine, University of California, San Francisco, California 94143
6. Department of Anatomy, University of California, San Francisco, California 94143
7. Human Embryonic Stem Cell Program, University of California, San Francisco, California 94143
8. Department of Medicine, University of California San Francisco, San Francisco.

Author Contributions:

S.K.T. generated CTB EVs. L.B. performed pancreas experiments. M.S.G. and S.J.F. supervised this project.

The pancreas, β-cells, and insulin production

The pancreas regulates metabolism and is made up of two parts with distinct functions: exocrine and endocrine (Zhou and Melton, 2018). Exocrine acinar cells produce digestive enzymes, which are secreted into the pancreatic ducts for release into the small intestine (Roder *et al.*, 2016). The endocrine component of the pancreas is organized into islets containing 5 cell types: insulin-producing β-cells, glucagon-producing α-cells, somatostatin-producing δ-cells, pancreatic polypeptide-producing (PP) cells, and ghrelin-producing ε-cells (Zhou and Melton, 2018).

β-cells and α-cells exert opposing functions to maintain normoglycemia. In response to high blood glucose, β-cells secrete insulin, which signals for muscle and adipose tissue to take up excess glucose, returning circulating concentrations to normal (Roder *et al.*, 2016). When blood glucose levels drop, α-cells release glucagon, which stimulates liver gluconeogenesis, restoring homeostasis (Goke, 2008). Pancreatic islet dysfunction disrupts the balance between β-cells and α-cells, resulting in metabolic disease. For example, insufficient insulin and excess glucagon is a hallmark of type 2 diabetes mellitus and gestational diabetes mellitus (Beis *et al.*, 2005; Goke, 2008).

Placental lactogen mediates rodent β-cell adaptation to pregnancy

In human pregnancy, maternal organs become insulin resistant to promote glucose uptake by the feto-placental unit (Lain and Catalano, 2007). To meet demand for increased insulin secretion, the pancreas increases in size, and β-cells increase in number (Butler *et al.*, 2010; Van Assche *et al.*, 1978). The mechanisms underlying these changes are unknown. It is unclear whether cell numbers increase by β-cell proliferation or by another population transdifferentiating into insulin-producing cells.

The mechanisms behind maternal pancreatic adaptation to pregnancy have been defined in rodent models. In rat pregnancy, cells in pancreatic islets proliferate and are labelled with BrdU beginning at day 10 of pregnancy and peaking at day 14 (Figure 4.1, left panel) (Parsons *et al.*, 1992). This event coincides with the detection of placental lactogen in maternal circulation starting at day 10 and with bimodal peaks at days 12 and 18 (Figure 4.1, left panel) (Parsons *et al.*, 1992). Although both β-cell proliferation and lactogen secretion begin at day 10, overall activities of the two are not parallel. This may reflect the fact that lactogen comprises the initial signal required for proliferation after which other messengers from the placenta and elsewhere may be required to sustain this process.

In addition to increasing β-cell number, pregnancy also enhances insulin secretion. Pancreatic islets isolated from pregnant mice (gestational day 13) release more insulin in response increasing glucose concentrations compared to those from non-pregnant controls (Figure 4.2) (Ohara-Imaizumi *et al.*, 2013). The difference between the two groups increases at higher levels of glucose, perhaps plateauing between 20 and 25 mM.

The mechanism underlying mouse pancreatic adaptation to pregnancy is well defined (Figure 4.3). The placenta releases placental lactogen into the maternal circulation (Welsch, 1979). The hormone binds to the prolactin receptor (PRLR) on β-cells, resulting in the transcription of tryptophan hydroxylase (TPH), which increases serotonin (5HT) synthesis from tryptophan (Trp) (Kim *et al.*, 2010). This neurotransmitter is secreted into the extracellular space, where it acts in an autocrine/paracrine manner and binds to its receptors HTR2B and HTR3A on β-cells (Kim *et al.*, 2010; Ohara-Imaizumi *et al.*, 2013). HTR2B promotes cell cycle progression and proliferation, while the sodium ion channel HTR3A increases insulin secretion (Kim *et al.*, 2010; Ohara-Imaizumi *et al.*, 2013). Towards the end of pregnancy, expression of HTR2B returns to normal levels, while expression of the inhibitory receptor HTR1D increases, decreasing proliferation (Kim 2010).

Mechanisms of pancreatic adaptation to pregnancy differ between human and mouse

Adult human β-cells are resistant to proliferation (Wang *et al.*, 2015). Mouse β-cell mitogens do not promote a similar response in human cells (Baeyens *et al.*, 2018). For example, placental lactogen does not stimulate replication in human islets as measured by EdU incorporation (Figure 4.4).

To determine whether murine pregnancy can drive human β-cell proliferation, adult human islets were transplanted beneath the mouse kidney capsule (Figure 4.5 A). After allowing for engraftment, a portion of the mice were impregnated. Concentrations of human C-peptide, a byproduct of insulin production, did not differ between non-pregnant and pregnant mice (Figure 4.5 B). In both groups, human β-cells did not proliferate as determined by EdU incorporation (Figure 4.5 C). In contrast, mouse β-cells in the pregnant mice replicated, and 10% were positive for EdU (Figure 4.5 D). Therefore, mechanisms underlying pancreatic adaptation to pregnancy are species-specific.

Human cytotrophoblast 100,000 x g extracellular vesicles promote β-cell proliferation and insulin secretion

Because the placenta mediates pancreatic adaptation to pregnancy in mice, we investigated whether human placental cytotrophoblasts (CTBs) and their extracellular vesicles (EVs) promote β-cell proliferation and insulin secretion. Mice transplanted with human pancreatic islets underwent one of two treatments: CTBs were transplanted under the other kidney capsule or CTB 100,000 x g EVs were injected into the tail vein (Figure 4.6). Both treatments dramatically increased human β-cell proliferation as measured by EdU incorporation (Figure 4.7). Only mouse pregnancy enhanced mouse β-cell proliferation, reinforcing the

overarching principal that the mechanisms of pancreatic adaptation to pregnancy are different in mice and humans.

We asked whether this mitogenic activity was specific to the 100,000 x g EV population or a general property of CTB EVs. In these experiments, either CTB 16,500 x g EVs or 100,000 x g EVs were injected into the tail veins of mice transplanted with human islets. Only the 100,000 x g fraction increased the transplanted cells' incorporation of EdU (Figures 4.8 and 4.9). The proliferating cells retained expression of Nkx6.1, a marker of mature β-cells, and continued to secrete insulin (Figure 4.8). In contrast, CTB 16,500 x g EVs did not stimulate EdU incorporation. Additionally, the mitogenic activity, which was restricted to the 100,000 x g fraction, was sustained over the course of the experiment, which lasted for 64 days (Figure 4.9). Together, these experiments indicate that the 100,000 x g EVs had the unusual property of inducing β-cell proliferation without loss of mature markers or insulin secretion.

In additional experiments, we investigated whether the observed effects were cell type-specific. To this end, we generated HeLa cell 100,000 x g EVs. These vesicles did not stimulate β-cell proliferation as measured by EdU incorporation *in vivo* (Figure 4.7). To test whether other HeLa cell EV populations could drive β-cell replication *in vitro*, we cultured human islets with vesicles isolated at 3 different speeds: 2,000 x g, 16,500 x g, and 100,000 x g. HeLa EVs failed to increase β-cell proliferation as measured by EdU incorporation (Figure 4.10, upper panel) and Ki67 staining (Figure 4.10, lower panel). Together, these data suggest that the ability of 100,000 x g EVs to drive β-cell proliferation is specific to those derived from CTBs.

We addressed whether human placental lactogen synergizes with CTB 100,000 x g EVs to drive β-cell proliferation and insulin production *in vitro*. Human islets were cultured with 3 populations of CTB EVs: 2,000 x g, 16,500 x g, and 100,000 x g. Only CTB 100,000 x g EVs increased β-cell proliferation as measured by EdU incorporation, and human placental lactogen had no additional effects (Figure 4.11, upper panel). In agreement with this result, only CTB

100,000 x g EVs increased the number of proliferating Ki67-positive, insulin-producing cells, and again placental lactogen had no effect (Figure 4.11, lower panel). The proliferating Ki67-positive cells retained insulin secretion, suggesting that mature β-cells replicate without dedifferentiation. Furthermore, only the CTB 100,000 x g EVs increased glucose-stimulated insulin secretion; the addition of human placental lactogen further enhanced this activity (Figure 4.12). Thus, CTB 100,000 x g EVs increased β-cell proliferation and insulin secretion.

Because serotonin induces mouse β-cell proliferation, we investigated whether this neurotransmitter synergizes with CTB 100,000 x g EVs. Addition of serotonin to pancreatic islets did not influence alter CTB EV-induced β-cell proliferation as measured by EdU incorporation (Figure 4.13). This reinforces the principle that mechanisms of pancreatic adaptation to pregnancy differ between human and mouse.

To further investigate the mechanism underlying CTB 100,000 x g EV-induced β-cell proliferation, we disrupted the vesicles by sonication prior to adding them to pancreatic islets. Sonication abolished proliferative effects of CTB 100,000 x g EVs as measured by EdU incorporation (Figure 4.14). Therefore, vesicle structure must be intact to deliver the activator, which could be an RNA or protein. Of note, this experiment was performed a single time and replicates are needed to reach a firm conclusion.

We next compared the *in vitro* effects of CTB 100,000 x g EVs on human pancreatic islets to those of known β-cell mitogens. The vesicles stimulated proliferation of β-cells to a greater extent than the drugs and compounds tested (Figure 4.15). Additionally, CTB 100,000 x g EVs had no effect on α-cell proliferation. Thus, the vesicles specifically targeted β-cells to promote adaptation to pregnancy.

To gain insights into possible mechanisms, RNA-seq was performed on pancreatic islets treated with CTB 100,000 x g EVs versus a negative control. Gene set enrichment analysis (GSEA) revealed that the vesicles upregulated the expression of genes involved in cell cycle

progression (Figure 4.16). Thus, these experiments confirmed the results described above in terms of vesicle stimulation of pancreatic islet EdU incorporation and Ki67 staining.

Cytotrophoblast 100,000 x g extracellular vesicles promote human embryonic stem cell differentiation into β-cells

Since CTB 100,000 x g EVs stimulated primary β-cell proliferation without the loss of mature markers, we asked whether the vesicles could enhance human embryonic stem cells (hESCs) differentiation into this cell type. To this end, we treated β-like cells with CTB EVs isolated at 2,000 x g, 16,500 x g, and 100,000 x g. Only CTB 100,000 x g EVs increased the percentage of cells positive for C-peptide as measured by flow cytometry (Figure 4.17, left panel). In terms of function, glucose-stimulated insulin secretion (GSIS) of hESC-derived β-like cells was calculated by dividing insulin secretion at high glucose (20 mM) by response at low glucose (2.8 mM). Only CTB 100,000 x g EVs increased glucose responsiveness of β-like cells (Figure 4.17, right panel). Thus, these vesicles improved differentiation and function of these cells by enhancing their insulin secretion.

Discussion

Here, we investigate the role of CTB 100,000 x g EVs at sites beyond the uterus. Specifically, we examined their effects in terms of maternal pancreatic adaptation to pregnancy. These vesicles stimulated human pancreatic β-cell proliferation and insulin secretion both *in vivo* and *in vitro*. Proliferating cells maintained expression of the mature β-cell marker Nkx6.1. This indicates that increased β-cell number is due to replication of mature cells, rather dedifferentiation to a precursor prior to proliferation or transdifferentiation of other cell types into β-cells. The effect was specific to both cell type and vesicle type, as HeLa 100,000 x g EVs and other CTB EVs isolated at 2,000 x g and 16,500 x g did not increase β-cell proliferation.

Furthermore, the mechanisms were distinct from those in mice, as mouse pregnancy had no effect on human cells. Placental lactogen synergized with CTB 100,000 x g EVs to promote insulin production, but not proliferation. The vesicles stimulated β-cell, but not α-cell, proliferation to a greater extent than known mitogens. Finally, CTB 100,000 x g EVs enhanced differentiation of hESC-derived β-like cells. Overall, the data suggest that CTBs play an important role in pancreatic adaptation to pregnancy through EVs released into the maternal circulation.

Additional studies are needed to identify the specific cargo within CTB EVs that promotes β-cell proliferation and insulin production, as well as hESC differentiation. It could be one of many RNA species or proteins identified in CTB EVs by mass spectrometry. RNA-sequencing of the vesicle contents is challenging due to limited quantities of starting material but may become more feasible as methods improve and/or trophoblast cell lines that produce these EVs are identified. It may be possible to identify miRNA candidates by analyzing sequences of differentially expressed genes. Different bioinformatic approaches to analyze EV-induced changes in β-cell gene expression could reveal additional insights into mechanisms and mediators.

It is logical to predict that gestational diabetes mellitus could be the result of defective CTB 100,000 x g EV communication with maternal pancreatic β-cells. The problem could lie in the vesicle contents or islet responses. This complication does not always recur in second pregnancies (Kim *et al.*, 2007), suggesting that defective β-cell proliferation is due to a missing feto-placental signal. Future studies comparing the contents and functions of CTB EVs from normal versus gestational diabetic pregnancies could uncover the root causes of this pregnancy complication.

CTB 100,000 x g EVs specifically induced proliferation of β-, but not α-cells, suggesting that the mechanism could be used to correct the insulin-glucagon imbalance observed in

gestational diabetes mellitus and type 2 diabetes mellitus. The vesicles themselves may not be a viable therapy. Their contents and functions are not fully known and understood, which could result in undesirable off-target effects. However, uncovering the mechanism underlying increased β-cell proliferation and function will lead to new therapeutic developments. For example, enhancing insulin secretion of hESC-derived β-like cells could improve transplantation therapies. Furthermore, understanding the pathway could identify druggable targets and lead to the generation of new pharmaceuticals to treat diabetes. Thus, maternal adaptation to pregnancy can be co-opted to treat human disease.

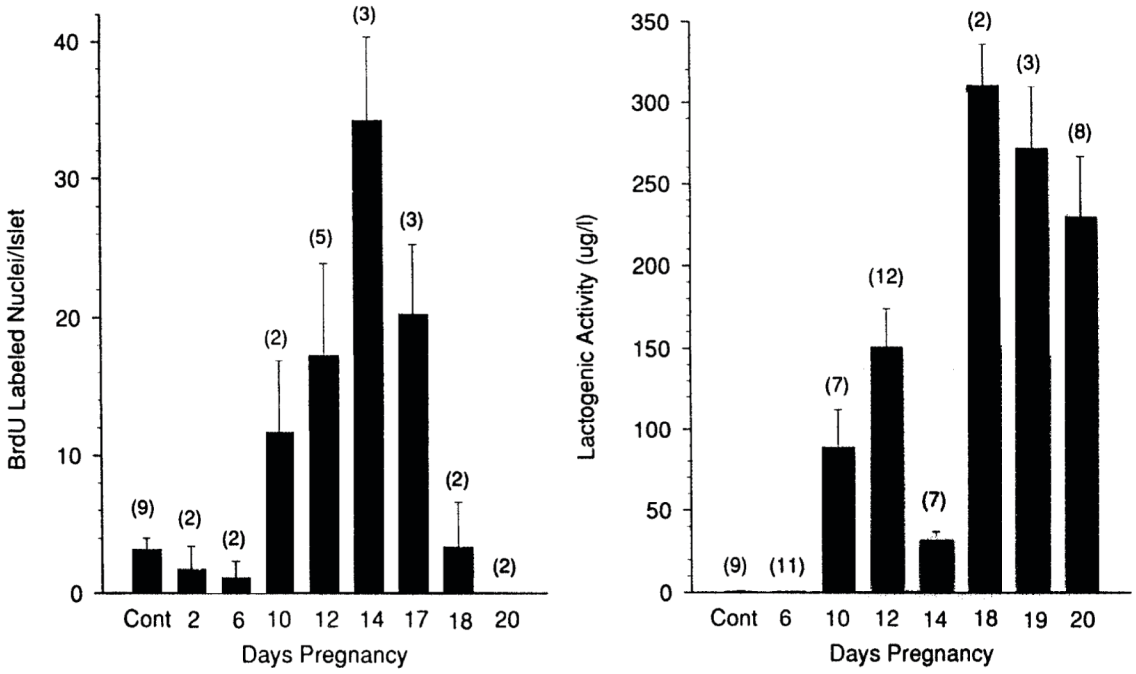

Figure 4.1 The start of pancreatic islet β-cell proliferation overlaps with the beginning of placental lactogen secretion in rats.

(Left) Islet proliferation, as measured by BrdU incorporation, increases from days 10 to 17 of pregnancy compared to the control (Cont). Numbers in parentheses denote (n) animals. (Right) Compared to the control (Cont), lactogenic activity in serum increases starting at day 10 of pregnancy. Reprinted from Parsons *et al.* (1992).

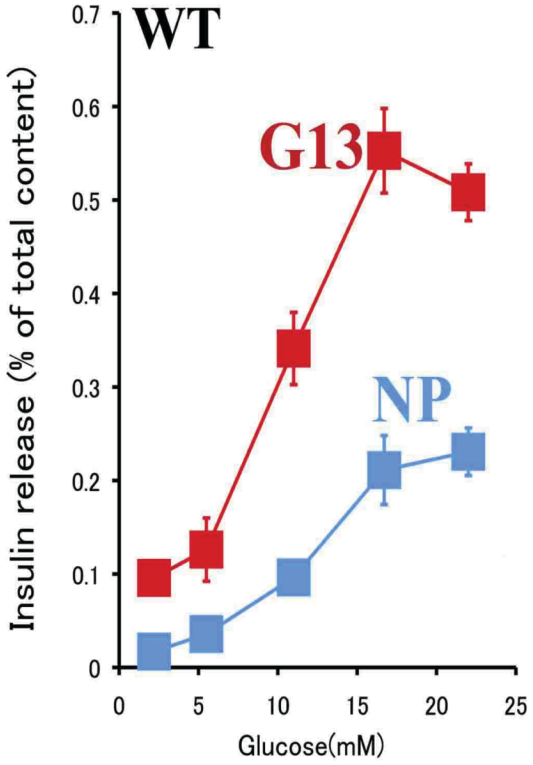

Figure 4.2 At gestational day 13, β-cells from wildtype pregnant mice (G13) secrete higher levels of insulin in response to glucose stimulation than non-pregnant mice (NP).

Adapted from Ohara-Imaizumi *et al.* (2013).

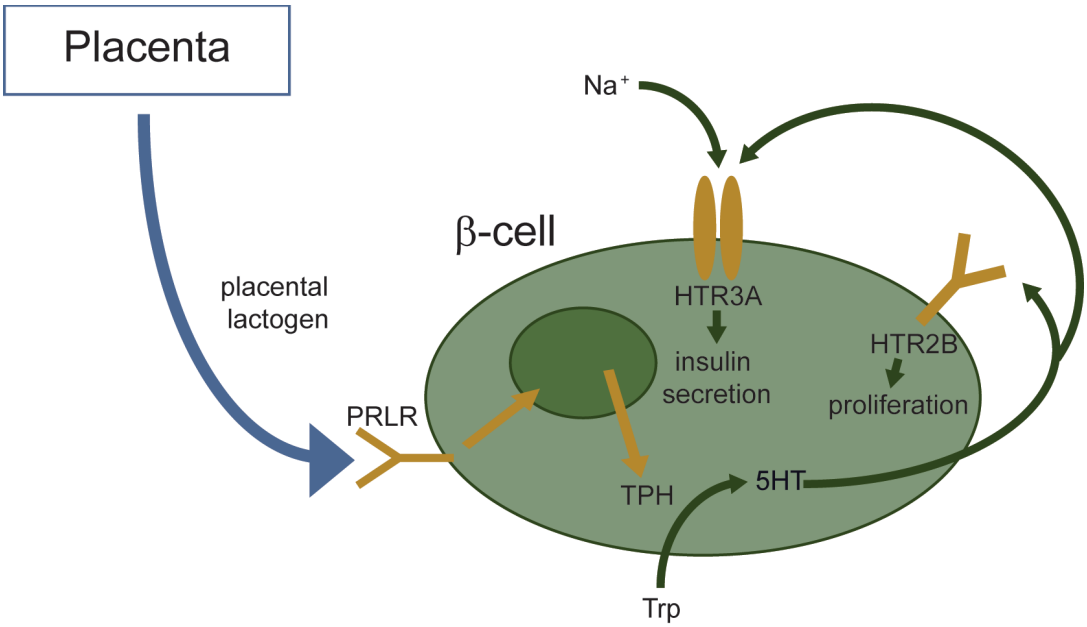

Figure 4.3 Pathway by which placental lactogen stimulates β-cell proliferation during mouse pregnancy.

In mouse pregnancy, the placenta secretes placental lactogen, which binds to the prolactin receptor (PRLR), driving tryptophan hydroxylase (TPH) production in β-cells. TPH increases tryptophan (Trp) conversion to serotonin (5HT), which then binds to the receptors HTR2B and HTR3A. The former interaction increases proliferation and the latter drives insulin secretion.

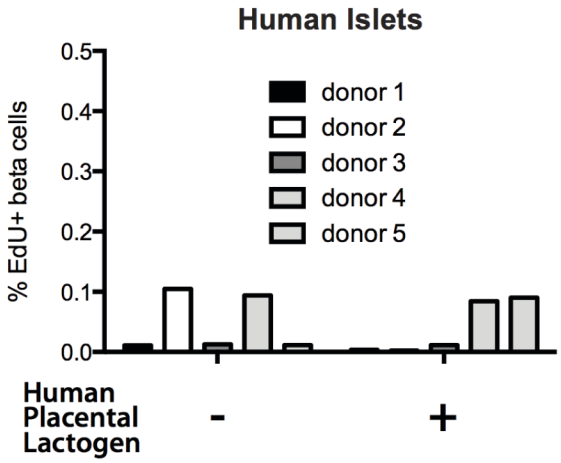

Figure 4.4 Placental lactogen fails to increase human β-cell proliferation.

Percentage of EdU-positive β-cells in human islets treated with placental lactogen. n=5.

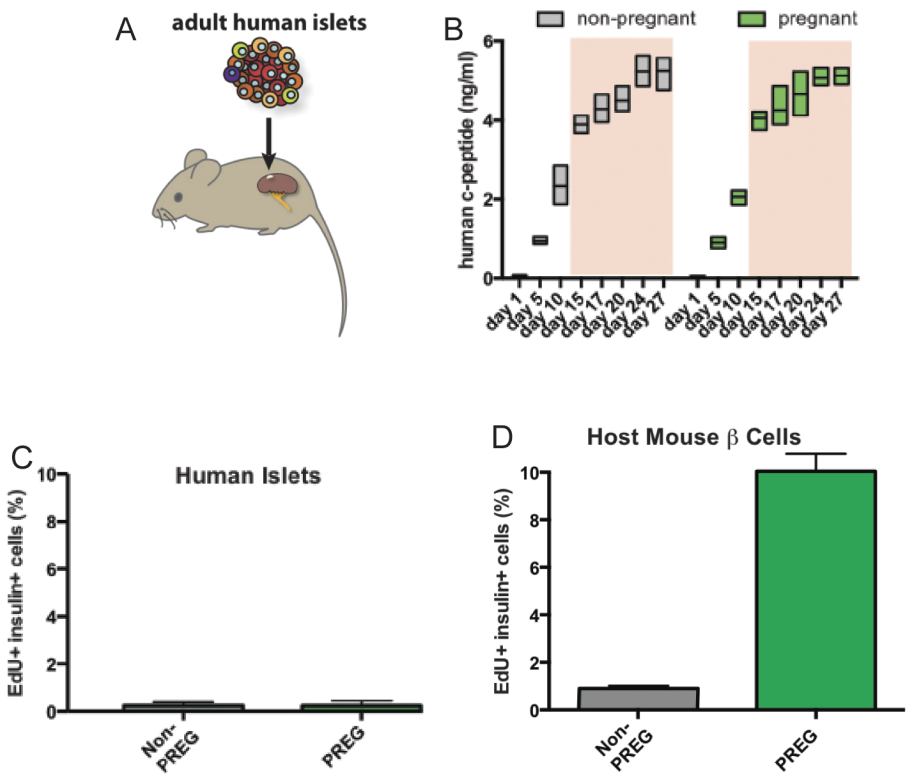

Figure 4.5 Mouse pregnancy does not promote human β-cell proliferation.

(A) Adult human islets were transplanted under the kidney capsules of mice, which were later impregnated. (B) Pregnancy did not impact human C-peptide concentrations, a measure of human insulin production, in the transplanted mice. (C) Pregnancy did not increase the proliferation of transplanted human β-cells as measured by EdU incorporation. (D) In contrast, mouse β-cells proliferated and incorporated EdU.

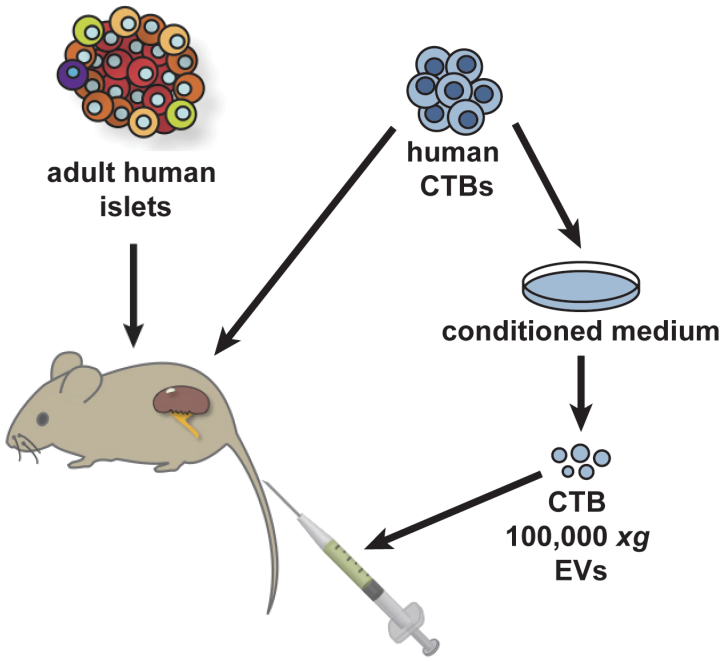

Figure 4.6 In the mouse model shown in Figure 4.5A, human CTBs or 100,000 x g EVs isolated from these cells stimulated adult human β-cell proliferation.

Adult human islets were transplanted under the capsule of one kidney. To test whether the placenta induces β-cell adaptation to pregnancy, human CTBs were transplanted beneath the other kidney capsule or their EVs were injected into the tail vein.

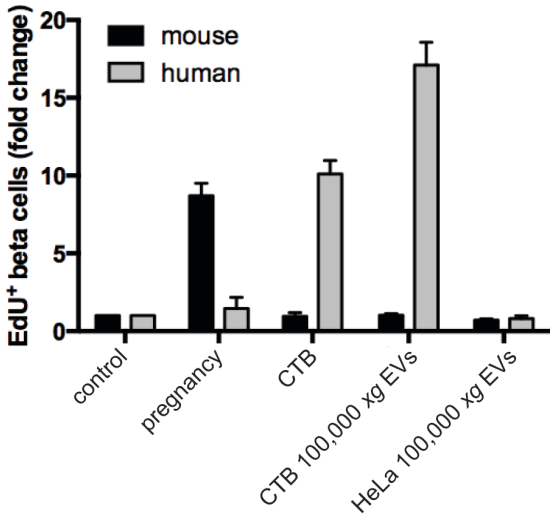

Figure 4.7 CTBs and their EVs increased human β-cell proliferation in an *in vivo* mouse model.

Mouse pregnancy specifically increased mouse β-cell proliferation as measured by EdU incorporation. CTBs transplanted beneath the kidney capsule promoted proliferation of human β-cells with no effect on mouse β-cells. Tail vein injection of CTB 100,000 x g EVs similarly increased human β-cell proliferation. In contrast, injection of HeLa cell 100,000 x g EVs failed to promote β-cell replication of either species.

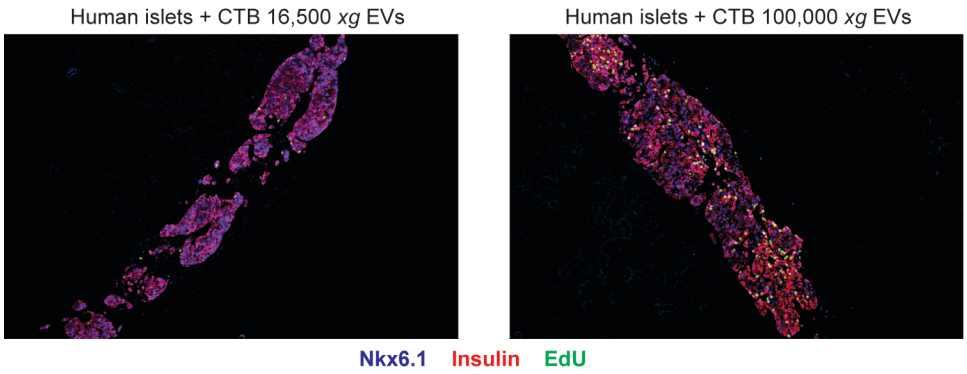

Figure 4.8 CTB 100,000 x g EVs induced β-cell proliferation *in vivo.*

Unlike CTB 16,500 x g EVs, the 100,000 x g fraction increased EdU incorporation (green) in human β-cells, which retained expression of Nkx6.1 (blue), a marker of mature cells, and insulin secretion (red).

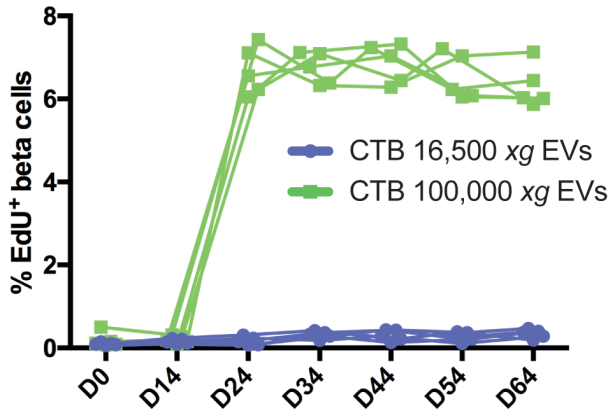

Figure 4.9 CTB 100,000 x g EV-stimulated β-cell proliferation was stable over several weeks.

Mice transplanted with human pancreatic islets were injected with two populations of CTB EVs: 16,500 x g and 100,000 x g. The percentage of EdU-positive human β-cells was calculated over time. The results showed that only the 100,000 x g EV fraction stimulated β-cell proliferation, an effect that was sustained over the course of these experiments.

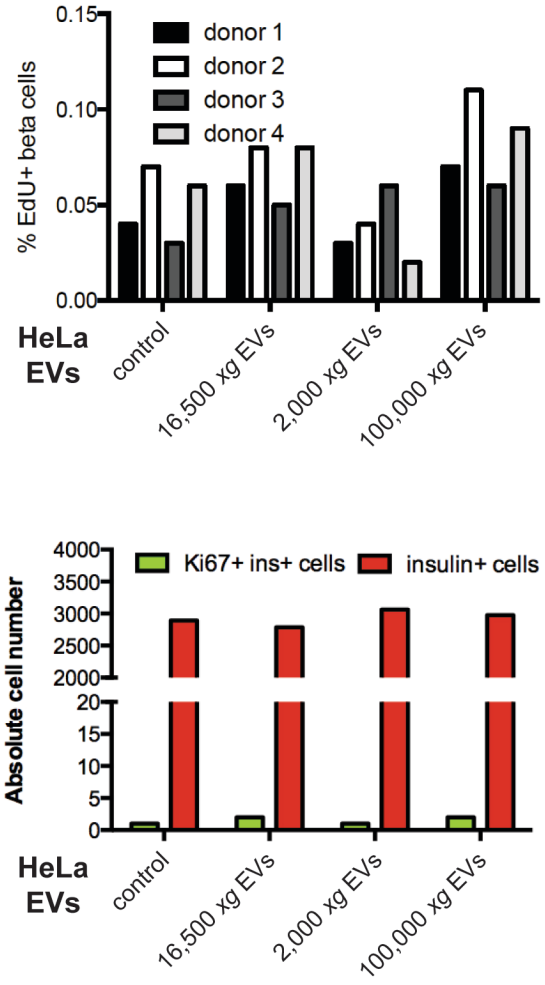

Figure 4.10 HeLa cell EVs did not induce β-cell proliferation *in vitro*

Human pancreatic islets were cultured with HeLa cell EVs isolated at 3 speeds: 2,000 x g, 16,500 x g, and 100,000 x g. (Upper panel) EdU incorporation by β-cells did not increase with any HeLa EV treatment. (Lower panel) Ki67 staining of insulin+ cells was used as an additional marker proliferation. HeLa EVs had no effect. n=4 biological replicates.

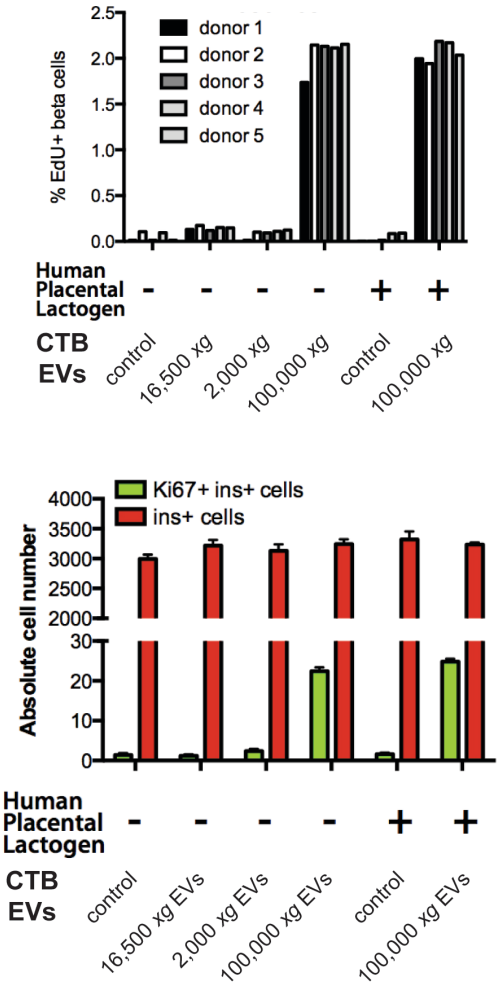

Figure 4.11 Placental lactogen did not enhance CTB 100,000 x g EV-induced β-cell proliferation *in vitro*.

Islets were treated with CTB EVs. EdU incorporation (upper panel) and Ki67 (lower panel) were used as markers of proliferating cells. Only 100,000 x g EVs increased proliferation. Addition of human placental lactogen had no effect. n=5 biological replicates.

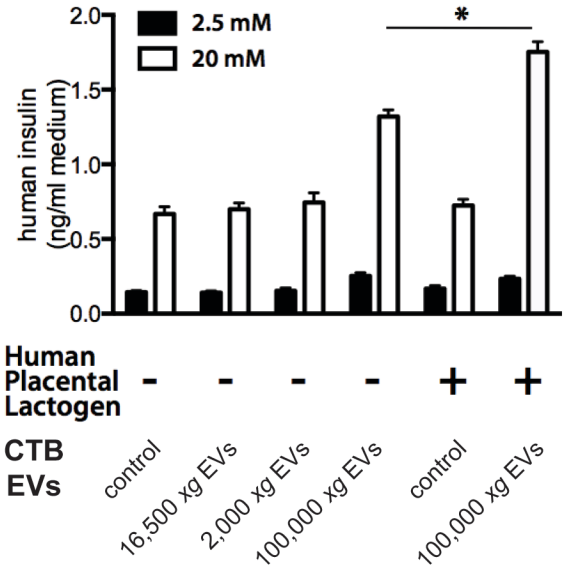

Figure 4.12 CTB 100,000 x g EVs increased pancreatic islet insulin secretion *in vitro*, which was further enhanced by the addition of human placental lactogen.

Islets were treated with CTB EVs and insulin response to low (2.5 mM) and high (20mM) glucose was measured. Only 100,000 x g EVs increased insulin secretion. Addition of human placental lactogen further enhanced this response.

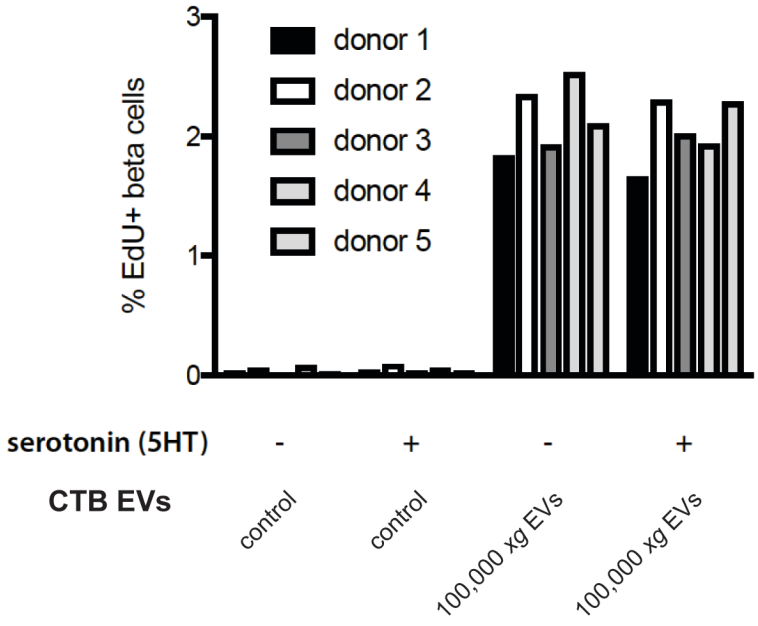

Figure 4.13 Serotonin did not impact β-cell proliferation *in vitro.*

Pancreatic islets were treated with CTB 100,000 x g EVs and serotonin (5HT). Addition of 5HT had no effect on β-cell proliferation as measured by EdU incorporation. n=5 biological replicates.

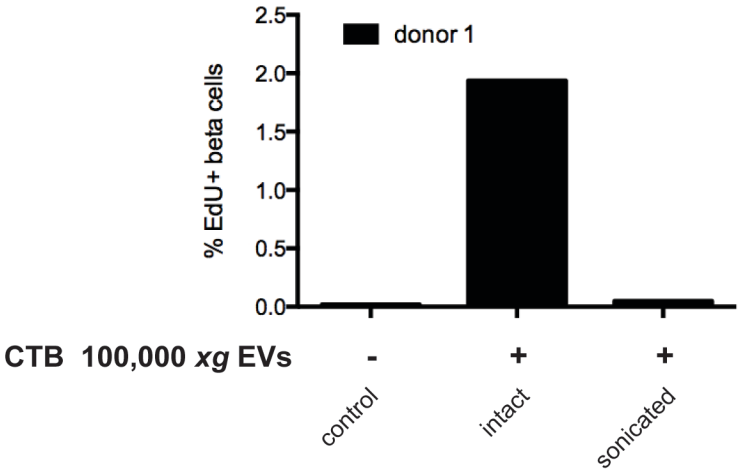

Figure 4.14 Sonication disrupted CTB EV-induced β-cell proliferation

Pancreatic islets were treated with intact or sonicated CTB 100,000 x g EVs. Sonication abolished CTB EV-induced β-cell proliferation, which was measured by EdU incorporation. n=1.

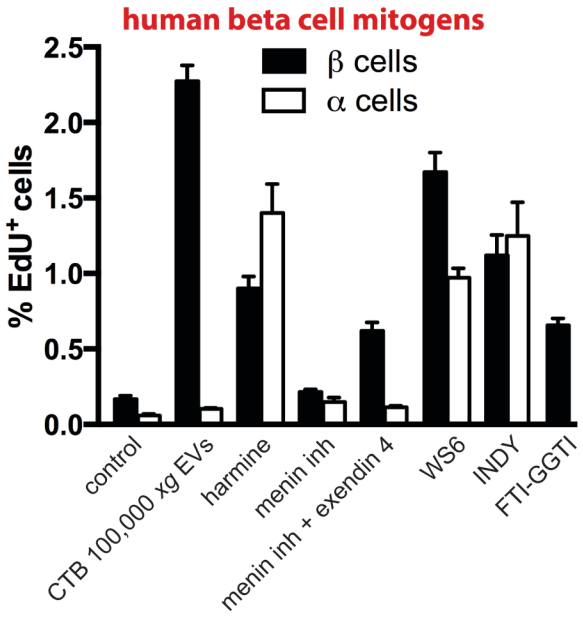

Figure 4.15 CTB 100,000 x g EVs specifically stimulated β-cell proliferation to a greater extent than other known mitogens *in vitro.*

Human pancreatic islets were cultured with CTB 100,000 x g EVs or known mitogens: harmine, menin inhibitor (menin inh), exendin 4, small molecule WS6, inhibitor of dual specificity tyrosine-regulated kinase-1a (INDY), and farnesyl:protein transferase inhibitor combined with GGPTase-I inhibitor (FTI-GGTI). Percentage of EdU incorporation was calculated for both β-cells and α-cells. CTB 100,000 x g EVs specifically increased β-cell proliferation to a greater extent and with more specificity than known mitogens.

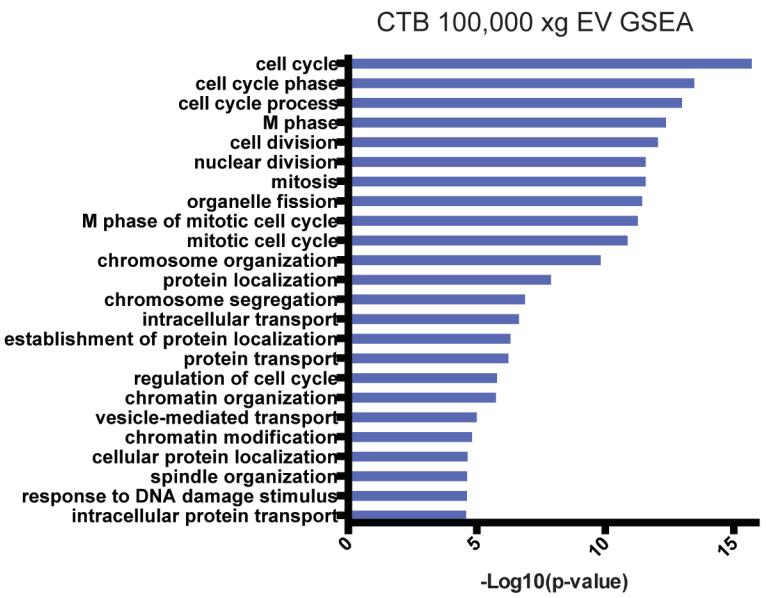

Figure 4.16 CTB 100,000 x g EVs upregulated the expression of cell cycle genes by pancreatic islets.

Gene Set Enrichment Analysis (GSEA) was performed for differentially expressed RNAs. The results showed that CTB 100,000 x g EVs upregulated genes involved in numerous biological processes related to proliferation.

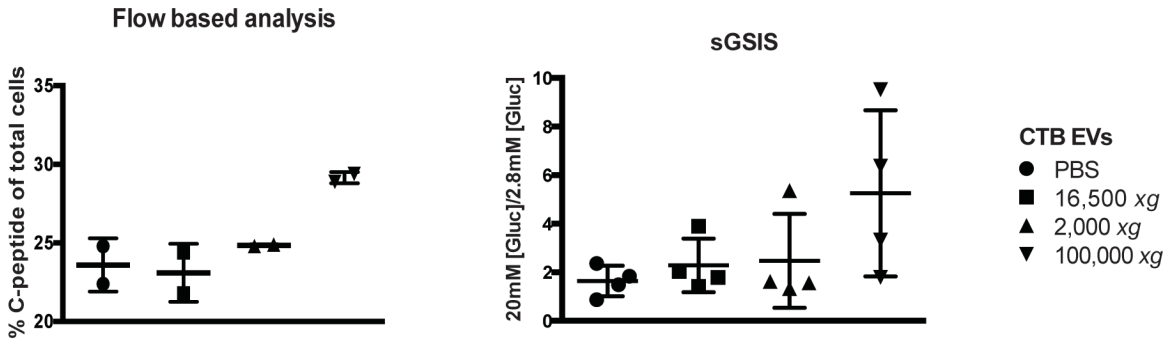

Figure 4.17 CTB 100,000 x g EVs improved generation of β-like cells from human embryonic stem cells (hESCs)

(Left panel) Percentage of C-peptide-producing cells were enumerated by flow cytometry. (Right panel) Glucose-stimulated insulin secretion (GSIS) was calculated as the response at high glucose (20mM) divided by that at low glucose (2.8mM). Only CTB 100,000 x g EVs increased insulin production of hESC-derived β-like cells in these experiments.

Chapter 5: Future Directions

Sara K. Taylor[1,2,3], Susan J. Fisher[1,2,3,4,5,6]

1. Center for Reproductive Sciences, University of California, San Francisco, California 94143
2. Department of Obstetrics, Gynecology, and Reproductive Sciences, University of California, San Francisco, California 94143
3. Eli and Edythe Broad Center for Regeneration Medicine and Stem Cell Research, University of California, San Francisco, California 94143
4. Division of Maternal Fetal Medicine, University of California, San Francisco, California 94143
5. Department of Anatomy, University of California, San Francisco, California 94143
6. Human Embryonic Stem Cell Program, University of California, San Francisco, California 94143

Summary

In these studies, we characterized CTB EV contents and functions in promoting maternal adaptation to pregnancy at local and distant sites. In Chapter 2, I characterized CTB EVs by transmission electron microscopy and immunoblotting methods. I also profiled the global protein contents by mass spectrometry. In Chapter 3, I reported that these vesicles mediated inflammatory signals in the uterus, a local site. Specifically, CTB 100,000 x g EVs enhanced decidualized endometrial stromal fibroblast (dESF) transcription and secretion of immunomodulators with previously reported functions in endothelial cells, immune cells, and CTBs. Finally, in Chapter 4, we describe our discovery that that these vesicles promoted maternal adaptation to pregnancy in the pancreas, a distant organ. Specifically, these vesicles stimulated pancreatic β-cell proliferation and insulin secretion. Future studies will identify additional roles of these vesicles in mediating pregnancy-related changes in other maternal organs and tissues. The following summarizes the many directions in which this work could lead.

Potential roles for placental extracellular vesicles at local sites

The EVs we studied likely have effects on neighboring CTBs. For example, the 100,000 x g fraction is rich in fibronectin (Figure 2.8). Another group reported that migrating fibrosarcoma cells create an exosome trail that promotes paracrine motility via a mechanism that partially involves vesicular fibronectin (Sung *et al.*, 2015; Sung and Weaver, 2017). Furthermore, CTB 16,500 x g EVs contained Ephrin receptors, patterning molecules that influence CTB organization as they invade into the decidua (Red-Horse *et al.*, 2005). Thus, CTB EVs may organize and promote CTB invasion from the cell column into the uterus. Understanding these processes in normal pregnancy will provide insights into what goes wrong in preeclampsia and placenta percreta, complications characterized by faulty invasion.

CTB EVs likely have other roles in the decidua. For example, it has long been known that decidualization proceeds in advance of invading trophoblasts (Kindelberger and Nucci, 2009). It is tempting to speculate that this observation could be explained by the cells' release of EVs that signal endometrial stromal fibroblasts to decidualize.

CTBs could also promote spiral artery remodeling. For example, first trimester extravillous trophoblasts induce cell death in endothelial cells of the spiral artery in an explant model (Ashton *et al.*, 2005). TNF-α in CTB 100,000 x g EVs may facilitate this endothelial cell death. Furthermore, I identified glia-derived nexin in CTB 100,000 x g EVs by mass spectrometry. This molecule promotes vascular mimicry in tumor cells (Wagenblast *et al.*, 2015), a process that is integral to spiral artery remodeling.

Placental vesicles could play a role in triggering parturition. CTB EVs contained the inflammatory cytokine TNF-α and induced NF-κB signaling in dESFs. Activating these pathways in the myometrium combined with inflammatory cytokines released by dESFs may promote labor. Furthermore, mass spectrometry analyses revealed that CTB EVs contained components of the prostaglandin pathway, additional possible mediators of parturition. EVs from term placentas collected following labor versus elective cesarean section will likely differ in contents and their ability to induce myometrial contraction, suggesting stimulation of parturition. Identifying mechanisms in the context of normal pregnancy will provide a foundation for understanding what goes wrong in pre-term labor or in cases of stalled labor.

CTB 100,000 x g EVs contained a number of immune molecules, including HLA-G, PD-L1, TNF-α, CD276, CD47, and CD59. The vesicular form of these immunomodulators may be key to their functions in pregnancy. For example, CTB EVs were enriched for dimeric HLA-G (Figure 2.6). Using mass spectrometry, we detected multiple protein disulfide isomerases, which likely promote dimerization of this MHC class I molecule, increasing its affinity for the inhibitory receptors LILRB1 and LILRB2 (Bulleid and Ellgaard, 2011; Lynch *et al.*, 2009; Shiroishi *et al.*,

2006). In both vesicle types (16,500 x g and 100,000 x g), we also identified multiple proteasome subunits, which process antigens for peptide presentation by HLA molecules (Vigneron *et al.*, 2017), suggesting that HLA-G present in CTB EVs may have antigen-presenting capability.

Additional studies are needed to understand how EV proteins modulate the immune balance of pregnancy. For example, placental vesicles could promote recruitment of specific subsets of potentially beneficial immune cells to the decidua. Additionally, *in vitro* experiments could identify EV-induced changes in specific populations of peripheral or decidual cells. Models involving multiple immune cell types, such as antigen-presenting cells and T cells, or the addition of stromal cells may be required to identify other placental vesicle functions of this type.

Potential roles for placental extracellular vesicles at distant sites

CTBs are in direct contact with maternal blood and secrete EVs into the circulation. Future studies will identify additional functions of these vesicles in mediating pregnancy-associated changes throughout the mother's body. For example, mouse pregnancy stimulates neurogenesis in the maternal olfactory bulb via a prolactin-mediated mechanism (Medina and Workman, 2018; Shingo *et al.*, 2003). It is unclear whether a similar mechanism exists in humans, where adult neurogenesis is rare but occurs when neural stem cells in the subventricular zone give rise to neurons that migrate into the olfactory bulb (Sanai *et al.*, 2011; Sorrells *et al.*, 2018). It is tempting to speculate that the well-known sensitivity to certain olfactory stimuli that some pregnant women experience could be related to proliferation of neurons at this site. Prolactin, produced by the placenta, induces fetal neural stem cell proliferation *in vitro* (Pathipati *et al.*, 2011). Although we failed to detect prolactin in CTB EVs, these vesicles could synergize with this hormone to promote adult neurogenesis during pregnancy.

In addition to pancreatic changes, placental vesicles may influence other metabolic adaptations to pregnancy. Liver expansion during pregnancy is thought to be due to increased blood volume, as the number of hepatocytes does not increase in mice (Hollister *et al.*, 1987). CTB EVs may increase hepatocyte proliferation or functions, including enzyme production and nutrient synthesis.

During pregnancy, total fat mass and adipocyte size increase (Svensson *et al.*, 2016). Additionally, fat distribution shifts from subcutaneous to preperitoneal, possibly as a metabolic adaptation to pregnancy or to prepare for lactation (Selovic *et al.*, 2016; Straughen *et al.*, 2013). The mechanisms are unknown. Circulating EVs and hormones produced by the placenta may trigger these changes in body fat.

During late mouse pregnancy, there are drastic changes in mammary gland adipocytes (Cinti 2018). These cells transdifferentiate into secretory epithelial cells containing large, cytoplasmic lipid droplets (De Matteis *et al.*, 2009; Morroni *et al.*, 2004). When lactation ends, these cells revert to white adipocytes, returning the gland to its pre-pregnancy state (Morroni *et al.*, 2004). The mechanisms underlying this phenomenon are not well understood. Exogenous *Elf5* expression promotes adipocyte production of whey acidic protein, a component of milk, but is not sufficient to drive conversion into secretory epithelial cells (Prokesch *et al.*, 2014). Removal of the ductal component of the mammary gland prevents adipocyte trans-differentiation during pregnancy, indicating that a signal from ductal cells is required for this process (Prokesch *et al.*, 2014). Conversion of adipocytes during mouse pregnancy and lactation is likely dependent on a complex network of signals from multiple cell types.

Additional studies are needed to determine whether a similar process occurs in humans and the extent of mechanistic overlap between species, especially given the rapid evolution of the placenta and its secreted products (Chuong *et al.*, 2013). In terms of species-specific differences, the non-lactating human mammary gland contains much more stroma than its mouse counterpart (McNally and Stein, 2017). Stromal cell signals may be critical for human

mammary gland development during pregnancy. The contents of placental EVs may shift as pregnancy progresses to initiate mammary gland development; identifying cargo changes may provide mechanistic insights. Overall, future studies may implicate placental vesicles as the source of signals to adipocytes, ductal cells, and stromal cells in the mammary gland to initiate adipocyte conversion and preparation of the mother for lactation.

In normal pregnancy, vascular resistance decreases despite increases in total blood volume and cardiac output (Clark *et al.*, 1989; Hytten, 1985). Uterine vascular resistance drops to a greater extent than the systemic decrease, increasing blood flow to the developing feto-placental unit. (Bird *et al.*, 2003). As discussed above, CTB remodeling of spiral arteries plays an important role in this process. In terms of other mechanisms, pregnancy is associated with an increase in vasodilators, such as nitric oxide and prostacyclin (Poston *et al.*, 1995; Suzuki *et al.*, 2002). Placental vesicles may play a role in systemic delivery of these molecules, as STB EVs contain endothelial nitric oxide synthase and nitric oxide (Motta-Mejia *et al.*, 2017). Future studies may identify a function of CTB EVs in vascular relaxation, possibly due to known vasodilators or by acting on other pathways.

Placental vesicles may promote pregnancy complications, such as hyperemesis gravidarum, a severe and dangerous form of morning sickness. The mechanisms underlying nausea and vomiting during pregnancy are not understood, but gastric dysrhythmia is observed (Austin *et al.*, 2019; Koch *et al.*, 1990). Estrogen, which increases throughout gestation, inhibits gastric smooth muscle contractility in rats (Al-Shboul *et al.*, 2019). Placental EVs may synergize with pregnancy-associated hormones to influence gut motility. Testing the effects of CTB EVs on digestive tract smooth muscle activity could yield clues to the mechanisms underlying morning sickness.

Stem cell systems for modelling human adaptation to pregnancy

The species-specificity of pancreatic adaptation to pregnancy emphasizes the rapid evolution of the placenta and highlights the need for human models (Chuong *et al.*, 2013). Labeled placental vesicles injected into mice or other model organisms may not target the correct tissues or induce pregnancy-related changes due to species-specific differences. In Chapters 3 and 4, adult human tissues were used to study functions of CTB EVs. However, acquisition of healthy adult tissue is difficult, creating a very significant barrier to probing the effects of these vesicles across different organs.

Differentiated stem cell models are an alternative to difficult-to-acquire patient samples for testing placenta-mediated maternal physiologic changes. For example, stem cells can be differentiated into neurons and other brain cell types (Dutta *et al.*, 2017). Generation of potential vesicle targets by differentiating human embryonic stem cells could be a powerful approach for studying CTB EV functions during pregnancy.

Stem cell systems for increasing cytotrophoblast extracellular vesicle yield

The biggest barrier of the work presented here was limited numbers of primary CTBs, resulting in relatively low quantities of vesicles for downstream analyses and preventing additional purification steps. Generating CTBs from blastomere-derived stem cells or trophoblast progenitor cells could provide an alternative to primary cells (Genbacev *et al.*, 2011; Zdravkovic *et al.*, 2015). This system would allow for genetic manipulation to probe specific mechanisms underlying maternal changes induced by CTB EVs. Furthermore, increased cell numbers would allow for additional purification steps required for exosome isolation or for sufficient quantities of vesicles for RNA-sequencing.

Diagnostic and therapeutic potential of placental extracellular vesicles

A deeper understanding of CTB EV contents could result in the identification of sets of biomarkers associated with normal pregnancy or pregnancy complications. The probability that this approach will be feasible is increased by the emergence of circulating tumor exosome cargo as biomarkers of cancer progression (Wong and Chen, 2019). Higher concentrations of circulating placental vesicles are a feature of preeclampsia and gestational diabetes mellitus compared to normal pregnancy, indicating that the number of EVs in maternal circulation could serve as a biomarker of these complications (Germain *et al.*, 2007; Knight *et al.*, 1998; Lok *et al.*, 2008; Salomon *et al.*, 2016).

Although this work focused on the protein contents of CTB EVs (Chapter 2), future studies should also investigate the RNA cargo of placental vesicles as well as other molecules, such as metabolites, including lipids. Comparing the contents and functions of EVs from normal placentas versus those from complicated pregnancies will identify new disease markers, allowing for the diagnosis of pregnancy-related problems such as preeclampsia and gestational diabetes mellitus before symptoms appear. Because the majority of circulating vesicles are derived from platelets (Aatonen *et al.*, 2017; Yuana *et al.*, 2014), immuno-affinity isolation would be required to separate CTB EVs from contaminating material, enriching the placental signal. Future studies using antibodies against HLA-G and PLAP would determine the feasibility of this approach.

CTB EVs themselves are likely not a viable therapy. Their contents and functions are not entirely understood; their clinical use would likely result in off-target effects. However, understanding the mechanisms could enable their co-option for therapeutic use in a range of pregnancy complications and other diseases.

For example, in Chapter 4, we report that CTB 100,000 x g EVs promoted human pancreatic β-cell proliferation and insulin production, without increasing α-cell number. The mechanism could be mimicked to correct the insulin-glucagon imbalance that characterizes both

gestational diabetes mellitus and type 2 diabetes mellitus (Beis *et al.*, 2005; Goke, 2008). Understanding the pathway could to the development of druggable targets. Alternatively, the mechanism could be used to improve stem cell differentiation into β-like cells before transplantation within an encapsulation device as a treatment for both type 1 and 2 diabetes mellitus (Figure 4.17) (Kirk *et al.*, 2014; Pepper *et al.*, 2015; Vegas *et al.*, 2016).

Understanding CTB EV functions may result in treatments for pregnancy complications. For example, uncovering how these vesicles regulate invasion would provide insight into what goes wrong in preeclampsia and placenta percreta, possibly allowing for improved diagnostics, earlier interventions, and new treatments.

Mechanisms underlying placental vesicle functions could be co-opted to treat diseases outside of pregnancy. For example, uncovering how these EVs modulate tolerance of the semi-allogeneic feto-placental unit may lead to new developments to prevent or treat organ transplant rejection or allergic diseases. Additionally, understanding the pathways involved in increasing body fat and changing distribution during pregnancy may result in the development of therapeutics for obesity. Furthermore, understanding how the placenta promotes uterine vascular relaxation could be co-opted to treat systemic high blood pressure.

Finally, understanding mechanisms underlying CTB invasion may provide insights into cancer. Carcinogenesis mimics processes required for normal pregnancy and vice versa. Tumors frequently express placenta-specific proteins, suggesting that they hijack placental pathways to promote disease progression (Bjerregaard *et al.*, 2006; Devor *et al.*, 2014). For example, in Chapter 2, I identified AHNAK, which promotes cancer invasion and vesicle release, and glia-derived nexin, which modulates vascular mimicry, in CTB EVs (Shankar *et al.*, 2010; Silva *et al.*, 2016; Wagenblast *et al.*, 2015). Additionally, these vesicles contained lactate dehydrogenase, which is secreted by glioblastoma cells to stimulate myeloid cell expression of Natural killer group 2, member D ligands (NKG2D ligands), promoting immune evasion (Crane *et al.*, 2014). Understanding how onco-fetal-placental proteins function in the original, tightly-

regulated context of pregnancy and development may provide insight into how cancer hijacks these pathways and give rise to new druggable targets. Overall, future experiments identifying mechanisms of CTB EV-mediated adaptations to pregnancy can be exploited to treat a variety of diseases and improve human health.

Chapter 6: References

AATONEN, M., VALKONEN, S., BOING, A., YUANA, Y., NIEUWLAND, R. & SILJANDER, P. 2017. Isolation of Platelet-Derived Extracellular Vesicles. *Methods Mol Biol,* 1545**,** 177-188.

ABED, M., VERSCHUEREN, E., BUDAYEVA, H., LIU, P., KIRKPATRICK, D. S., REJA, R., KUMMERFELD, S. K., WEBSTER, J. D., GIERKE, S., REICHELT, M., ANDERSON, K. R., NEWMAN, R. J., ROOSE-GIRMA, M., MODRUSAN, Z., PEKTAS, H., MALTEPE, E., NEWTON, K. & DIXIT, V. M. 2019. The Gag protein PEG10 binds to RNA and regulates trophoblast stem cell lineage specification. *PLoS One,* 14**,** e0214110.

ABELS, E. R., MAAS, S. L. N., NIELAND, L., WEI, Z., CHEAH, P. S., TAI, E., KOLSTEEG, C. J., DUSOSWA, S. A., TING, D. T., HICKMAN, S., EL KHOURY, J., KRICHEVSKY, A. M., BROEKMAN, M. L. D. & BREAKEFIELD, X. O. 2019. Glioblastoma-Associated Microglia Reprogramming Is Mediated by Functional Transfer of Extracellular miR-21. *Cell Rep,* 28**,** 3105-3119 e7.

ABRAHAMS, V. M., STRASZEWSKI-CHAVEZ, S. L., GULLER, S. & MOR, G. 2004. First trimester trophoblast cells secrete Fas ligand which induces immune cell apoptosis. *Mol Hum Reprod,* 10**,** 55-63.

ADMYRE, C., BOHLE, B., JOHANSSON, S. M., FOCKE-TEJKL, M., VALENTA, R., SCHEYNIUS, A. & GABRIELSSON, S. 2007. B cell-derived exosomes can present allergen peptides and activate allergen-specific T cells to proliferate and produce TH2-like cytokines. *J Allergy Clin Immunol,* 120**,** 1418-24.

AL-SHBOUL, O. A., AL-RSHOUD, H. J., AL-DWAIRI, A. N., ALQUDAH, M. A., ALFAQIH, M. A., MUSTAFA, A. G. & JAAFAR, M. 2019. Changes in Gastric Smooth Muscle Cell Contraction during Pregnancy: Effect of Estrogen. *J Pregnancy,* 2019**,** 4302309.

ALAM, S. M. K., JASTI, S., KSHIRSAGAR, S. K., TANNETTA, D. S., DRAGOVIC, R. A., REDMAN, C. W., SARGENT, I. L., HODES, H. C., NAUSER, T. L., FORTES, T., FILLER, A. M., BEHAN, K., MARTIN, D. R., FIELDS, T. A., PETROFF, B. K. & PETROFF, M. G. 2018. Trophoblast Glycoprotein (TPGB/5T4) in Human Placenta: Expression, Regulation, and Presence in Extracellular Microvesicles and Exosomes. *Reprod Sci,* 25**,** 185-197.

ALDO, P. B., RACICOT, K., CRAVIERO, V., GULLER, S., ROMERO, R. & MOR, G. 2014. Trophoblast induces monocyte differentiation into CD14+/CD16+ macrophages. *Am J Reprod Immunol,* 72**,** 270-84.

ALLAVENA, P., BIANCHI, G., ZHOU, D., VAN DAMME, J., JILEK, P., SOZZANI, S. & MANTOVANI, A. 1994. Induction of natural killer cell migration by monocyte chemotactic protein-1, -2 and -3. *Eur J Immunol,* 24**,** 3233-6.

ANDREOLA, G., RIVOLTINI, L., CASTELLI, C., HUBER, V., PEREGO, P., DEHO, P., SQUARCINA, P., ACCORNERO, P., LOZUPONE, F., LUGINI, L., STRINGARO, A., MOLINARI, A., ARANCIA, G., GENTILE, M., PARMIANI, G. & FAIS, S. 2002. Induction of lymphocyte apoptosis by tumor cell secretion of FasL-bearing microvesicles. *J Exp Med,* 195**,** 1303-16.

ANISOWICZ, A., MESSINEO, M., LEE, S. W. & SAGER, R. 1991. An NF-kappa B-like transcription factor mediates IL-1/TNF-alpha induction of gro in human fibroblasts. *J Immunol,* 147**,** 520-7.

ASHTON, S. V., WHITLEY, G. S., DASH, P. R., WAREING, M., CROCKER, I. P., BAKER, P. N. & CARTWRIGHT, J. E. 2005. Uterine spiral artery remodeling involves endothelial apoptosis induced by extravillous trophoblasts through Fas/FasL interactions. *Arterioscler Thromb Vasc Biol,* 25**,** 102-8.

AUSTIN, K., WILSON, K. & SAHA, S. 2019. Hyperemesis Gravidarum. *Nutr Clin Pract,* 34**,** 226-241.

BAEYENS, L., LEMPER, M., STAELS, W., DE GROEF, S., DE LEU, N., HEREMANS, Y., GERMAN, M. S. & HEIMBERG, H. 2018. (Re)generating Human Beta Cells: Status, Pitfalls, and Perspectives. *Physiol Rev,* 98**,** 1143-1167.

BALL, E., BULMER, J. N., AYIS, S., LYALL, F. & ROBSON, S. C. 2006. Late sporadic miscarriage is associated with abnormalities in spiral artery transformation and trophoblast invasion. *J Pathol,* 208**,** 535-42.

BANFER, S., SCHNEIDER, D., DEWES, J., STRAUSS, M. T., FREIBERT, S. A., HEIMERL, T., MAIER, U. G., ELSASSER, H. P., JUNGMANN, R. & JACOB, R. 2018. Molecular mechanism to recruit galectin-3 into multivesicular bodies for polarized exosomal secretion. *Proc Natl Acad Sci U S A,* 115**,** E4396-E4405.

BEIS, C., GRIGORAKIS, S. I., PHILIPPOU, G., ALEVIZAKI, M. & ANASTASIOU, E. 2005. Lack of suppression of plasma glucagon levels in late pregnancy persists postpartum only in women with previous gestational diabetes mellitus. *Acta Diabetol,* 42**,** 31-5.

BIRD, I. M., ZHANG, L. & MAGNESS, R. R. 2003. Possible mechanisms underlying pregnancy-induced changes in uterine artery endothelial function. *Am J Physiol Regul Integr Comp Physiol,* 284**,** R245-58.

BJERREGAARD, B., HOLCK, S., CHRISTENSEN, I. J. & LARSSON, L. I. 2006. Syncytin is involved in breast cancer-endothelial cell fusions. *Cell Mol Life Sci,* 63**,** 1906-11.

BOELENS, M. C., WU, T. J., NABET, B. Y., XU, B., QIU, Y., YOON, T., AZZAM, D. J., TWYMAN-SAINT VICTOR, C., WIEMANN, B. Z., ISHWARAN, H., TER BRUGGE, P. J., JONKERS, J., SLINGERLAND, J. & MINN, A. J. 2014. Exosome transfer from stromal to breast cancer cells regulates therapy resistance pathways. *Cell,* 159**,** 499-513.

BOISVERT, W. A., ROSE, D. M., JOHNSON, K. A., FUENTES, M. E., LIRA, S. A., CURTISS, L. K. & TERKELTAUB, R. A. 2006. Up-regulated expression of the CXCR2 ligand KC/GRO-alpha in atherosclerotic lesions plays a central role in macrophage accumulation and lesion progression. *Am J Pathol,* 168**,** 1385-95.

BORGHESAN, M., FAFIAN-LABORA, J., ELEFTHERIADOU, O., CARPINTERO-FERNANDEZ, P., PAEZ-RIBES, M., VIZCAY-BARRENA, G., SWISA, A., KOLODKIN-GAL, D., XIMENEZ-EMBUN, P., LOWE, R., MARTIN-MARTIN, B., PEINADO, H., MUNOZ, J., FLECK, R. A., DOR, Y., BEN-PORATH, I., VOSSENKAMPER, A., MUNOZ-ESPIN, D. & O'LOGHLEN, A. 2019. Small Extracellular Vesicles Are Key Regulators of Non-cell Autonomous Intercellular Communication in Senescence via the Interferon Protein IFITM3. *Cell Rep,* 27**,** 3956-3971 e6.

BOYSON, J. E., ERSKINE, R., WHITMAN, M. C., CHIU, M., LAU, J. M., KOOPMAN, L. A., VALTER, M. M., ANGELISOVA, P., HOREJSI, V. & STROMINGER, J. L. 2002. Disulfide bond-mediated dimerization of HLA-G on the cell surface. *Proc Natl Acad Sci U S A,* 99**,** 16180-5.

BRACH, M. A., HENSCHLER, R., MERTELSMANN, R. H. & HERRMANN, F. 1991. Regulation of M-CSF expression by M-CSF: role of protein kinase C and transcription factor NF kappa B. *Pathobiology,* 59**,** 284-8.

BREN, G. D., SOLAN, N. J., MIYOSHI, H., PENNINGTON, K. N., POBST, L. J. & PAYA, C. V. 2001. Transcription of the RelB gene is regulated by NF-kappaB. *Oncogene,* 20**,** 7722-33.

BULLEID, N. J. & ELLGAARD, L. 2011. Multiple ways to make disulfides. *Trends Biochem Sci,* 36**,** 485-92.

BUTLER, A. E., CAO-MINH, L., GALASSO, R., RIZZA, R. A., CORRADIN, A., COBELLI, C. & BUTLER, P. C. 2010. Adaptive changes in pancreatic beta cell fractional area and beta cell turnover in human pregnancy. *Diabetologia,* 53**,** 2167-76.

CAMPOY, I., LANAU, L., ALTADILL, T., SEQUEIROS, T., CABRERA, S., CUBO-ABERT, M., PEREZ-BENAVENTE, A., GARCIA, A., BORROS, S., SANTAMARIA, A., PONCE, J., MATIAS-GUIU, X., REVENTOS, J., GIL-MORENO, A., RIGAU, M. & COLAS, E. 2016.

Exosome-like vesicles in uterine aspirates: a comparison of ultracentrifugation-based isolation protocols. *J Transl Med,* 14**,** 180.

CAPELLO, M., VYKOUKAL, J. V., KATAYAMA, H., BANTIS, L. E., WANG, H., KUNDNANI, D. L., AGUILAR-BONAVIDES, C., AGUILAR, M., TRIPATHI, S. C., DHILLON, D. S., MOMIN, A. A., PETERS, H., KATZ, M. H., ALVAREZ, H., BERNARD, V., FERRI-BORGOGNO, S., BRAND, R., ADLER, D. G., FIRPO, M. A., MULVIHILL, S. J., MOLLDREM, J. J., FENG, Z., TAGUCHI, A., MAITRA, A. & HANASH, S. M. 2019. Exosomes harbor B cell targets in pancreatic adenocarcinoma and exert decoy function against complement-mediated cytotoxicity. *Nat Commun,* 10**,** 254.

CARR, M. W., ROTH, S. J., LUTHER, E., ROSE, S. S. & SPRINGER, T. A. 1994. Monocyte chemoattractant protein 1 acts as a T-lymphocyte chemoattractant. *Proc Natl Acad Sci U S A,* 91**,** 3652-6.

CHEN, G., HUANG, A. C., ZHANG, W., ZHANG, G., WU, M., XU, W., YU, Z., YANG, J., WANG, B., SUN, H., XIA, H., MAN, Q., ZHONG, W., ANTELO, L. F., WU, B., XIONG, X., LIU, X., GUAN, L., LI, T., LIU, S., YANG, R., LU, Y., DONG, L., MCGETTIGAN, S., SOMASUNDARAM, R., RADHAKRISHNAN, R., MILLS, G., LU, Y., KIM, J., CHEN, Y. H., DONG, H., ZHAO, Y., KARAKOUSIS, G. C., MITCHELL, T. C., SCHUCHTER, L. M., HERLYN, M., WHERRY, E. J., XU, X. & GUO, W. 2018. Exosomal PD-L1 contributes to immunosuppression and is associated with anti-PD-1 response. *Nature,* 560**,** 382-386.

CHOI, H. W., SUWANPRADID, J., KIM, I. H., STAATS, H. F., HANIFFA, M., MACLEOD, A. S. & ABRAHAM, S. N. 2018. Perivascular dendritic cells elicit anaphylaxis by relaying allergens to mast cells via microvesicles. *Science,* 362.

CHUONG, E. B., HANNIBAL, R. L., GREEN, S. L. & BAKER, J. C. 2013. Evolutionary perspectives into placental biology and disease. *Appl Transl Genom,* 2**,** 64-69.

CLARK, S. L., COTTON, D. B., LEE, W., BISHOP, C., HILL, T., SOUTHWICK, J., PIVARNIK, J., SPILLMAN, T., DEVORE, G. R., PHELAN, J. & ET AL. 1989. Central hemodynamic assessment of normal term pregnancy. *Am J Obstet Gynecol,* 161**,** 1439-42.

CLAYTON, A., MITCHELL, J. P., COURT, J., MASON, M. D. & TABI, Z. 2007. Human tumor-derived exosomes selectively impair lymphocyte responses to interleukin-2. *Cancer Res,* 67**,** 7458-66.

CO, E. C., GORMLEY, M., KAPIDZIC, M., ROSEN, D. B., SCOTT, M. A., STOLP, H. A., MCMASTER, M., LANIER, L. L., BARCENA, A. & FISHER, S. J. 2013. Maternal decidual macrophages inhibit NK cell killing of invasive cytotrophoblasts during human pregnancy. *Biol Reprod,* 88**,** 155.

COLLINS, B. C., HUNTER, C. L., LIU, Y., SCHILLING, B., ROSENBERGER, G., BADER, S. L., CHAN, D. W., GIBSON, B. W., GINGRAS, A. C., HELD, J. M., HIRAYAMA-KUROGI, M., HOU, G., KRISP, C., LARSEN, B., LIN, L., LIU, S., MOLLOY, M. P., MORITZ, R. L., OHTSUKI, S., SCHLAPBACH, R., SELEVSEK, N., THOMAS, S. N., TZENG, S. C., ZHANG, H. & AEBERSOLD, R. 2017. Multi-laboratory assessment of reproducibility, qualitative and quantitative performance of SWATH-mass spectrometry. *Nat Commun,* 8**,** 291.

CONDE-VANCELLS, J., RODRIGUEZ-SUAREZ, E., EMBADE, N., GIL, D., MATTHIESEN, R., VALLE, M., ELORTZA, F., LU, S. C., MATO, J. M. & FALCON-PEREZ, J. M. 2008. Characterization and comprehensive proteome profiling of exosomes secreted by hepatocytes. *J Proteome Res,* 7**,** 5157-66.

COOKSON, V. J. & CHAPMAN, N. R. 2010. NF-kappaB function in the human myometrium during pregnancy and parturition. *Histol Histopathol,* 25**,** 945-56.

CORTI, A., FASSINA, G., MARCUCCI, F., BARBANTI, E. & CASSANI, G. 1992. Oligomeric tumour necrosis factor alpha slowly converts into inactive forms at bioactive levels. *Biochem J,* 284 (Pt 3)**,** 905-10.

COSTA-SILVA, B., AIELLO, N. M., OCEAN, A. J., SINGH, S., ZHANG, H., THAKUR, B. K., BECKER, A., HOSHINO, A., MARK, M. T., MOLINA, H., XIANG, J., ZHANG, T., THEILEN, T. M., GARCIA-SANTOS, G., WILLIAMS, C., ARARSO, Y., HUANG, Y., RODRIGUES, G., SHEN, T. L., LABORI, K. J., LOTHE, I. M., KURE, E. H., HERNANDEZ, J., DOUSSOT, A., EBBESEN, S. H., GRANDGENETT, P. M., HOLLINGSWORTH, M. A., JAIN, M., MALLYA, K., BATRA, S. K., JARNAGIN, W. R., SCHWARTZ, R. E., MATEI, I., PEINADO, H., STANGER, B. Z., BROMBERG, J. & LYDEN, D. 2015. Pancreatic cancer exosomes initiate pre-metastatic niche formation in the liver. *Nat Cell Biol,* 17**,** 816-26.

COUMANS, F. A. W., BRISSON, A. R., BUZAS, E. I., DIGNAT-GEORGE, F., DREES, E. E. E., EL-ANDALOUSSI, S., EMANUELI, C., GASECKA, A., HENDRIX, A., HILL, A. F., LACROIX, R., LEE, Y., VAN LEEUWEN, T. G., MACKMAN, N., MAGER, I., NOLAN, J. P., VAN DER POL, E., PEGTEL, D. M., SAHOO, S., SILJANDER, P. R. M., STURK, G., DE WEVER, O. & NIEUWLAND, R. 2017. Methodological Guidelines to Study Extracellular Vesicles. *Circ Res,* 120**,** 1632-1648.

CRANE, C. A., AUSTGEN, K., HABERTHUR, K., HOFMANN, C., MOYES, K. W., AVANESYAN, L., FONG, L., CAMPBELL, M. J., COOPER, S., OAKES, S. A., PARSA, A. T. & LANIER, L. L. 2014. Immune evasion mediated by tumor-derived lactate dehydrogenase induction of NKG2D ligands on myeloid cells in glioblastoma patients. *Proc Natl Acad Sci U S A,* 111**,** 12823-8.

DAMSKY, C. H. & FISHER, S. J. 1998. Trophoblast pseudo-vasculogenesis: faking it with endothelial adhesion receptors. *Curr Opin Cell Biol,* 10**,** 660-6.

DAMSKY, C. H., FITZGERALD, M. L. & FISHER, S. J. 1992. Distribution patterns of extracellular matrix components and adhesion receptors are intricately modulated during first trimester cytotrophoblast differentiation along the invasive pathway, in vivo. *J Clin Invest,* 89**,** 210-22.

DE MATTEIS, R., ZINGARETTI, M. C., MURANO, I., VITALI, A., FRONTINI, A., GIANNULIS, I., BARBATELLI, G., MARCUCCI, F., BORDICCHIA, M., SARZANI, R., RAVIOLA, E. & CINTI, S. 2009. In vivo physiological transdifferentiation of adult adipose cells. *Stem Cells,* 27**,** 2761-8.

DELORME-AXFORD, E., DONKER, R. B., MOUILLET, J. F., CHU, T., BAYER, A., OUYANG, Y., WANG, T., STOLZ, D. B., SARKAR, S. N., MORELLI, A. E., SADOVSKY, Y. & COYNE, C. B. 2013. Human placental trophoblasts confer viral resistance to recipient cells. *Proc Natl Acad Sci U S A,* 110**,** 12048-53.

DEVOR, E. J., REYES, H. D., SANTILLAN, D. A., SANTILLAN, M. K., ONUKWUGHA, C., GOODHEART, M. J. & LESLIE, K. K. 2014. Placenta-specific protein 1: a potential key to many oncofetal-placental OB/GYN research questions. *Obstet Gynecol Int,* 2014**,** 678984.

DOMINGUEZ, F., MARTINEZ, S., QUINONERO, A., LORO, F., HORCAJADAS, J. A., PELLICER, A. & SIMON, C. 2008. CXCL10 and IL-6 induce chemotaxis in human trophoblast cell lines. *Mol Hum Reprod,* 14**,** 423-30.

DONG, H., STROME, S. E., SALOMAO, D. R., TAMURA, H., HIRANO, F., FLIES, D. B., ROCHE, P. C., LU, J., ZHU, G., TAMADA, K., LENNON, V. A., CELIS, E. & CHEN, L. 2002. Tumor-associated B7-H1 promotes T-cell apoptosis: a potential mechanism of immune evasion. *Nat Med,* 8**,** 793-800.

DONKER, R. B., MOUILLET, J. F., CHU, T., HUBEL, C. A., STOLZ, D. B., MORELLI, A. E. & SADOVSKY, Y. 2012. The expression profile of C19MC microRNAs in primary human trophoblast cells and exosomes. *Mol Hum Reprod,* 18**,** 417-24.

DRAGOVIC, R. A., COLLETT, G. P., HOLE, P., FERGUSON, D. J., REDMAN, C. W., SARGENT, I. L. & TANNETTA, D. S. 2015. Isolation of syncytiotrophoblast microvesicles and exosomes and their characterisation by multicolour flow cytometry and fluorescence Nanoparticle Tracking Analysis. *Methods,* 87**,** 64-74.

DRAKE, P. M., RED-HORSE, K. & FISHER, S. J. 2004. Reciprocal chemokine receptor and ligand expression in the human placenta: implications for cytotrophoblast differentiation. *Dev Dyn,* 229**,** 877-85.

DUONG, P., CHUNG, A., BOUCHAREYCHAS, L. & RAFFAI, R. L. 2019. Cushioned-Density Gradient Ultracentrifugation (C-DGUC) improves the isolation efficiency of extracellular vesicles. *PLoS One,* 14**,** e0215324.

DUTTA, D., HEO, I. & CLEVERS, H. 2017. Disease Modeling in Stem Cell-Derived 3D Organoid Systems. *Trends Mol Med,* 23**,** 393-410.

EL-AZZAMY, H., BALOGH, A., ROMERO, R., XU, Y., LAJEUNESSE, C., PLAZYO, O., XU, Z., PRICE, T. G., DONG, Z., TARCA, A. L., PAPP, Z., HASSAN, S. S., CHAIWORAPONGSA, T., KIM, C. J., GOMEZ-LOPEZ, N. & THAN, N. G. 2017. Characteristic Changes in Decidual Gene Expression Signature in Spontaneous Term Parturition. *J Pathol Transl Med,* 51**,** 264-283.

ELLIS, S. A., SARGENT, I. L., REDMAN, C. W. & MCMICHAEL, A. J. 1986. Evidence for a novel HLA antigen found on human extravillous trophoblast and a choriocarcinoma cell line. *Immunology,* 59**,** 595-601.

EVANS, J., RAI, A., NGUYEN, H. P. T., POH, Q. H., ELGLASS, K., SIMPSON, R. J., SALAMONSEN, L. A. & GREENING, D. W. 2019. Human Endometrial Extracellular Vesicles Functionally Prepare Human Trophectoderm Model for Implantation: Understanding Bidirectional Maternal-Embryo Communication. *Proteomics***,** e1800423.

FISHER, S. J. 2015. Why is placentation abnormal in preeclampsia? *Am J Obstet Gynecol,* 213**,** S115-22.

FLAHERTY, S. E., 3RD, GRIJALVA, A., XU, X., ABLES, E., NOMANI, A. & FERRANTE, A. W., JR. 2019. A lipase-independent pathway of lipid release and immune modulation by adipocytes. *Science,* 363**,** 989-993.

FRANZ, C., BOING, A. N., MONTAG, M., STROWITZKI, T., MARKERT, U. R., MASTENBROEK, S., NIEUWLAND, R. & TOTH, B. 2016. Extracellular vesicles in human follicular fluid do not promote coagulation. *Reprod Biomed Online,* 33**,** 652-655.

GAMEZ-VALERO, A., MONGUIO-TORTAJADA, M., CARRERAS-PLANELLA, L., FRANQUESA, M., BEYER, K. & BORRAS, F. E. 2016. Size-Exclusion Chromatography-based isolation minimally alters Extracellular Vesicles' characteristics compared to precipitating agents. *Sci Rep,* 6**,** 33641.

GAO, W., LIU, H., YUAN, J., WU, C., HUANG, D., MA, Y., ZHU, J., MA, L., GUO, J., SHI, H., ZOU, Y. & GE, J. 2016. Exosomes derived from mature dendritic cells increase endothelial inflammation and atherosclerosis via membrane TNF-alpha mediated NF-kappaB pathway. *J Cell Mol Med,* 20**,** 2318-2327.

GARRICK, M. D. 2011. Human iron transporters. *Genes Nutr,* 6**,** 45-54.

GAW, S. L., HROMATKA, B. S., NGELEZA, S., BUARPUNG, S., OZARSLAN, N., TSHEFU, A. & FISHER, S. J. 2019. Differential Activation of Fetal Hofbauer Cells in Primigravidas Is Associated with Decreased Birth Weight in Symptomatic Placental Malaria. *Malar Res Treat,* 2019**,** 1378174.

GENBACEV, O., DONNE, M., KAPIDZIC, M., GORMLEY, M., LAMB, J., GILMORE, J., LAROCQUE, N., GOLDFIEN, G., ZDRAVKOVIC, T., MCMASTER, M. T. & FISHER, S. J. 2011. Establishment of human trophoblast progenitor cell lines from the chorion. *Stem Cells,* 29**,** 1427-36.

GERMAIN, S. J., SACKS, G. P., SOORANNA, S. R., SARGENT, I. L. & REDMAN, C. W. 2007. Systemic inflammatory priming in normal pregnancy and preeclampsia: the role of circulating syncytiotrophoblast microparticles. *J Immunol,* 178**,** 5949-56.

GOKE, B. 2008. Islet cell function: alpha and beta cells--partners towards normoglycaemia. *Int J Clin Pract Suppl***,** 2-7.

GRANGE, C., TAPPARO, M., TRITTA, S., DEREGIBUS, M. C., BATTAGLIA, A., GONTERO, P., FREA, B. & CAMUSSI, G. 2015. Role of HLA-G and extracellular vesicles in renal cancer stem cell-induced inhibition of dendritic cell differentiation. *BMC Cancer,* 15**,** 1009.

GREENING, D. W., NGUYEN, H. P., ELGASS, K., SIMPSON, R. J. & SALAMONSEN, L. A. 2016. Human Endometrial Exosomes Contain Hormone-Specific Cargo Modulating Trophoblast Adhesive Capacity: Insights into Endometrial-Embryo Interactions. *Biol Reprod,* 94**,** 38.

GRIFFITH, O. W., CHAVAN, A. R., PROTOPAPAS, S., MAZIARZ, J., ROMERO, R. & WAGNER, G. P. 2017. Embryo implantation evolved from an ancestral inflammatory attachment reaction. *Proc Natl Acad Sci U S A,* 114**,** E6566-E6575.

GUESCINI, M., GENEDANI, S., STOCCHI, V. & AGNATI, L. F. 2010. Astrocytes and Glioblastoma cells release exosomes carrying mtDNA. *J Neural Transm (Vienna),* 117**,** 1-4.

GUPTA, A. K., RUSTERHOLZ, C., HOLZGREVE, W. & HAHN, S. 2005a. Syncytiotrophoblast micro-particles do not induce apoptosis in peripheral T lymphocytes, but differ in their activity depending on the mode of preparation. *J Reprod Immunol,* 68**,** 15-26.

GUPTA, A. K., RUSTERHOLZ, C., HUPPERTZ, B., MALEK, A., SCHNEIDER, H., HOLZGREVE, W. & HAHN, S. 2005b. A comparative study of the effect of three different syncytiotrophoblast micro-particles preparations on endothelial cells. *Placenta,* 26**,** 59-66.

HADERK, F., SCHULZ, R., ISKAR, M., CID, L. L., WORST, T., WILLMUND, K. V., SCHULZ, A., WARNKEN, U., SEILER, J., BENNER, A., NESSLING, M., ZENZ, T., GOBEL, M., DURIG, J., DIEDERICHS, S., PAGGETTI, J., MOUSSAY, E., STILGENBAUER, S., ZAPATKA, M., LICHTER, P. & SEIFFERT, M. 2017. Tumor-derived exosomes modulate PD-L1 expression in monocytes. *Sci Immunol,* 2.

HANNA, J., GOLDMAN-WOHL, D., HAMANI, Y., AVRAHAM, I., GREENFIELD, C., NATANSON-YARON, S., PRUS, D., COHEN-DANIEL, L., ARNON, T. I., MANASTER, I., GAZIT, R., YUTKIN, V., BENHARROCH, D., PORGADOR, A., KESHET, E., YAGEL, S. & MANDELBOIM, O. 2006. Decidual NK cells regulate key developmental processes at the human fetal-maternal interface. *Nat Med,* 12**,** 1065-74.

HANNAN, N. J., PAIVA, P., DIMITRIADIS, E. & SALAMONSEN, L. A. 2010. Models for study of human embryo implantation: choice of cell lines? *Biol Reprod,* 82**,** 235-45.

HAO, S., BAI, O., LI, F., YUAN, J., LAFERTE, S. & XIANG, J. 2007. Mature dendritic cells pulsed with exosomes stimulate efficient cytotoxic T-lymphocyte responses and antitumour immunity. *Immunology,* 120**,** 90-102.

HARDING, C., HEUSER, J. & STAHL, P. 1984. Endocytosis and intracellular processing of transferrin and colloidal gold-transferrin in rat reticulocytes: demonstration of a pathway for receptor shedding. *Eur J Cell Biol,* 35**,** 256-63.

HARRIS, L. K., KEOGH, R. J., WAREING, M., BAKER, P. N., CARTWRIGHT, J. E., APLIN, J. D. & WHITLEY, G. S. 2006. Invasive trophoblasts stimulate vascular smooth muscle cell apoptosis by a fas ligand-dependent mechanism. *Am J Pathol,* 169**,** 1863-74.

HEMBERGER, M. 2013. Immune balance at the foeto-maternal interface as the fulcrum of reproductive success. *J Reprod Immunol,* 97**,** 36-42.

HESS, A. P., HAMILTON, A. E., TALBI, S., DOSIOU, C., NYEGAARD, M., NAYAK, N., GENBECEV-KRTOLICA, O., MAVROGIANIS, P., FERRER, K., KRUESSEL, J., FAZLEABAS, A. T., FISHER, S. J. & GIUDICE, L. C. 2007. Decidual stromal cell response to paracrine signals from the trophoblast: amplification of immune and angiogenic modulators. *Biol Reprod,* 76**,** 102-17.

HESSVIK, N. P. & LLORENTE, A. 2018. Current knowledge on exosome biogenesis and release. *Cell Mol Life Sci,* 75**,** 193-208.

HOELTZENBEIN, M., BECK, E., RAJWANSHI, R., GOTESTAM SKORPEN, C., BERBER, E., SCHAEFER, C. & OSTENSEN, M. 2016. Tocilizumab use in pregnancy: Analysis of a global safety database including data from clinical trials and post-marketing data. *Semin Arthritis Rheum,* 46**,** 238-245.

HOHENSINNER, P. J., KAUN, C., RYCHLI, K., NIESSNER, A., PFAFFENBERGER, S., REGA, G., DE MARTIN, R., MAURER, G., ULLRICH, R., HUBER, K. & WOJTA, J. 2007. Macrophage colony stimulating factor expression in human cardiac cells is upregulated by tumor necrosis factor-alpha via an NF-kappaB dependent mechanism. *J Thromb Haemost,* 5**,** 2520-8.

HOLDER, B., JONES, T., SANCHO SHIMIZU, V., RICE, T. F., DONALDSON, B., BOUQUEAU, M., FORBES, K. & KAMPMANN, B. 2016. Macrophage Exosomes Induce Placental Inflammatory Cytokines: A Novel Mode of Maternal-Placental Messaging. *Traffic,* 17**,** 168-78.

HOLLISTER, A., OKUBARA, P., WATSON, J. G. & CHAYKIN, S. 1987. Reproduction in mice: liver enlargement in mice during pregnancy and lactation. *Life Sci,* 40**,** 11-8.

HOOG, J. L. & LOTVALL, J. 2015. Diversity of extracellular vesicles in human ejaculates revealed by cryo-electron microscopy. *J Extracell Vesicles,* 4**,** 28680.

HOSHINO, A., COSTA-SILVA, B., SHEN, T. L., RODRIGUES, G., HASHIMOTO, A., TESIC MARK, M., MOLINA, H., KOHSAKA, S., DI GIANNATALE, A., CEDER, S., SINGH, S., WILLIAMS, C., SOPLOP, N., URYU, K., PHARMER, L., KING, T., BOJMAR, L., DAVIES, A. E., ARARSO, Y., ZHANG, T., ZHANG, H., HERNANDEZ, J., WEISS, J. M., DUMONT-COLE, V. D., KRAMER, K., WEXLER, L. H., NARENDRAN, A., SCHWARTZ, G. K., HEALEY, J. H., SANDSTROM, P., LABORI, K. J., KURE, E. H., GRANDGENETT, P. M., HOLLINGSWORTH, M. A., DE SOUSA, M., KAUR, S., JAIN, M., MALLYA, K., BATRA, S. K., JARNAGIN, W. R., BRADY, M. S., FODSTAD, O., MULLER, V., PANTEL, K., MINN, A. J., BISSELL, M. J., GARCIA, B. A., KANG, Y., RAJASEKHAR, V.

K., GHAJAR, C. M., MATEI, I., PEINADO, H., BROMBERG, J. & LYDEN, D. 2015. Tumour exosome integrins determine organotropic metastasis. *Nature,* 527**,** 329-35.

HOUSHDARAN, S., ZELENKO, Z., IRWIN, J. C. & GIUDICE, L. C. 2014. Human endometrial DNA methylome is cycle-dependent and is associated with gene expression regulation. *Mol Endocrinol,* 28**,** 1118-35.

HUANG, D. W., SHERMAN, B. T., TAN, Q., COLLINS, J. R., ALVORD, W. G., ROAYAEI, J., STEPHENS, R., BASELER, M. W., LANE, H. C. & LEMPICKI, R. A. 2007. The DAVID Gene Functional Classification Tool: a novel biological module-centric algorithm to functionally analyze large gene lists. *Genome Biol,* 8**,** R183.

HUANG, Z. & FENG, Y. 2017. Exosomes Derived From Hypoxic Colorectal Cancer Cells Promote Angiogenesis Through Wnt4-Induced beta-Catenin Signaling in Endothelial Cells. *Oncol Res,* 25**,** 651-661.

HUNKAPILLER, N. M. & FISHER, S. J. 2008. Chapter 12. Placental remodeling of the uterine vasculature. *Methods Enzymol,* 445**,** 281-302.

HYTTEN, F. 1985. Blood volume changes in normal pregnancy. *Clin Haematol,* 14**,** 601-12.

IRWIN, J. C., KIRK, D., KING, R. J., QUIGLEY, M. M. & GWATKIN, R. B. 1989. Hormonal regulation of human endometrial stromal cells in culture: an in vitro model for decidualization. *Fertil Steril,* 52**,** 761-8.

JI, Y., QI, D., LI, L., SU, H., LI, X., LUO, Y., SUN, B., ZHANG, F., LIN, B., LIU, T. & LU, Y. 2019. Multiplexed profiling of single-cell extracellular vesicles secretion. *Proc Natl Acad Sci U S A,* 116**,** 5979-5984.

JOHANSEN, C. B., JIMENEZ-SOLEM, E., HAERSKJOLD, A., SAND, F. L. & THOMSEN, S. F. 2018. The Use and Safety of TNF Inhibitors during Pregnancy in Women with Psoriasis: A Review. *Int J Mol Sci,* 19.

KANADA, M., BACHMANN, M. H., HARDY, J. W., FRIMANNSON, D. O., BRONSART, L., WANG, A., SYLVESTER, M. D., SCHMIDT, T. L., KASPAR, R. L., BUTTE, M. J.,

MATIN, A. C. & CONTAG, C. H. 2015. Differential fates of biomolecules delivered to target cells via extracellular vesicles. *Proc Natl Acad Sci U S A,* 112**,** E1433-42.

KANDZIJA, N., ZHANG, W., MOTTA-MEJIA, C., MHLOMI, V., MCGOWAN-DOWNEY, J., JAMES, T., CERDEIRA, A. S., TANNETTA, D., SARGENT, I., REDMAN, C. W., BASTIE, C. C. & VATISH, M. 2019. Placental extracellular vesicles express active dipeptidyl peptidase IV; levels are increased in gestational diabetes mellitus. *J Extracell Vesicles,* 8**,** 1617000.

KANG, H. B., KIM, Y. E., KWON, H. J., SOK, D. E. & LEE, Y. 2007. Enhancement of NF-kappaB expression and activity upon differentiation of human embryonic stem cell line SNUhES3. *Stem Cells Dev,* 16**,** 615-23.

KELLY, R. W., HOLLAND, P., SKIBINSKI, G., HARRISON, C., MCMILLAN, L., HARGREAVE, T. & JAMES, K. 1991. Extracellular organelles (prostasomes) are immunosuppressive components of human semen. *Clin Exp Immunol,* 86**,** 550-6.

KIM, C., BERGER, D. K. & CHAMANY, S. 2007. Recurrence of gestational diabetes mellitus: a systematic review. *Diabetes Care,* 30**,** 1314-9.

KIM, H., TOYOFUKU, Y., LYNN, F. C., CHAK, E., UCHIDA, T., MIZUKAMI, H., FUJITANI, Y., KAWAMORI, R., MIYATSUKA, T., KOSAKA, Y., YANG, K., HONIG, G., VAN DER HART, M., KISHIMOTO, N., WANG, J., YAGIHASHI, S., TECOTT, L. H., WATADA, H. & GERMAN, M. S. 2010. Serotonin regulates pancreatic beta cell mass during pregnancy. *Nat Med,* 16**,** 804-8.

KINDELBERGER, D. W. & NUCCI, M. R. 2009. Benign Endometrium. *In:* NUCCI, M. R. & OLIVA, E. (eds.) *Gynecologic Pathology: A Volume in the Series: Foundations in Diagnostic Pathology.* Elsevier Health Sciences.

KIRK, K., HAO, E., LAHMY, R. & ITKIN-ANSARI, P. 2014. Human embryonic stem cell derived islet progenitors mature inside an encapsulation device without evidence of increased biomass or cell escape. *Stem Cell Res,* 12**,** 807-14.

KNIGHT, M., REDMAN, C. W., LINTON, E. A. & SARGENT, I. L. 1998. Shedding of syncytiotrophoblast microvilli into the maternal circulation in pre-eclamptic pregnancies. *Br J Obstet Gynaecol,* 105**,** 632-40.

KOCH, K. L., STERN, R. M., VASEY, M., BOTTI, J. J., CREASY, G. W. & DWYER, A. 1990. Gastric dysrhythmias and nausea of pregnancy. *Dig Dis Sci,* 35**,** 961-8.

KOVATS, S., MAIN, E. K., LIBRACH, C., STUBBLEBINE, M., FISHER, S. J. & DEMARS, R. 1990. A class I antigen, HLA-G, expressed in human trophoblasts. *Science,* 248**,** 220-3.

KUNSCH, C. & ROSEN, C. A. 1993. NF-kappa B subunit-specific regulation of the interleukin-8 promoter. *Mol Cell Biol,* 13**,** 6137-46.

LAIN, K. Y. & CATALANO, P. M. 2007. Metabolic changes in pregnancy. *Clin Obstet Gynecol,* 50**,** 938-48.

LEE, H. M., CHOI, E. J., KIM, J. H., KIM, T. D., KIM, Y. K., KANG, C. & GHO, Y. S. 2010. A membranous form of ICAM-1 on exosomes efficiently blocks leukocyte adhesion to activated endothelial cells. *Biochem Biophys Res Commun,* 397**,** 251-6.

LIBERMANN, T. A. & BALTIMORE, D. 1990. Activation of interleukin-6 gene expression through the NF-kappa B transcription factor. *Mol Cell Biol,* 10**,** 2327-34.

LOK, C. A., VAN DER POST, J. A., SARGENT, I. L., HAU, C. M., STURK, A., BOER, K. & NIEUWLAND, R. 2008. Changes in microparticle numbers and cellular origin during pregnancy and preeclampsia. *Hypertens Pregnancy,* 27**,** 344-60.

LOKOSSOU, A. G., TOUDIC, C., NGUYEN, P. T., ELISSEEFF, X., VARGAS, A., RASSART, E., LAFOND, J., LEDUC, L., BOURGAULT, S., GILBERT, C., SCORZA, T., TOLOSA, J. & BARBEAU, B. 2019. Endogenous retrovirus-encoded Syncytin-2 contributes to exosome-mediated immunosuppression of T cells. *Biol Reprod*.

LOMBARDI, L., CIANA, P., CAPPELLINI, C., TRECCA, D., GUERRINI, L., MIGLIAZZA, A., MAIOLO, A. T. & NERI, A. 1995. Structural and functional characterization of the promoter regions of the NFKB2 gene. *Nucleic Acids Res,* 23**,** 2328-36.

LU, B., RUTLEDGE, B. J., GU, L., FIORILLO, J., LUKACS, N. W., KUNKEL, S. L., NORTH, R., GERARD, C. & ROLLINS, B. J. 1998. Abnormalities in monocyte recruitment and cytokine expression in monocyte chemoattractant protein 1-deficient mice. *J Exp Med,* 187**,** 601-8.

LYNCH, S., SANTOS, S. G., CAMPBELL, E. C., NIMMO, A. M., BOTTING, C., PRESCOTT, A., ANTONIOU, A. N. & POWIS, S. J. 2009. Novel MHC class I structures on exosomes. *J Immunol,* 183**,** 1884-91.

MACKENZIE, A., WILSON, H. L., KISS-TOTH, E., DOWER, S. K., NORTH, R. A. & SURPRENANT, A. 2001. Rapid secretion of interleukin-1beta by microvesicle shedding. *Immunity,* 15**,** 825-35.

MALTEPE, E. & FISHER, S. J. 2015. Placenta: the forgotten organ. *Annu Rev Cell Dev Biol,* 31**,** 523-52.

MARINO, M. W., DUNN, A., GRAIL, D., INGLESE, M., NOGUCHI, Y., RICHARDS, E., JUNGBLUTH, A., WADA, H., MOORE, M., WILLIAMSON, B., BASU, S. & OLD, L. J. 1997. Characterization of tumor necrosis factor-deficient mice. *Proc Natl Acad Sci U S A,* 94**,** 8093-8.

MATSUSHIMA, K., LARSEN, C. G., DUBOIS, G. C. & OPPENHEIM, J. J. 1989. Purification and characterization of a novel monocyte chemotactic and activating factor produced by a human myelomonocytic cell line. *J Exp Med,* 169**,** 1485-90.

MCMASTER, M., ZHOU, Y., SHORTER, S., KAPASI, K., GERAGHTY, D., LIM, K. H. & FISHER, S. 1998. HLA-G isoforms produced by placental cytotrophoblasts and found in amniotic fluid are due to unusual glycosylation. *J Immunol,* 160**,** 5922-8.

MCMASTER, M. T., LIBRACH, C. L., ZHOU, Y., LIM, K. H., JANATPOUR, M. J., DEMARS, R., KOVATS, S., DAMSKY, C. & FISHER, S. J. 1995. Human placental HLA-G expression is restricted to differentiated cytotrophoblasts. *J Immunol,* 154**,** 3771-8.

MCNALLY, S. & STEIN, T. 2017. Overview of Mammary Gland Development: A Comparison of Mouse and Human. *Methods Mol Biol,* 1501**,** 1-17.

MEDINA, J. & WORKMAN, J. L. 2018. Maternal experience and adult neurogenesis in mammals: Implications for maternal care, cognition, and mental health. *J Neurosci Res*.

MESSERLI, M., MAY, K., HANSSON, S. R., SCHNEIDER, H., HOLZGREVE, W., HAHN, S. & RUSTERHOLZ, C. 2010. Feto-maternal interactions in pregnancies: placental microparticles activate peripheral blood monocytes. *Placenta,* 31**,** 106-12.

MONTECALVO, A., SHUFESKY, W. J., STOLZ, D. B., SULLIVAN, M. G., WANG, Z., DIVITO, S. J., PAPWORTH, G. D., WATKINS, S. C., ROBBINS, P. D., LARREGINA, A. T. & MORELLI, A. E. 2008. Exosomes as a short-range mechanism to spread alloantigen between dendritic cells during T cell allorecognition. *J Immunol,* 180**,** 3081-90.

MORRONI, M., GIORDANO, A., ZINGARETTI, M. C., BOIANI, R., DE MATTEIS, R., KAHN, B. B., NISOLI, E., TONELLO, C., PISOSCHI, C., LUCHETTI, M. M., MARELLI, M. & CINTI, S. 2004. Reversible transdifferentiation of secretory epithelial cells into adipocytes in the mammary gland. *Proc Natl Acad Sci U S A,* 101**,** 16801-6.

MOTTA-MEJIA, C., KANDZIJA, N., ZHANG, W., MHLOMI, V., CERDEIRA, A. S., BURDUJAN, A., TANNETTA, D., DRAGOVIC, R., SARGENT, I. L., REDMAN, C. W., KISHORE, U. & VATISH, M. 2017. Placental Vesicles Carry Active Endothelial Nitric Oxide Synthase and Their Activity is Reduced in Preeclampsia. *Hypertension,* 70**,** 372-381.

MUNICH, S., SOBO-VUJANOVIC, A., BUCHSER, W. J., BEER-STOLZ, D. & VUJANOVIC, N. L. 2012. Dendritic cell exosomes directly kill tumor cells and activate natural killer cells via TNF superfamily ligands. *Oncoimmunology,* 1**,** 1074-1083.

MURDICA, V., GIACOMINI, E., ALTERI, A., BARTOLACCI, A., CERMISONI, G. C., ZAROVNI, N., PAPALEO, E., MONTORSI, F., SALONIA, A., VIGANO, P. & VAGO, R. 2019. Seminal plasma of men with severe asthenozoospermia contain exosomes that affect spermatozoa motility and capacitation. *Fertil Steril,* 111**,** 897-908 e2.

NABET, B. Y., QIU, Y., SHABASON, J. E., WU, T. J., YOON, T., KIM, B. C., BENCI, J. L., DEMICHELE, A. M., TCHOU, J., MARCOTRIGIANO, J. & MINN, A. J. 2017. Exosome RNA Unshielding Couples Stromal Activation to Pattern Recognition Receptor Signaling in Cancer. *Cell,* 170**,** 352-366 e13.

NAKAMURA, H., KIMURA, T., OGITA, K., KOYAMA, S., TSUJIE, T., TSUTSUI, T., SHIMOYA, K., KOYAMA, M., KANEDA, Y. & MURATA, Y. 2004. Alteration of the timing of implantation by in vivo gene transfer: delay of implantation by suppression of nuclear factor kappaB activity and partial rescue by leukemia inhibitory factor. *Biochem Biophys Res Commun,* 321**,** 886-92.

NANCY, P., TAGLIANI, E., TAY, C. S., ASP, P., LEVY, D. E. & ERLEBACHER, A. 2012. Chemokine gene silencing in decidual stromal cells limits T cell access to the maternal-fetal interface. *Science,* 336**,** 1317-21.

NG, Y. H., ROME, S., JALABERT, A., FORTERRE, A., SINGH, H., HINCKS, C. L. & SALAMONSEN, L. A. 2013. Endometrial exosomes/microvesicles in the uterine microenvironment: a new paradigm for embryo-endometrial cross talk at implantation. *PLoS One,* 8**,** e58502.

NOVAKOVIC, B., GORDON, L., WONG, N. C., MOFFETT, A., MANUELPILLAI, U., CRAIG, J. M., SHARKEY, A. & SAFFERY, R. 2011. Wide-ranging DNA methylation differences of primary trophoblast cell populations and derived cell lines: implications and opportunities for understanding trophoblast function. *Mol Hum Reprod,* 17**,** 344-53.

OBER, C., ALDRICH, C., ROSINSKY, B., ROBERTSON, A., WALKER, M. A., WILLADSEN, S., VERP, M. S., GERAGHTY, D. E. & HUNT, J. S. 1998. HLA-G1 protein expression is not essential for fetal survival. *Placenta,* 19**,** 127-32.

OBER, C., ALDRICH, C. L., CHERVONEVA, I., BILLSTRAND, C., RAHIMOV, F., GRAY, H. L. & HYSLOP, T. 2003. Variation in the HLA-G promoter region influences miscarriage rates. *Am J Hum Genet,* 72**,** 1425-35.

OBREGON, C., ROTHEN-RUTISHAUSER, B., GERBER, P., GEHR, P. & NICOD, L. P. 2009. Active uptake of dendritic cell-derived exovesicles by epithelial cells induces the release of inflammatory mediators through a TNF-alpha-mediated pathway. *Am J Pathol,* 175**,** 696-705.

OECKINGHAUS, A. & GHOSH, S. 2009. The NF-kappaB family of transcription factors and its regulation. *Cold Spring Harb Perspect Biol,* 1**,** a000034.

OHARA-IMAIZUMI, M., KIM, H., YOSHIDA, M., FUJIWARA, T., AOYAGI, K., TOYOFUKU, Y., NAKAMICHI, Y., NISHIWAKI, C., OKAMURA, T., UCHIDA, T., FUJITANI, Y., AKAGAWA, K., KAKEI, M., WATADA, H., GERMAN, M. S. & NAGAMATSU, S. 2013. Serotonin regulates glucose-stimulated insulin secretion from pancreatic beta cells during pregnancy. *Proc Natl Acad Sci U S A,* 110**,** 19420-5.

ONO, M., KOSAKA, N., TOMINAGA, N., YOSHIOKA, Y., TAKESHITA, F., TAKAHASHI, R. U., YOSHIDA, M., TSUDA, H., TAMURA, K. & OCHIYA, T. 2014. Exosomes from bone marrow mesenchymal stem cells contain a microRNA that promotes dormancy in metastatic breast cancer cells. *Sci Signal,* 7**,** ra63.

OSMERS, R. G., BLASER, J., KUHN, W. & TSCHESCHE, H. 1995. Interleukin-8 synthesis and the onset of labor. *Obstet Gynecol,* 86**,** 223-9.

OUYANG, Y., BAYER, A., CHU, T., TYURIN, V. A., KAGAN, V. E., MORELLI, A. E., COYNE, C. B. & SADOVSKY, Y. 2016. Isolation of human trophoblastic extracellular vesicles and characterization of their cargo and antiviral activity. *Placenta,* 47**,** 86-95.

PAKTINAT, S., HASHEMI, S. M., GHAFFARI NOVIN, M., MOHAMMADI-YEGANEH, S., SALEHPOUR, S., KARAMIAN, A. & NAZARIAN, H. 2019. Seminal exosomes induce interleukin-6 and interleukin-8 secretion by human endometrial stromal cells. *Eur J Obstet Gynecol Reprod Biol,* 235**,** 71-76.

PAN, B. T., TENG, K., WU, C., ADAM, M. & JOHNSTONE, R. M. 1985. Electron microscopic evidence for externalization of the transferrin receptor in vesicular form in sheep reticulocytes. *J Cell Biol,* 101**,** 942-8.

PARSONS, J. A., BRELJE, T. C. & SORENSON, R. L. 1992. Adaptation of islets of Langerhans to pregnancy: increased islet cell proliferation and insulin secretion correlates with the onset of placental lactogen secretion. *Endocrinology,* 130**,** 1459-66.

PASCOLO, S., GINHOUX, F., LAHAM, N., WALTER, S., SCHOOR, O., PROBST, J., ROHRLICH, P., OBERMAYR, F., FISCH, P., DANOS, O., EHRLICH, R., LEMONNIER, F. A. & RAMMENSEE, H. G. 2005. The non-classical HLA class I molecule HFE does not influence the NK-like activity contained in fresh human PBMCs and does not interact with NK cells. *Int Immunol,* 17**,** 117-22.

PASPARAKIS, M., ALEXOPOULOU, L., EPISKOPOU, V. & KOLLIAS, G. 1996. Immune and inflammatory responses in TNF alpha-deficient mice: a critical requirement for TNF alpha in the formation of primary B cell follicles, follicular dendritic cell networks and germinal centers, and in the maturation of the humoral immune response. *J Exp Med,* 184**,** 1397-411.

PATEL, G. K., KHAN, M. A., ZUBAIR, H., SRIVASTAVA, S. K., KHUSHMAN, M., SINGH, S. & SINGH, A. P. 2019. Comparative analysis of exosome isolation methods using culture supernatant for optimum yield, purity and downstream applications. *Sci Rep,* 9**,** 5335.

PATHIPATI, P., GORBA, T., SCHEEPENS, A., GOFFIN, V., SUN, Y. & FRASER, M. 2011. Growth hormone and prolactin regulate human neural stem cell regenerative activity. *Neuroscience,* 190**,** 409-27.

PAVLYUKOV, M. S., YU, H., BASTOLA, S., MINATA, M., SHENDER, V. O., LEE, Y., ZHANG, S., WANG, J., KOMAROVA, S., WANG, J., YAMAGUCHI, S., ALSHEIKH, H. A., SHI, J., CHEN, D., MOHYELDIN, A., KIM, S. H., SHIN, Y. J., ANUFRIEVA, K., EVTUSHENKO, E. G., ANTIPOVA, N. V., ARAPIDI, G. P., GOVORUN, V., PESTOV, N. B.,

SHAKHPARONOV, M. I., LEE, L. J., NAM, D. H. & NAKANO, I. 2018. Apoptotic Cell-Derived Extracellular Vesicles Promote Malignancy of Glioblastoma Via Intercellular Transfer of Splicing Factors. *Cancer Cell,* 34**,** 119-135 e10.

PEINADO, H., ALECKOVIC, M., LAVOTSHKIN, S., MATEI, I., COSTA-SILVA, B., MORENO-BUENO, G., HERGUETA-REDONDO, M., WILLIAMS, C., GARCIA-SANTOS, G., GHAJAR, C., NITADORI-HOSHINO, A., HOFFMAN, C., BADAL, K., GARCIA, B. A., CALLAHAN, M. K., YUAN, J., MARTINS, V. R., SKOG, J., KAPLAN, R. N., BRADY, M. S., WOLCHOK, J. D., CHAPMAN, P. B., KANG, Y., BROMBERG, J. & LYDEN, D. 2012. Melanoma exosomes educate bone marrow progenitor cells toward a pro-metastatic phenotype through MET. *Nat Med,* 18**,** 883-91.

PEPPER, A. R., GALA-LOPEZ, B., PAWLICK, R., MERANI, S., KIN, T. & SHAPIRO, A. M. 2015. A prevascularized subcutaneous device-less site for islet and cellular transplantation. *Nat Biotechnol,* 33**,** 518-23.

PIJNENBORG, R., MCLAUGHLIN, P. J., VERCRUYSSE, L., HANSSENS, M., JOHNSON, P. M., KEITH, J. C., JR. & VAN ASSCHE, F. A. 1998. Immunolocalization of tumour necrosis factor-alpha (TNF-alpha) in the placental bed of normotensive and hypertensive human pregnancies. *Placenta,* 19**,** 231-9.

POGGIO, M., HU, T., PAI, C. C., CHU, B., BELAIR, C. D., CHANG, A., MONTABANA, E., LANG, U. E., FU, Q., FONG, L. & BLELLOCH, R. 2019. Suppression of Exosomal PD-L1 Induces Systemic Anti-tumor Immunity and Memory. *Cell,* 177**,** 414-427 e13.

POSTON, L., MCCARTHY, A. L. & RITTER, J. M. 1995. Control of vascular resistance in the maternal and feto-placental arterial beds. *Pharmacol Ther,* 65**,** 215-39.

PROKESCH, A., SMORLESI, A., PERUGINI, J., MANIERI, M., CIARMELA, P., MONDINI, E., TRAJANOSKI, Z., KRISTIANSEN, K., GIORDANO, A., BOGNER-STRAUSS, J. G. & CINTI, S. 2014. Molecular aspects of adipoepithelial transdifferentiation in mouse mammary gland. *Stem Cells,* 32**,** 2756-66.

RAPOSO, G., NIJMAN, H. W., STOORVOGEL, W., LIEJENDEKKER, R., HARDING, C. V., MELIEF, C. J. & GEUZE, H. J. 1996. B lymphocytes secrete antigen-presenting vesicles. *J Exp Med,* 183**,** 1161-72.

RAPOSO, G. & STOORVOGEL, W. 2013. Extracellular vesicles: exosomes, microvesicles, and friends. *J Cell Biol,* 200**,** 373-83.

RED-HORSE, K., DRAKE, P. M., GUNN, M. D. & FISHER, S. J. 2001. Chemokine ligand and receptor expression in the pregnant uterus: reciprocal patterns in complementary cell subsets suggest functional roles. *Am J Pathol,* 159**,** 2199-213.

RED-HORSE, K., KAPIDZIC, M., ZHOU, Y., FENG, K. T., SINGH, H. & FISHER, S. J. 2005. EPHB4 regulates chemokine-evoked trophoblast responses: a mechanism for incorporating the human placenta into the maternal circulation. *Development,* 132**,** 4097-106.

RED-HORSE, K., RIVERA, J., SCHANZ, A., ZHOU, Y., WINN, V., KAPIDZIC, M., MALTEPE, E., OKAZAKI, K., KOCHMAN, R., VO, K. C., GIUDICE, L., ERLEBACHER, A., MCCUNE, J. M., STODDART, C. A. & FISHER, S. J. 2006. Cytotrophoblast induction of arterial apoptosis and lymphangiogenesis in an in vivo model of human placentation. *J Clin Invest,* 116**,** 2643-52.

REYES, L., WOLFE, B. & GOLOS, T. 2017. Hofbauer Cells: Placental Macrophages of Fetal Origin. *Results Probl Cell Differ,* 62**,** 45-60.

RICKLEFS, F. L., ALAYO, Q., KRENZLIN, H., MAHMOUD, A. B., SPERANZA, M. C., NAKASHIMA, H., HAYES, J. L., LEE, K., BALAJ, L., PASSARO, C., ROOJ, A. K., KRASEMANN, S., CARTER, B. S., CHEN, C. C., STEED, T., TREIBER, J., RODIG, S., YANG, K., NAKANO, I., LEE, H., WEISSLEDER, R., BREAKEFIELD, X. O., GODLEWSKI, J., WESTPHAL, M., LAMSZUS, K., FREEMAN, G. J., BRONISZ, A., LAWLER, S. E. & CHIOCCA, E. A. 2018. Immune evasion mediated by PD-L1 on glioblastoma-derived extracellular vesicles. *Sci Adv,* 4**,** eaar2766.

RIECK, S. & KAESTNER, K. H. 2010. Expansion of beta-cell mass in response to pregnancy. *Trends Endocrinol Metab,* 21**,** 151-8.

RINALDI, S. F., MAKIEVA, S., SAUNDERS, P. T., ROSSI, A. G. & NORMAN, J. E. 2017. Immune cell and transcriptomic analysis of the human decidua in term and preterm parturition. *Mol Hum Reprod,* 23**,** 708-724.

RIVOLTINI, L., CHIODONI, C., SQUARCINA, P., TORTORETO, M., VILLA, A., VERGANI, B., BURDEK, M., BOTTI, L., ARIOLI, I., COVA, A., MAURI, G., VERGANI, E., BIANCHI, B., DELLA MINA, P., CANTONE, L., BOLLATI, V., ZAFFARONI, N., GIANNI, A. M., COLOMBO, M. P. & HUBER, V. 2016. TNF-Related Apoptosis-Inducing Ligand (TRAIL)-Armed Exosomes Deliver Proapoptotic Signals to Tumor Site. *Clin Cancer Res,* 22**,** 3499-512.

ROBERTSON, S. A., CHRISTIAENS, I., DORIAN, C. L., ZARAGOZA, D. B., CARE, A. S., BANKS, A. M. & OLSON, D. M. 2010. Interleukin-6 is an essential determinant of on-time parturition in the mouse. *Endocrinology,* 151**,** 3996-4006.

ROBINSON, J. F., KAPIDZIC, M., GORMLEY, M., ONA, K., DENT, T., SEIFIKAR, H., HAMILTON, E. G. & FISHER, S. J. 2017. Transcriptional Dynamics of Cultured Human Villous Cytotrophoblasts. *Endocrinology,* 158**,** 1581-1594.

RODER, P. V., WU, B., LIU, Y. & HAN, W. 2016. Pancreatic regulation of glucose homeostasis. *Exp Mol Med,* 48**,** e219.

SAJI, F., SAMEJIMA, Y., KAMIURA, S. & KOYAMA, M. 1999. Dynamics of immunoglobulins at the feto-maternal interface. *Rev Reprod,* 4**,** 81-9.

SAKAMOTO, Y., MORAN, P., SEARLE, R. F., BULMER, J. N. & ROBSON, S. C. 2004. Interleukin-8 is involved in cervical dilatation but not in prelabour cervical ripening. *Clin Exp Immunol,* 138**,** 151-7.

SALOMON, C., SCHOLZ-ROMERO, K., SARKER, S., SWEENEY, E., KOBAYASHI, M., CORREA, P., LONGO, S., DUNCOMBE, G., MITCHELL, M. D., RICE, G. E. &

ILLANES, S. E. 2016. Gestational Diabetes Mellitus Is Associated With Changes in the Concentration and Bioactivity of Placenta-Derived Exosomes in Maternal Circulation Across Gestation. *Diabetes,* 65**,** 598-609.

SALOMON, C., TORRES, M. J., KOBAYASHI, M., SCHOLZ-ROMERO, K., SOBREVIA, L., DOBIERZEWSKA, A., ILLANES, S. E., MITCHELL, M. D. & RICE, G. E. 2014. A gestational profile of placental exosomes in maternal plasma and their effects on endothelial cell migration. *PLoS One,* 9**,** e98667.

SANAI, N., NGUYEN, T., IHRIE, R. A., MIRZADEH, Z., TSAI, H. H., WONG, M., GUPTA, N., BERGER, M. S., HUANG, E., GARCIA-VERDUGO, J. M., ROWITCH, D. H. & ALVAREZ-BUYLLA, A. 2011. Corridors of migrating neurons in the human brain and their decline during infancy. *Nature,* 478**,** 382-6.

SANSONE, P., SAVINI, C., KURELAC, I., CHANG, Q., AMATO, L. B., STRILLACCI, A., STEPANOVA, A., IOMMARINI, L., MASTROLEO, C., DALY, L., GALKIN, A., THAKUR, B. K., SOPLOP, N., URYU, K., HOSHINO, A., NORTON, L., BONAFE, M., CRICCA, M., GASPARRE, G., LYDEN, D. & BROMBERG, J. 2017. Packaging and transfer of mitochondrial DNA via exosomes regulate escape from dormancy in hormonal therapy-resistant breast cancer. *Proc Natl Acad Sci U S A,* 114**,** E9066-E9075.

SANTONOCITO, M., VENTO, M., GUGLIELMINO, M. R., BATTAGLIA, R., WAHLGREN, J., RAGUSA, M., BARBAGALLO, D., BORZI, P., RIZZARI, S., MAUGERI, M., SCOLLO, P., TATONE, C., VALADI, H., PURRELLO, M. & DI PIETRO, C. 2014. Molecular characterization of exosomes and their microRNA cargo in human follicular fluid: bioinformatic analysis reveals that exosomal microRNAs control pathways involved in follicular maturation. *Fertil Steril,* 102**,** 1751-61 e1.

SARKER, S., SCHOLZ-ROMERO, K., PEREZ, A., ILLANES, S. E., MITCHELL, M. D., RICE, G. E. & SALOMON, C. 2014. Placenta-derived exosomes continuously increase in maternal circulation over the first trimester of pregnancy. *J Transl Med,* 12**,** 204.

SAVINA, A., VIDAL, M. & COLOMBO, M. I. 2002. The exosome pathway in K562 cells is regulated by Rab11. *J Cell Sci,* 115**,** 2505-15.

SEGURA, E., GUERIN, C., HOGG, N., AMIGORENA, S. & THERY, C. 2007. CD8+ dendritic cells use LFA-1 to capture MHC-peptide complexes from exosomes in vivo. *J Immunol,* 179**,** 1489-96.

SEGURA, E., NICCO, C., LOMBARD, B., VERON, P., RAPOSO, G., BATTEUX, F., AMIGORENA, S. & THERY, C. 2005. ICAM-1 on exosomes from mature dendritic cells is critical for efficient naive T-cell priming. *Blood,* 106**,** 216-23.

SELOVIC, A., SARAC, J. & MISSONI, S. 2016. Changes in adipose tissue distribution during pregnancy estimated by ultrasonography. *J Matern Fetal Neonatal Med,* 29**,** 2131-7.

SHAH, R., PATEL, T. & FREEDMAN, J. E. 2018. Circulating Extracellular Vesicles in Human Disease. *N Engl J Med,* 379**,** 958-966.

SHANKAR, J., MESSENBERG, A., CHAN, J., UNDERHILL, T. M., FOSTER, L. J. & NABI, I. R. 2010. Pseudopodial actin dynamics control epithelial-mesenchymal transition in metastatic cancer cells. *Cancer Res,* 70**,** 3780-90.

SHINGO, T., GREGG, C., ENWERE, E., FUJIKAWA, H., HASSAM, R., GEARY, C., CROSS, J. C. & WEISS, S. 2003. Pregnancy-stimulated neurogenesis in the adult female forebrain mediated by prolactin. *Science,* 299**,** 117-20.

SHIROISHI, M., KUROKI, K., OSE, T., RASUBALA, L., SHIRATORI, I., ARASE, H., TSUMOTO, K., KUMAGAI, I., KOHDA, D. & MAENAKA, K. 2006. Efficient leukocyte Ig-like receptor signaling and crystal structure of disulfide-linked HLA-G dimer. *J Biol Chem,* 281**,** 10439-47.

SHURTLEFF, M. J., TEMOCHE-DIAZ, M. M., KARFILIS, K. V., RI, S. & SCHEKMAN, R. 2016. Y-box protein 1 is required to sort microRNAs into exosomes in cells and in a cell-free reaction. *Elife,* 5.

SHURTLEFF, M. J., YAO, J., QIN, Y., NOTTINGHAM, R. M., TEMOCHE-DIAZ, M. M., SCHEKMAN, R. & LAMBOWITZ, A. M. 2017. Broad role for YBX1 in defining the small noncoding RNA composition of exosomes. *Proc Natl Acad Sci U S A,* 114**,** E8987-E8995.

SILVA, T. A., SMUCZEK, B., VALADAO, I. C., DZIK, L. M., IGLESIA, R. P., CRUZ, M. C., ZELANIS, A., DE SIQUEIRA, A. S., SERRANO, S. M., GOLDBERG, G. S., JAEGER, R. G. & FREITAS, V. M. 2016. AHNAK enables mammary carcinoma cells to produce extracellular vesicles that increase neighboring fibroblast cell motility. *Oncotarget,* 7**,** 49998-50016.

SIMISTER, N. E. & MOSTOV, K. E. 1989. An Fc receptor structurally related to MHC class I antigens. *Nature,* 337**,** 184-7.

SIMISTER, N. E., STORY, C. M., CHEN, H. L. & HUNT, J. S. 1996. An IgG-transporting Fc receptor expressed in the syncytiotrophoblast of human placenta. *Eur J Immunol,* 26**,** 1527-31.

SKIBINSKI, G., KELLY, R. W., HARKISS, D. & JAMES, K. 1992. Immunosuppression by human seminal plasma--extracellular organelles (prostasomes) modulate activity of phagocytic cells. *Am J Reprod Immunol,* 28**,** 97-103.

SKOKOS, D., BOTROS, H. G., DEMEURE, C., MORIN, J., PERONET, R., BIRKENMEIER, G., BOUDALY, S. & MECHERI, S. 2003. Mast cell-derived exosomes induce phenotypic and functional maturation of dendritic cells and elicit specific immune responses in vivo. *J Immunol,* 170**,** 3037-45.

SMARASON, A. K., SARGENT, I. L., STARKEY, P. M. & REDMAN, C. W. 1993. The effect of placental syncytiotrophoblast microvillous membranes from normal and pre-eclamptic women on the growth of endothelial cells in vitro. *Br J Obstet Gynaecol,* 100**,** 943-9.

SMITH, C. H., NELSON, D. M., KING, B. F., DONOHUE, T. M., RUZYCKI, S. & KELLEY, L. K. 1977. Characterization of a microvillous membrane preparation from human placental

syncytiotrophoblast: a morphologic, biochemical, and physiologic, study. *Am J Obstet Gynecol,* 128**,** 190-6.

SON, Y. H., JEONG, Y. T., LEE, K. A., CHOI, K. H., KIM, S. M., RHIM, B. Y. & KIM, K. 2008. Roles of MAPK and NF-kappaB in interleukin-6 induction by lipopolysaccharide in vascular smooth muscle cells. *J Cardiovasc Pharmacol,* 51**,** 71-7.

SONI, S., O'DEA, K. P., TAN, Y. Y., CHO, K., ABE, E., ROMANO, R., CUI, J., MA, D., SARATHCHANDRA, P., WILSON, M. R. & TAKATA, M. 2019. ATP redirects cytokine trafficking and promotes novel membrane TNF signaling via microvesicles. *FASEB J,* 33**,** 6442-6455.

SORRELLS, S. F., PAREDES, M. F., CEBRIAN-SILLA, A., SANDOVAL, K., QI, D., KELLEY, K. W., JAMES, D., MAYER, S., CHANG, J., AUGUSTE, K. I., CHANG, E. F., GUTIERREZ, A. J., KRIEGSTEIN, A. R., MATHERN, G. W., OLDHAM, M. C., HUANG, E. J., GARCIA-VERDUGO, J. M., YANG, Z. & ALVAREZ-BUYLLA, A. 2018. Human hippocampal neurogenesis drops sharply in children to undetectable levels in adults. *Nature,* 555**,** 377-381.

SOUTHCOMBE, J., TANNETTA, D., REDMAN, C. & SARGENT, I. 2011. The immunomodulatory role of syncytiotrophoblast microvesicles. *PLoS One,* 6**,** e20245.

STENQVIST, A. C., NAGAEVA, O., BARANOV, V. & MINCHEVA-NILSSON, L. 2013. Exosomes secreted by human placenta carry functional Fas ligand and TRAIL molecules and convey apoptosis in activated immune cells, suggesting exosome-mediated immune privilege of the fetus. *J Immunol,* 191**,** 5515-23.

STERZENBACH, U., PUTZ, U., LOW, L. H., SILKE, J., TAN, S. S. & HOWITT, J. 2017. Engineered Exosomes as Vehicles for Biologically Active Proteins. *Mol Ther,* 25**,** 1269-1278.

STRAUGHEN, J. K., TRUDEAU, S. & MISRA, V. K. 2013. Changes in adipose tissue distribution during pregnancy in overweight and obese compared with normal weight women. *Nutr Diabetes,* 3**,** e84.

SUNG, B. H., KETOVA, T., HOSHINO, D., ZIJLSTRA, A. & WEAVER, A. M. 2015. Directional cell movement through tissues is controlled by exosome secretion. *Nat Commun,* 6**,** 7164.

SUNG, B. H. & WEAVER, A. M. 2017. Exosome secretion promotes chemotaxis of cancer cells. *Cell Adh Migr,* 11**,** 187-195.

SUZUKI, Y., HATTORI, T., KAJIKURI, J., YAMAMOTO, T., SUZUMORI, K. & ITOH, T. 2002. Reduced function of endothelial prostacyclin in human omental resistance arteries in pre-eclampsia. *J Physiol,* 545**,** 269-77.

SVENSSON, H., WETTERLING, L., BOSAEUS, M., ODEN, B., ODEN, A., JENNISCHE, E., EDEN, S., HOLMANG, A. & LONN, M. 2016. Body fat mass and the proportion of very large adipocytes in pregnant women are associated with gestational insulin resistance. *Int J Obes (Lond),* 40**,** 646-53.

TANNETTA, D. S., DRAGOVIC, R. A., GARDINER, C., REDMAN, C. W. & SARGENT, I. L. 2013. Characterisation of syncytiotrophoblast vesicles in normal pregnancy and pre-eclampsia: expression of Flt-1 and endoglin. *PLoS One,* 8**,** e56754.

TANNETTA, D. S., HUNT, K., JONES, C. I., DAVIDSON, N., COXON, C. H., FERGUSON, D., REDMAN, C. W., GIBBINS, J. M., SARGENT, I. L. & TUCKER, K. L. 2015. Syncytiotrophoblast Extracellular Vesicles from Pre-Eclampsia Placentas Differentially Affect Platelet Function. *PLoS One,* 10**,** e0142538.

TEN, R. M., PAYA, C. V., ISRAEL, N., LE BAIL, O., MATTEI, M. G., VIRELIZIER, J. L., KOURILSKY, P. & ISRAEL, A. 1992. The characterization of the promoter of the gene encoding the p50 subunit of NF-kappa B indicates that it participates in its own regulation. *EMBO J,* 11**,** 195-203.

THAKUR, B. K., ZHANG, H., BECKER, A., MATEI, I., HUANG, Y., COSTA-SILVA, B., ZHENG, Y., HOSHINO, A., BRAZIER, H., XIANG, J., WILLIAMS, C., RODRIGUEZ-BARRUECO, R., SILVA, J. M., ZHANG, W., HEARN, S., ELEMENTO, O., PAKNEJAD, N., MANOVA-TODOROVA, K., WELTE, K., BROMBERG, J., PEINADO, H. & LYDEN, D. 2014. Double-stranded DNA in exosomes: a novel biomarker in cancer detection. *Cell Res,* 24**,** 766-9.

THERY, C., AMIGORENA, S., RAPOSO, G. & CLAYTON, A. 2006. Isolation and characterization of exosomes from cell culture supernatants and biological fluids. *Curr Protoc Cell Biol,* Chapter 3**,** Unit 3 22.

UEDA, A., OKUDA, K., OHNO, S., SHIRAI, A., IGARASHI, T., MATSUNAGA, K., FUKUSHIMA, J., KAWAMOTO, S., ISHIGATSUBO, Y. & OKUBO, T. 1994. NF-kappa B and Sp1 regulate transcription of the human monocyte chemoattractant protein-1 gene. *J Immunol,* 153**,** 2052-63.

VALADI, H., EKSTROM, K., BOSSIOS, A., SJOSTRAND, M., LEE, J. J. & LOTVALL, J. O. 2007. Exosome-mediated transfer of mRNAs and microRNAs is a novel mechanism of genetic exchange between cells. *Nat Cell Biol,* 9**,** 654-9.

VALENTE, A. J., GRAVES, D. T., VIALLE-VALENTIN, C. E., DELGADO, R. & SCHWARTZ, C. J. 1988. Purification of a monocyte chemotactic factor secreted by nonhuman primate vascular cells in culture. *Biochemistry,* 27**,** 4162-8.

VALENTI, R., HUBER, V., FILIPAZZI, P., PILLA, L., SOVENA, G., VILLA, A., CORBELLI, A., FAIS, S., PARMIANI, G. & RIVOLTINI, L. 2006. Human tumor-released microvesicles promote the differentiation of myeloid cells with transforming growth factor-beta-mediated suppressive activity on T lymphocytes. *Cancer Res,* 66**,** 9290-8.

VAN ASSCHE, F. A., AERTS, L. & DE PRINS, F. 1978. A morphological study of the endocrine pancreas in human pregnancy. *Br J Obstet Gynaecol,* 85**,** 818-20.

VAN DE STOLPE, A., CALDENHOVEN, E., STADE, B. G., KOENDERMAN, L., RAAIJMAKERS, J. A., JOHNSON, J. P. & VAN DER SAAG, P. T. 1994. 12-O-tetradecanoylphorbol-13-acetate- and tumor necrosis factor alpha-mediated induction of intercellular adhesion molecule-1 is inhibited by dexamethasone. Functional analysis of the human intercellular adhesion molecular-1 promoter. *J Biol Chem,* 269**,** 6185-92.

VAN DE VLEKKERT, D., DEMMERS, J., NGUYEN, X. X., CAMPOS, Y., MACHADO, E., ANNUNZIATA, I., HU, H., GOMERO, E., QIU, X., BONGIOVANNI, A., FEGHALI-BOSTWICK, C. A. & D'AZZO, A. 2019. Excessive exosome release is the pathogenic pathway linking a lysosomal deficiency to generalized fibrosis. *Sci Adv,* 5**,** eaav3270.

VAN NIEL, G., D'ANGELO, G. & RAPOSO, G. 2018. Shedding light on the cell biology of extracellular vesicles. *Nat Rev Mol Cell Biol,* 19**,** 213-228.

VEGAS, A. J., VEISEH, O., GURTLER, M., MILLMAN, J. R., PAGLIUCA, F. W., BADER, A. R., DOLOFF, J. C., LI, J., CHEN, M., OLEJNIK, K., TAM, H. H., JHUNJHUNWALA, S., LANGAN, E., ARESTA-DASILVA, S., GANDHAM, S., MCGARRIGLE, J. J., BOCHENEK, M. A., HOLLISTER-LOCK, J., OBERHOLZER, J., GREINER, D. L., WEIR, G. C., MELTON, D. A., LANGER, R. & ANDERSON, D. G. 2016. Long-term glycemic control using polymer-encapsulated human stem cell-derived beta cells in immune-competent mice. *Nat Med,* 22**,** 306-11.

VIGNERON, N., FERRARI, V., STROOBANT, V., ABI HABIB, J. & VAN DEN EYNDE, B. J. 2017. Peptide splicing by the proteasome. *J Biol Chem,* 292**,** 21170-21179.

VILELLA, F., MORENO-MOYA, J. M., BALAGUER, N., GRASSO, A., HERRERO, M., MARTINEZ, S., MARCILLA, A. & SIMON, C. 2015. Hsa-miR-30d, secreted by the human endometrium, is taken up by the pre-implantation embryo and might modify its transcriptome. *Development,* 142**,** 3210-21.

VILLARROYA-BELTRI, C., GUTIERREZ-VAZQUEZ, C., SANCHEZ-CABO, F., PEREZ-HERNANDEZ, D., VAZQUEZ, J., MARTIN-COFRECES, N., MARTINEZ-HERRERA, D.

J., PASCUAL-MONTANO, A., MITTELBRUNN, M. & SANCHEZ-MADRID, F. 2013. Sumoylated hnRNPA2B1 controls the sorting of miRNAs into exosomes through binding to specific motifs. *Nat Commun,* 4**,** 2980.

VOJTECH, L., ZHANG, M., DAVE, V., LEVY, C., HUGHES, S. M., WANG, R., CALIENES, F., PRLIC, M., NANCE, E. & HLADIK, F. 2019. Extracellular vesicles in human semen modulate antigen-presenting cell function and decrease downstream antiviral T cell responses. *PLoS One,* 14**,** e0223901.

WAGENBLAST, E., SOTO, M., GUTIERREZ-ANGEL, S., HARTL, C. A., GABLE, A. L., MACELI, A. R., ERARD, N., WILLIAMS, A. M., KIM, S. Y., DICKOPF, S., HARRELL, J. C., SMITH, A. D., PEROU, C. M., WILKINSON, J. E., HANNON, G. J. & KNOTT, S. R. 2015. A model of breast cancer heterogeneity reveals vascular mimicry as a driver of metastasis. *Nature,* 520**,** 358-62.

WAHLUND, C. J. E., GUCLULER, G., HILTBRUNNER, S., VEERMAN, R. E., NASLUND, T. I. & GABRIELSSON, S. 2017. Exosomes from antigen-pulsed dendritic cells induce stronger antigen-specific immune responses than microvesicles in vivo. *Sci Rep,* 7**,** 17095.

WAKIM, L. M. & BEVAN, M. J. 2011. Cross-dressed dendritic cells drive memory CD8+ T-cell activation after viral infection. *Nature,* 471**,** 629-32.

WANG, G. J., LIU, Y., QIN, A., SHAH, S. V., DENG, Z. B., XIANG, X., CHENG, Z., LIU, C., WANG, J., ZHANG, L., GRIZZLE, W. E. & ZHANG, H. G. 2008. Thymus exosomes-like particles induce regulatory T cells. *J Immunol,* 181**,** 5242-8.

WANG, P., FIASCHI-TAESCH, N. M., VASAVADA, R. C., SCOTT, D. K., GARCIA-OCANA, A. & STEWART, A. F. 2015. Diabetes mellitus--advances and challenges in human beta-cell proliferation. *Nat Rev Endocrinol,* 11**,** 201-12.

WEBBER, J., STEADMAN, R., MASON, M. D., TABI, Z. & CLAYTON, A. 2010. Cancer exosomes trigger fibroblast to myofibroblast differentiation. *Cancer Res,* 70**,** 9621-30.

WEBBER, J. P., SPARY, L. K., SANDERS, A. J., CHOWDHURY, R., JIANG, W. G., STEADMAN, R., WYMANT, J., JONES, A. T., KYNASTON, H., MASON, M. D., TABI, Z. & CLAYTON, A. 2015. Differentiation of tumour-promoting stromal myofibroblasts by cancer exosomes. *Oncogene,* 34**,** 290-302.

WEI, Z., BATAGOV, A. O., SCHINELLI, S., WANG, J., WANG, Y., EL FATIMY, R., RABINOVSKY, R., BALAJ, L., CHEN, C. C., HOCHBERG, F., CARTER, B., BREAKEFIELD, X. O. & KRICHEVSKY, A. M. 2017. Coding and noncoding landscape of extracellular RNA released by human glioma stem cells. *Nat Commun,* 8**,** 1145.

WELSCH, F. 1979. Release of human chorionic somatomammotrophin from isolated perfused lobules and superfused fragments of term placenta: spontaneous liberation and the effects of cholinergic drugs, dibutyrylcyclic adenosine monophosphate and calcium. *Res Commun Chem Pathol Pharmacol,* 24**,** 211-22.

WILLIAMS, C., PAZOS, R., ROYO, F., GONZALEZ, E., ROURA-FERRER, M., MARTINEZ, A., GAMIZ, J., REICHARDT, N. C. & FALCON-PEREZ, J. M. 2019. Assessing the role of surface glycans of extracellular vesicles on cellular uptake. *Sci Rep,* 9**,** 11920.

WOLFERS, J., LOZIER, A., RAPOSO, G., REGNAULT, A., THERY, C., MASURIER, C., FLAMENT, C., POUZIEUX, S., FAURE, F., TURSZ, T., ANGEVIN, E., AMIGORENA, S. & ZITVOGEL, L. 2001. Tumor-derived exosomes are a source of shared tumor rejection antigens for CTL cross-priming. *Nat Med,* 7**,** 297-303.

WONG, C. H. & CHEN, Y. C. 2019. Clinical significance of exosomes as potential biomarkers in cancer. *World J Clin Cases,* 7**,** 171-190.

YELAVARTHI, K. K., FISHBACK, J. L. & HUNT, J. S. 1991. Analysis of HLA-G mRNA in human placental and extraplacental membrane cells by in situ hybridization. *J Immunol,* 146**,** 2847-54.

YIE, S. M., LI, L. H., XIAO, R. & LIBRACH, C. L. 2008. A single base-pair mutation in the 3'-untranslated region of HLA-G mRNA is associated with pre-eclampsia. *Mol Hum Reprod,* 14**,** 649-53.

YU, S., LIU, C., SU, K., WANG, J., LIU, Y., ZHANG, L., LI, C., CONG, Y., KIMBERLY, R., GRIZZLE, W. E., FALKSON, C. & ZHANG, H. G. 2007. Tumor exosomes inhibit differentiation of bone marrow dendritic cells. *J Immunol,* 178**,** 6867-75.

YUANA, Y., LEVELS, J., GROOTEMAAT, A., STURK, A. & NIEUWLAND, R. 2014. Co-isolation of extracellular vesicles and high-density lipoproteins using density gradient ultracentrifugation. *J Extracell Vesicles,* 3.

ZDRAVKOVIC, T., NAZOR, K. L., LAROCQUE, N., GORMLEY, M., DONNE, M., HUNKAPILLAR, N., GIRITHARAN, G., BERNSTEIN, H. S., WEI, G., HEBROK, M., ZENG, X., GENBACEV, O., MATTIS, A., MCMASTER, M. T., KRTOLICA, A., VALBUENA, D., SIMON, C., LAURENT, L. C., LORING, J. F. & FISHER, S. J. 2015. Human stem cells from single blastomeres reveal pathways of embryonic or trophoblast fate specification. *Development,* 142**,** 4010-25.

ZHANG, H. G., LIU, C., SU, K., YU, S., ZHANG, L., ZHANG, S., WANG, J., CAO, X., GRIZZLE, W. & KIMBERLY, R. P. 2006. A membrane form of TNF-alpha presented by exosomes delays T cell activation-induced cell death. *J Immunol,* 176**,** 7385-93.

ZHOU, A., SCOGGIN, S., GAYNOR, R. B. & WILLIAMS, N. S. 2003. Identification of NF-kappa B-regulated genes induced by TNFalpha utilizing expression profiling and RNA interference. *Oncogene,* 22**,** 2054-64.

ZHOU, Q. & MELTON, D. A. 2018. Pancreas regeneration. *Nature,* 557**,** 351-358.

ZITVOGEL, L., REGNAULT, A., LOZIER, A., WOLFERS, J., FLAMENT, C., TENZA, D., RICCIARDI-CASTAGNOLI, P., RAPOSO, G. & AMIGORENA, S. 1998. Eradication of established murine tumors using a novel cell-free vaccine: dendritic cell-derived exosomes. *Nat Med,* 4**,** 594-600.

ZOMER, A., MAYNARD, C., VERWEIJ, F. J., KAMERMANS, A., SCHAFER, R., BEERLING, E., SCHIFFELERS, R. M., DE WIT, E., BERENGUER, J., ELLENBROEK, S. I. J., WURDINGER, T., PEGTEL, D. M. & VAN RHEENEN, J. 2015. In Vivo imaging reveals extracellular vesicle-mediated phenocopying of metastatic behavior. *Cell,* 161**,** 1046-1057.

Publishing Agreement

It is the policy of the University to encourage the distribution of all theses, dissertations, and manuscripts. Copies of all UCSF theses, dissertations, and manuscripts will be routed to the library via the Graduate Division. The library will make all theses, dissertations, and manuscripts accessible to the public and will preserve these to the best of their abilities, in perpetuity.

Please sign the following statement:

I hereby grant permission to the Graduate Division of the University of California, San Francisco to release copies of my thesis, dissertation, or manuscript to the Campus Library to provide access and preservation, in whole or in part, in perpetuity.

DocuSigned by:

A97C43FFE82D44E...

Author Signature

12/9/2019

Date